Pharmacological characterization and functional rescue of the giant panda and human melanocortin-4 receptors

by

Wei Wang

A dissertation submitted to the Graduate Faculty of
Auburn University
in partial fulfillment of the
requirements for the Degree of
Doctor of Philosophy

Auburn, Alabama
August 5, 2017

Keywords: G protein-coupled receptor, Melanocortin-4 receptor, Obesity, Naturally occurring mutations, Pharmacoperone

Approved by

Ya-Xiong Tao, Chair, Professor of Physiology
Robert Judd, Professor of Pharmacology
Satyanarayana Pondugula, Associate Professor of Anatomy
Ramesh Jeganathan, Associate Professor of Nutrition

Abstract

The melanocortin-4 receptor (MC4R) is a member of family A rhodopsin-like G protein-coupled receptors. It is well established that MC4R is critically involved in regulating food intake and energy expenditure in mammals. As the most common monogenic form of human obesity, more than 170 naturally occurring *MC4R* mutations have been identified from different patient cohorts. Functional characterization of mutant MC4Rs is indispensable for confirming the causal role of *MC4R* mutations in obesity pathogenesis.

In this study, giant panda (*Ailuropoda melanoleuca*) MC4R was cloned, expressed, and functionally characterized. Sequence analysis revealed that amMC4R was highly homologous (>88%) at nucleotide and amino acid sequence levels to human, mouse, rat, pig, cat, cattle, and dog MC4Rs. With human MC4R (hMC4R) as a control, four agonists, including [Nle^4, D-Phe^7]-α-melanocyte stimulating hormone (NDP-MSH), α-MSH, β-MSH, and a small molecule agonist, THIQ, were used in the binding and signaling assays to investigate the pharmacological properties of amMC4R. We showed that amMC4R bound NDP-MSH with the highest affinity followed by THIQ, α-MSH, and β-MSH, with the same ranking as hMC4R. Treatment of HEK293T cells expressing amMC4R with different concentrations of agonists resulted in dose-dependent accumulation of intracellular cAMP levels, with similar EC_{50}s for the four agonists. The results suggested that the cloned amMC4R encoded a functional MC4R. The availability of amMC4R and its binding and signaling properties will facilitate the investigation of MC4R in regulating food intake and energy expenditure in giant panda.

In addition, we reported systematic functional characterization of nine novel human *MC4R* mutations including L23R, K73R, T101N, T112K, M161T, L207V, M215L, R310K, and I316S. Mutants with defects in the receptor expression, ligand binding, and/or cAMP signaling were identified and classified based on a classification scheme that we proposed earlier. Consistent with previous reports, intracellular retention was demonstrated to be the most common defect in the nine mutants studied herein. Mutant M161T had normal cAMP production in stimulation with NDP-MSH but not α-MSH, MTII, or THIQ. In addition, we demonstrated that defective ERK1/2 signaling might be a cause of obesity in patients harboring Class V mutant MC4Rs. Five mutant receptors were identified as biased receptors in the cAMP and ERK1/2 signaling pathways. Furthermore, we showed that two MC4R inverse agonists, Ipsen 5i and ML00253764, acted as pharmacological chaperones to rescue the cell surface expression and function of thirteen intracellularly retained mutant MC4Rs. In summary, we provided detailed functional data and a potential therapeutic approach for the treatment of obese patients harboring these mutations.

Acknowledgments

First and foremost, I would like to acknowledge my advisor, Dr. Ya-Xiong Tao, for his endless guidance and support during my four-year study in his laboratory. Without his critical comments, constant encouragements, and constructive suggestions, I could not have this dissertation done.

I would also like to express my sincere gratitude to my committee members, Drs. Robert Judd, Satyanarayana Pondugula, and Ramesh Jeganathan for sharing their wisdom, experience, advice, and expertise during the past four years. I am thankful to my university reader, Dr. Mahmoud Mansour, for his careful review and precious suggestions of my dissertation.

My enormous appreciation also goes to my lab colleagues and alumni, Li-Kun Yang, Zhi-Shuai Hou, Zhuo-Yue Li, Xiao-Chen Yuan, Hai-Jie Zhang, Drs. Hui Huang, Zhao Yang, Xiu-Lei Mo, Meng-Hong Dai, Guang-Li Li, and Qi-Hui Yang, for their valuable contribution and discussion to the research projects. I would like to thank China Scholarship Council of the People's Republic of China for the financial support throughout these years.

Last but not least, I would like to thank my wife, Han Fang, my sister, my parents, and parents-in-law for their unselfish love and endless encouragement. I could not finish my graduate study without their support.

Table of Contents

List of Tables

List of Figures

List of Abbreviations

ACTH	Adrenocorticotrophic hormone
AgRP	Agouti-related peptide
ARC	Arcuate nucleus
AVPR2	Arginine vasopressin V2 receptor
B_{max}	Maximal binding
BMI	Body mass index
BSA	Bovine serum albumin
CART	Cocaine and amphetamine-regulated transcript
CCK	Cholecystokinin
CCK1R	Type 1 cholecystokinin receptor
CCK-8s	Sulfated 8-amino-acid form of cholecystokinin
CFTR	Cystic fibrosis transmembrane conductance regulator
CNS	Central nervous system
DMEM	Dulbecco's modified Eagle's medium
ERK	Extracellular signal-regulated kinase
HEK	Human embryonic kidney
Hsc70	Cytosolic cognate 70-kDa heat shock protein
HSP	Heat shock protein
GABA	γ-aminobutyric acid

GPCR	G protein-coupled receptor
MC1R	Melanocortin-1 receptor
MC2R	Melanocortin-2 receptor
MC3R	Melanocortin-3 receptor
MC4R	Melanocortin-4 receptor
MC5R	Melanocortin-5 receptor
MCR	Melanocortin receptor
MRAP	Melanocortin-2 receptor accessory protein
MSH	Melanocyte stimulating hormone
MTII	Melanotan II
NDI	Nephrogenic diabetes insipidus
NPY	Neuropeptide Y
NTS	Nucleus tractus solitaries
PBA	Phenylbutyrate
PC	Prohormone convertase
PYY	Peptide tyrosine tyrosine
POMC	Pro-opiomelanocortin
PVN	Paraventricular nucleus
WHO	World Health Organization
WT	Wild-type

Chapter 1

1.1 Introduction

The melanocortin-4 receptor (MC4R) is a downstream mediator of leptin action in the hypothalamus, where it plays a vital role in regulating energy homeostasis (Huszar et al., 1997). Mutations in the *MC4R* gene are the most common monogenic form of obesity with a prevalence as high as 6% in some ethnic populations (Farooqi et al., 2003). Therefore, the MC4R has been considered as a premier target for obesity treatment and has been extensively studied in molecular genetics of obesity. In addition to regulation of energy balance, the MC4R is also involved in several other key physiological functions such as glucose and lipid homeostasis, reproductive function and sexual behavior, cardiovascular function, pain perception, and brain inflammation (reviewed in (Tao, 2010)). Not only in rodents and humans, the MC4R has also been suggested to be a critical physiological regulator of energy homeostasis in other mammals such as rhesus monkeys (Koegler et al., 2001), sheep (Wagner et al., 2004), and pigs (Barb et al., 2004). However, its role in the living fossil endemic to China, the giant panda (*Ailuropoda melanoleuca*), remains to be investigated.

The MC4R is a G protein-coupled receptor (GPCR). It responds to the activation of two endogenous peptide agonists, α- and β-melanocyte stimulating hormones (MSHs) and to the inhibition of an endogenous antagonist/inverse agonist, agouti-related peptide (AgRP). Like other GPCRs, the MC4R signals through G protein-dependent and -independent pathways and its mutant forms may exhibit biased signaling (Breit et al., 2011; He and Tao, 2014; Huang and Tao,

2012; Tao, 2014).

Approximately 170 *MC4R* mutations have been identified from obese patients (Hinney et al., 2013). Detailed functional studies revealed that most of the inactivating mutants are retained intracellularly and that mutants defective in binding and signaling are rare (Tao, 2005, 2009, 2010), similar to the observations in naturally occurring mutations in other GPCRs (Tao, 2006; Tao and Conn, 2014). Several approaches using chemical chaperones, molecular chaperones, or pharmacological chaperones have been proposed to promote the anterograde trafficking of intracellularly retained mutants.

This chapter presents an overview of the obesity epidemic and current treatments. A brief summary of the central melanocortin system and its upstream signals are also discussed. Finally, the importance of MC4R in regulating energy homeostasis, including naturally occurring mutations, the underlying molecular mechanisms, and potential strategies used for treatment of human obesity caused by misfolded *MC4R* mutations are highlighted.

1.2 Obesity

1.2.1 The prevalence of obesity

Obesity is a multi-factorial disorder characterized by an excess amount of body fat. According to the World Health Organization (WHO), obesity is defined as a body mass index (BMI, body weight in kilograms divided by height in meters squared) at least 30 kg/m^2 and overweight as BMI between 25 and 29.9 kg/m^2. Obesity has been shown to be closely associated with type 2 diabetes (Manson et al., 1992), stroke (Rexrode et al., 1997), gallbladder disease (Kato et al., 1992; Stampfer et al., 1992), dyslipidemia (Rabkin et al., 1997), hypertension (Witteman et al., 1989), cardiovascular disease (Rimm et al., 1995), and certain types of cancers

(Moyad, 2001; Romiti et al., 1998; Sellers et al., 1992), raising the risk of morbidity and mortality. Indeed, a pilot study performed by Allison and colleagues showed that the maximum years of life lost for white men aged 20 to 30 years with a severe level of obesity (BMI > 45) is 13, representing a 22% reduction in expected remaining life span (Fontaine et al., 2003). In addition, obesity can also result in a variety of psychological and social consequences. Therefore, obesity itself is currently recognized as a disease by the Obesity Society and the American Heart Association (Jensen et al., 2014).

The prevalence of obesity and overweight is increasing at an alarming rate in both developed and developing countries. According to the latest statistics provided by the WHO, worldwide obesity has more than doubled since 1980, with more than 1.9 billion adults being overweight and over 600 million being obese in 2014. Another study published in International Journal of Obesity predicts that, by the year of 2030, the absolute numbers will be total 2.16 billion overweight and 1.12 billion obese individuals, accounting for 38% and 20% of the world's adult population, respectively (Kelly et al., 2008). In the United States, data obtained from the 2011-2014 National Health and Nutrition Examination Survey showed that 36% adults and 17% youth are classified as obese (Ogden et al., 2015). Interestingly, the prevalence of obesity is higher in women (38.3%) than in men (34.3%) (Ogden et al., 2015).

Childhood obesity is also increasing rapidly and has become one of the most serious public health challenges of the 21th century. The worldwide prevalence of childhood overweight and obesity increases from 4.2% in 1990 to 6.7% in 2010 (de Onis et al., 2010). In 2010, 43 million children (35 million in developing countries) are estimated to be overweight and obese and 92 million are at risk of overweight (de Onis et al., 2010). The detrimental effects of childhood obesity include a higher risk for the development of obesity-associated diseases such as type 2

diabetes mellitus, atherosclerosis, and heart disease (Juonala et al., 2011; Lobstein et al., 2004; Tirosh et al., 2011). Indeed, over 10% of obese children have pre-diabetes, a condition characterized by high blood sugar levels, continuing weight gain, and will progress into type 2 diabetes without intervention (Morrison et al., 2007). About 10.3% and 25% of obese children and adolescents have impaired glucose tolerance and a clustering of cardiovascular risk factors (Sabin et al., 2006) and their medium-term chance of heart disease increases dramatically by 10 folds compared with normal children (Morrison et al., 2007).

Besides the enormous health burden, rising rates of overweight and obesity also causes significant economic expenditure in healthcare systems. In the United States, overweight- and obesity-attributable medical spending increases from $79 billion in 1998 (Finkelstein et al., 2003) to $147 billion in 2008 (Finkelstein et al., 2009), and this number is projected to be as high as $344 billion by 2018 (Trogdon et al., 2012). The majority of these medical costs are financed by Medicare and Medicaid (Finkelstein et al., 2009). Across all payers, obese people have medical spending that is $1,429 greater than spending for normal-weight people in 2006 (Finkelstein et al., 2009).

1.2.2 Current treatments for obesity

Although research over the past few decades has broadened our understanding of central and peripheral mechanisms in regulating energy homeostasis, there has been a major lag in the development of effective therapies for obesity. Currently, the main effective treatment options with sufficient evidence-based support are lifestyle intervention, pharmacotherapy, and bariatric surgery.

Lifestyle interventions, including dietary therapy, physical activity, and behavioral therapy, are usually recommended to the vast majority of obese individuals for weight management given their low cost and the minimal risk of complications. Indeed, among ten studies comparing diet, exercise, and behavioral intervention with minimal intervention, eight reported absolute weight change between the intervention and control groups, the weight differences range from -1.0 kg to -10.2 kg and the follow-up intervals range from 3 months to 24 months (Hassan et al., 2016). However, due to the highly conserved nature of the biological defense of human body weight, the lifestyle intervention often fails to succeed in long-term weight loss (Guyenet and Schwartz, 2012).

Pharmacotherapy can be used as an adjunct to lifestyle intervention since effects of lifestyle intervention are not always satisfactory in all cases. Clinically, drugs prescribed for weight loss can be classified into appetite suppressant or lipase inhibitor. Appetite suppressant, such as sibutramine, a serotonin and noradrenaline reuptake inhibitor that inhibits appetite, has been prescribed for treatment of obesity for half a century. However, sibutramine has been withdrawn from North America and Europe since 2010 when it was found to be associated with increased risks of myocardial infarction and nonfatal stroke (James et al., 2010). Orlistat, the only gastrointestinal lipase inhibitor currently available in the market, was approved by the FDA in 1999 for the treatment of obesity (McNeely and Benfield, 1998). In addition, orlistat also improves blood pressure, insulin resistance and serum lipid levels (Siebenhofer et al., 2009; Torgerson et al., 2004). However, oral consumption of orlistat has been reported to be related to some side-effects including diarrhea, flatulence, bloating, abdominal pain and dyspepsia (Siebenhofer et al., 2009).

Bariatric surgery is by far the most effective medical treatment for obesity and it has been proven to remarkably reduce total mortality in patients with a BMI of 40 kg/m^2 or greater. Roux-en-Y gastric bypass, the most commonly used procedure, can yield an average of approximately 60% loss of excess body weight in morbidly obese patients. Independent of weight loss, bariatric surgery can prevent development of type 2 diabetes in obese patients, with a rapid reduction in the use of oral hypoglycemic agents and insulin (Ackroyd et al., 2006). After studying 1658 patients who underwent bariatric surgery and 1771 obese matched controls with usual care, Carlsson *et al.* showed that bariatric surgery reduces the long-term incidence of type 2 diabetes by 78% in obese patients, and this preventive effect is particularly obvious in participants with impaired fasting glucose (Carlsson et al., 2012). However, few obese patients are qualified for bariatric surgery because of safety issues and enormous costs (Terranova et al., 2012). A study reported that the 30-day rate of death among obese patients who undergo a bariatric surgery is 0.3%, while a total of 4.1% of patients have at least one major adverse outcome (Longitudinal Assessment of Bariatric Surgery et al., 2009).

1.3 The melanocortin system

1.3.1 Overview of the melanocortin system

The melanocortin system consists of several agonists, two antagonists, and five melanocortin receptors (MCRs). The melanocortin peptides, including α-, β-, γ-melanocyte-stimulating hormones (MSHs), and adrenocorticotropic hormone (ACTH), are derived from the posttranslational processing of a larger precursor molecule called pro-opiomelanocortin (POMC) protein. POMC undergoes post-translational processing in a tissue-specific manner (Pritchard et al., 2002). In the anterior pituitary, it is cleaved into ACTH, β-lipotroin, N-terminal peptide and

joining peptide by prohormone convertase (PC) 1. In the hypothalamus and pars intermedia where both PC1 and PC2 are expressed, these products are further cleaved into α-, β-, and γ-MSH (reviewed in (Shimizu et al., 2007)). Importantly, the melanocortin peptides all share a common amino acid sequence His-Phe-Arg-Trp (HFRW), the core sequence required for receptor binding, activation, and physiological effects. The uniqueness of the melanocortin system is due to the existence of two natural antagonists/inverse agonists, Agouti and AgRP. Agouti is a high-affinity, competitive antagonist of the melanocortin peptides at MC1R and MC4R whereas AgRP is a competitive antagonist of MC3R and MC4R with equal potency (reviewed in (Gantz and Fong, 2003)).

To date, five closely related GPCRs, MC1R to MC5R, have been cloned and named by the sequence of their cloning. The MC1R is the classical MSH receptor expressed in skin and hair follicles that regulates pigmentation. The MC2R, responsive only to ACTH and thus also known as the classical ACTH receptor, is expressed in the adrenal cortex that regulates adrenal steroidogenesis. The MC3R and MC4R, also known as neural MCRs, are expressed primarily in the central nervous system (CNS) that regulate energy homeostasis. The MC5R is expressed widely in the brain and numerous peripheral tissues that regulates sebogenesis and lipid metabolism. Sequence comparison of human MCRs shows high homologies, with a 38% identity between MC2R and MC4R and 60% between MC4R and MC5R (Catania et al., 2004). The MCRs are the smallest GPCRs known to date, with short amino- and carboxyl-terminal ends and second extracellular loop. Once activated by the agonists, the MCRs are functionally coupled to stimulatory G protein and mediate their physiological effects primarily through the cAMP-dependent signaling pathway.

1.3.2 Energy homeostasis regulated by the melanocortin system

Energy homeostasis refers to the balance between energy intake, including food and drink consumption, and energy expenditure, including basal metabolism, physical exercise and thermogenesis over a prolonged period in adult animals. Therefore, in a normal adult where the energy homeostasis is under precise control, the body weight should be stable during adulthood (Guyenet and Schwartz, 2012).

The maintenance of energy hemostasis is achieved by incorporating both circulating dietary and central neuronal signals. The central integration of these signals modulates an intricate network of neurons capable of adjusting physiological and behavioral responses accordingly. One such element of this system is the melanocortin pathway. As one of the most fundamental components of centrally regulated energy balance, the melanocortin pathway employs two counteracting populations of interoceptive neurons in the arcuate nucleus of the hypothalamus (ARC), also known as first-order neurons, as the primary sensor of alteration of food intake and energy expenditure. The ARC^{POMC} neurons coexpressing POMC and cocaine and amphetamine-regulated transcript (CART) represents the catabolic arm of the melanocortin pathway activated by caloric sufficiency, whereas the ARC^{AgRP} neurons coexpressing the potent orexigenic peptides AgRP and neuropeptide Y (NPY) represents anabolic arm of the melanocortin pathway stimulated in response to caloric insufficiency. Consistent with their metabolic functions, the activity of ARC^{POMC} and ARC^{AgRP} neurons conveys the real-time awareness of energetic need, which in turn predicts neurotransmitter release and corresponding physiological output.

The opposing roles of POMC-derived peptides and AgRP in the regulation of food intake and energy expenditure are mediated through their opposing actions at neural MCRs (MC3R and MC4R) expressed in the paraventricular nucleus of hypothalamus (PVN). However, the

definitive role of MC3R in the regulation of energy homeostasis is still controversial and will not be discussed in this chapter. The MC4R is predominantly activated by the natural agonist, α-MSH, initiating a sequence of downstream signaling pathways that result in neural depolarization and action potential firing, and eventually increased satiety, energy expenditure, and weight loss, whereas AgRP acts as an antagonist and/or biased agonist inducing neural hyperpolarization, leading to increased food intake, energy conservation, and weight gain (reviewed in (Krashes et al., 2016)).

1.3.3 Upstream signals of the melanocortin system

Multiple lines of evidence have shown that the central melanocortin circuits can receive and integrate a variety of central neuronal and circulating hormonal signals. The actions of these signals affect the release of POMC-derived ligands and AgRP and the consequential modulation of downstream MC3R- and MC4R-dependent homeostatic pathways. The upstream hormonal signals include long-term adiposity signals, such as leptin and insulin, and short-term satiety signals, such as ghrelin, cholecystokinin (CCK), and peptide tyrosine tyrosine (PYY).

1.3.3.1 Chronic peripheral factors

Leptin, a principal regulator of long-term energy balance, is a hormone produced by the adipocytes. Circulating leptin levels are proportional to body fat mass, increasing with fat accumulation and decreasing with fat depletion. In addition, leptin levels are also responsive to acute nutritional state, increasing after food consumption and declining with food deprivation. Leptin serves as an ‘adipostat’ signal to inform the brain about the energy stores in the organism though a negative feedback loop. Leptin acts on its receptor in the CNS to inhibit food intake.

Concordantly, genetically modified rodents that lack the gene for leptin or leptin receptor, including *ob/ob* mice (leptin deficiency), *db/db* mice (leptin receptor deficiency), and Zucker *fa/fa* rat (leptin receptor deficiency), demonstrate a profound obesity phenotype, (reviewed in (Tao et al., 2013)).

By binding to the leptin receptors expressed in the ARC^{POMC} and ARC^{AgRP} neurons, leptin induces a sequence of signaling pathways ultimately stimulating ARC^{POMC} neurons and inhibiting ARC^{AgRP} neurons (Cowley et al., 2001). Transgenic mice with deficient leptin signaling at melanocortin neurons by specific deletion of leptin receptors in the ARC^{POMC} neurons (Balthasar et al., 2004) or signal transducer and activator of transcription-3 in the ARC^{AgRP} neurons, a downstream mediator of leptin signaling (Gong et al., 2008), demonstrate severe obesity, whereas mice with targeted overactivation of leptin signaling at the ARC^{AgRP} neurons by constitutive activation of signal transducer and activator of transcription-3, manifest a lean phenotype (Mesaros et al., 2008). These data suggest that the central melanocortin system mediates leptin's effects on food intake and energy expenditure.

Insulin, a peptide hormone released from the pancreas, has been known to decrease plasma glucose levels within the periphery. However, insulin also enters the brain from the circulation through several pathways including transport of insulin by brain microvascular endothelial cells from peripheral vessels and the delivery of insulin to cerebrospinal fluid via choroid plexus (Gray et al., 2014). Within the CNS, insulin is characterized as an anorexigenic factor in the energy homeostasis by inhibiting food intake.

It should be noted that, in similar manners to leptin, circulating levels of insulin are also positively correlated with body fat mass and the insulin receptors are widely expressed within the brain, including the ARC^{POMC} and ARC^{AgRP} neurons (Marks et al., 1990), suggesting insulin’s

effects in the food intake and body weight might also be mediated by the neural melanocortin system. Indeed, administration of insulin into the third cerebral ventricle of fasted rats increases expression of POMC mRNA whereas the reduction in food intake caused by third-ventricular insulin administration is prevented by a subthreshold dose of the melanocortin antagonist SHU9119 (Benoit et al., 2002). An elegant study by Qiu *et al.* further showed that insulin depolarizes ARC^{POMC} neurons via activation of transient receptor 5 potential channels expressed in the same neuronal populations whereas insulin hyperpolarizes and inhibites ARC^{AgRP} neurons via activation of K_{ATP} channels (Qiu et al., 2014). However, complexity of insulin signaling at the POMC neurons comes from data demonstrating that, genetically modified mice lacking insulin receptor substrate 2, a major mediator of the metabolic effects of insulin in the ARC^{POMC} neurons, manifest lean phenotype (Choudhury et al., 2005), and insulin actually hyperpolarizes ARC^{POMC} neurons with decreased neuronal firing rate (Plum et al., 2006). These results suggest that the anorexigenic effects of insulin are unlikely to be mediated through ARC^{POMC} neurons. Therefore, despite the widely known appetite-suppressive effect of insulin when administered to the CNS, the physiological significance of such action remains to be investigated.

1.3.3.2 Acute peripheral factors

Ghrelin, a 28-amino acid peptide released from gastrointestinal tract, is the only peripheral orexigenic hormone exerting effects upon the CNS. It is well established that ghrelin promotes a positive energy balance (increased food intake and decreased energy expenditure) and an increased adiposity gain in humans. In addition, ghrelin plays a physiological role in initiating food consumption since circulating levels of ghrelin rise during fasting and before meals and fall postprandially (reviewed in (Gil-Campos et al., 2006)).

The functional relevance of ghrelin and its relationship to the melanocortin system has been demonstrated through anatomic, electrophysiological, and pharmacological studies. It has been shown that ghrelin fibers form axo-somatic and axo-dendritic contact with both ARC^{POMC} and $ARC^{NPY/AGRP}$ neurons (Cowley et al., 2003) and ghrelin receptor that mediates the physiological functions of ghrelin is widely expressed in the hypothalamus, pituitary, and of particular note, the ventral $ARC^{NPY/AGRP}$ neurons (Howard et al., 1996; Willesen et al., 1999). In addition, electrophysiological studies demonstrated that ghrelin depolarizes ARC^{AgRP} neurons, and simultaneously hyperpolarizes the ARC^{POMC} neurons by increasing the GABAergic inhibitory postsynaptic currents onto ARC^{POMC} neurons (Cowley et al., 2003). A direct inhibition of firing of ARC^{POMC} neurons by ghrelin has been also observed (Riediger et al., 2003). Furthermore, both acute and chronic peripheral administration of ghrelin in rodents result in increased AgRP and NPY mRNA levels in the ARC (Asakawa et al., 2001; Kamegai et al., 2001). In addition, mice lacking Agouti, AGRP, and MC3R/MC4R compared to wild-type (WT) control, all show an attenuated feeding response following peripheral ghrelin administration, indicating that central melanocortin system plays a crucial role in mediating the orexigenic actions of ghrelin (Ellacott et al., 2006). Collectively, these data suggest that ghrelin opposes the action to leptin on the ARC^{POMC} and $ARC^{NPY/AGRP}$ neuronal network and the downstream melanocortin system.

CCK, a peptide hormone released from the gut, is a satiety-inducing peptide in response to food intake. Vagal afferent neurons, where the type 1 CCK receptor (CCK1R) is expressed, are the primary targets of CCK. Activation of CCK1R promotes the brainstem-mediated cessation of feeding by inducing bile acid and pancreatic digestive enzyme production, as well as inhibiting gastric acid secretion and gastric emptying (Ellacott et al., 2006). The anorexigenic effect of CKK is further supported by the evidence that a potent CCK1R antagonist L364718 attenuates

the reduction in food intake induced by exogenous CCK octapeptide in food-deprived rats (Hewson et al., 1988) and abnormal processing of CCK1R gene yielding a predominant product with an absent third exon to encode a nonfunctional receptor results in obesity in humans (Miller et al., 1995).

As mentioned above, the important role of leptin-regulated melanocortin circuit plays in the regulation of food intake and energy expenditure has been well established and leptin acts directly on the POMC neurons in nucleus tractus solitaries (NTS), a region known to receive inputs from the vagus and to be important in mediating the effects of satiety. It should be noted that CCK also controls the expression of receptors and peptide neurotransmitters by vagal afferent neurons, whose actions are potentiated by leptin, suggesting the important role of the central melanocortin system in mediating the effects of CCK. Indeed, using transgenic mice that express enhanced green fluorescent protein in the NTS POMC neurons, Fan *et al.* showed that intraperitoneal injection of the sulfated 8-amino-acid form of CCK (CCK-8s) activates NTS POMC neurons (Fan et al., 2004). In the same study, CCK-8s significantly reduced food intake in WT mice but not in the *Mc4r* knockout mice and central injection of the MC4R antagonist SHU9119 into either the third or fourth ventricle partially or completely attenuates the CKK-8s-induced inhibition of food intake, respectively (Fan et al., 2004), suggesting activation of the neural MC4R is required for CCK-induced suppression of feeding. Overall, the melanocortin system mediates the CCK satiety response, although the functional relationship between the distinct ARC and NTS neurons in this process remains to be investigated.

PYY, a 36 amino acid peptide with N-terminal tyrosine and C-terminal tyrosine amide, is secreted by enteroendocrine L cells in the ileum and colon in response of food intake (Bottcher et al., 1993). Two endogenous forms of PYY, $PYY_{1–36}$ and $PYY_{3–36}$, are released into the plasma

postprandially in response to a meal. In the circulation, $PYY_{3–36}$ is the predominant form, with approximately 40% of $PYY_{1–36}$ been cleaved by dipeptidyl peptidase-IV to produce $PYY_{3–36}$ (Grandt et al., 1994). The physiological functions of the PYY molecules are mediated through multiple G protein-coupled NPY receptors (Y1-Y5 receptors). While $PYY_{1–36}$ binds Y1, Y2 and Y5 receptors, $PYY_{3–36}$ preferentially binds to the Y2 receptor, an inhibitory presynaptic receptor highly expressed in the $ARC^{NPY/AgRP}$ neurons (Keire et al., 2000). Interestingly, central administration of PYY_{1-36} or $PYY_{3–36}$ is orexigenic, whereas peripheral administration has been shown to reduce food intake in a number of rodent models (Ellacott et al., 2006). Results from clinical trials demonstrated that continuous intravenous infusion of $PYY_{3–36}$ reduces food intake and hunger scores in small number of healthy and obese human individuals for 24 h (Batterham et al., 2003).

Several studies suggested that the anorexigenic effects of $PYY_{3–36}$ could be mediated by the central melanocortin system either directly through Y2 receptors on ARC^{POMC} neurons or indirectly through Y2 receptors on $ARC^{NPY/AgRP}$ neurons. Batterham *et al.* and Challis *et al.* demonstrated that peripheral administration of PYY_{3-36} upregulates POMC mRNA expression, increases c-FOS immunoreactivity within ARC^{POMC} neurons, and depolarizes ARC^{POMC} neurons by decreasing the inhibitory GABAergic inputs onto ARC^{POMC} neurons (Batterham et al., 2003; Challis et al., 2003). In a hypothalamic explant study, pretreatment with a Y2 receptor specific agonist significantly induces the release of the endogenous MC4R agonist α-MSH (Batterham et al., 2003). Furthermore, AgRP, the important component of the central melanocortin system, have also been suggested to be regulated by the PYY_{3-36}. Using a conditional Y2 receptor knockout model, Sainsbury *et al.* showed that hypothalamus-specific Y2 receptor-deleted mice have a significantly decreased body weight and increased food intake that is associated with

increased NPY and AgRP as well as decreased POMC and CART mRNA levels in the ARC (Sainsbury et al., 2002).

1.4 The melanocortin-4 receptor

1.4.1 Molecular cloning and tissue distribution of MC4R

The human MC4R (hMC4R) was independently cloned by the groups of Gantz and Cone through degenerate PCR and homology screening (Gantz et al., 1993; Mountjoy et al., 1994). The human *MC4R* gene, localized at chromosome 18q21.3, is an intronless gene with an open reading frame of 999 bp that encodes a protein of 332 amino acids. The MC4R shares the highest homology with the MC3R, with 58% identity and 76% similarity (reviewed in (Tao, 2010)).

Following the cloning of MC4R in rodent and human, the MC4R was cloned from mouse, rat, hamster, guinea pig, dog, cat, fox, pig, sheep, cow, and several primates including marmoset, cynomolgus macaque, vervet monkey, and orangutan, as well as several nonmammalian species including fish, chicken, and pigeon. Comparison of MC4R sequences from many different species showed that the amino acid sequences between the different species are highly conserved, with the identity ranging from 93% between rat and human MC4Rs to 71% between zebrafish and human MC4Rs (reviewed in (Tao, 2010)). However, evolutional analysis of MC4R sequences from many species demonstrated that the MC4R has been subject to high levels of continuous purifying selection with codon usage bias, resulting in the extremely low levels of silent polymorphisms in humans.

To date, extensive localization studies in rats showed that the MC4R mRNA is widely expressed in adult rat brain, including cortex, hippocampus, amygdala, septal region, corpus striatum, thalamus, hypothalamus, brainstem, and spinal cord (reviewed in (Siljee-Wong, 2011)).

In the hypothalamus, it is highly expressed in the PVN, including both parvicellular and magnocellular neurons.

In addition to neuronal distribution, the MC4R mRNA is also expressed in several peripheral tissues during the fetal period, including the developing heart, lung, kidney, and testis (Mountjoy et al., 2003). However, the potential physiological functions of the MC4R in these organs are still controversial and remain to be fully elucidated.

1.4.2 MC4R in energy homeostasis

Although early rodent studies demonstrated that ICV injection of α-MSH and ACTH suppresses food intake in rats (Poggioli et al., 1986; Vergoni et al., 1986), it was not until the molecular cloning of the MCRs that researchers began to realize the fundamental role of MC4R in regulating food intake and energy expenditure. In 1997, Fan *et al.* demonstrated that ICV administration of melanotan II (MTII), a superpotent and cyclic α-MSH analog, inhibits feeding behavior in four hyperphagic mouse models including *ob*/*ob*, A^y, fasted C57BL/6J, and NPY-treated mice, whereas coadministration SHU9119, a high-affinity cyclic antagonist of MC3R and MC4R, completely blocks this inhibition (Fan et al., 1997). In the same study, mice with SHU9119 injection alone have increased food intake (Fan et al., 1997). Administration of MTII or SHU9119 directly into the PVN accomplishes even more potent alterations in food intake, indicating that neurons in the PVN, which express very high levels of the MC4R, are predominant sites of action in melanocortin-induced inhibition of feeding behavior (Giraudo et al., 1998). In addition, ICV infusion of more specific synthesized MC4R antagonists, HS014 and HS024, results in increased food intake and body weight in rats (Kask et al., 1998; Vergoni et al., 2000), further supporting the critical role of MC4R in the regulation of feeding behavior.

In 1997, the construction of the *Mc4r* knockout mouse model by Huszar *et al.* provided the definitive evidence that MC4R plays an important role in regulating energy homeostasis in mice. The homozygous knockout mice develop a maturity onset obesity syndrome associated with hyperphagia, increased linear growth, hyperinsulinemia, and hyperglycemia, whereas the heterozygous mice have intermediate body weights compared with the WT littermates and homozygous mice, suggesting a gene dosage effect (Huszar et al., 1997). In addition to hyperphagia, the *Mc4r* deleted mice also have decreased energy expenditure. Using elegantly modified transgenic mice, Balthasar *et al.* demonstrated that alternation in food intake and energy expenditure account for 60% and 40% of the effect of the MC4R on energy balance, respectively (Balthasar et al., 2005). In young mice with similar body weights, the *Mc4r* deleted mice consume less oxygen than WT control, and pair feeding of the *Mc4r* deleted mice result in more weight gain than the WT littermates (Ste Marie et al., 2000).

Another important discovery in the year of 1997 regarding to the MC4R function in energy homeostasis is the cloning of human *AgRP* gene by several laboratories simultaneously (Fong et al., 1997; Graham et al., 1997; Ollmann et al., 1997). AgRP was initially identified as a neutral antagonist for the MC4R, when bound to the MC4R, could sterically block subsequent binding of agonist to the receptor without affecting receptor activity by itself. However, ensuing studies showed that it is in fact an inverse agonist for human and rodent MC4Rs decreasing basal signaling of WT or constitutively active mutant receptors (Chai et al., 2003; Haskell-Luevano and Monck, 2001; Nijenhuis et al., 2001).

The orexigenic role of AgRP has been demonstrated by extensive genetic and pharmacological studies (reviewed in (Ilnytska and Argyropoulos, 2008)). An elegant study by Ollmann *et al.* demonstrated that AgRP mRNA levels in *ob/ob* and *db/db* mice are increased at

least 8 folds and transgenic overexpression of AgRP in mice results in obesity (Ollmann et al., 1997). In addition, human genetic studies showed that single nucleotide polymorphisms in AgRP such as A67T are associated with anorexia nervosa and leanness, suggesting a protective role against obesity (Marks et al., 2004; Vink et al., 2001). However, the underlying mechanism for this protection remains to be fully elucidated. Pharmacologically, ICV administration of AgRP(83-132), an amidated carboxyl-terminal fragment of AgRP retaining the biological activity of full-length AgRP, into rats increases food intake with long lasting effect and blocks the inhibitory effect of α–MSH (Rossi et al., 1998). AgRP also reverses leptin-induced inhibition of food intake and body weight in a dose-dependent manner (Ebihara et al., 1999). Subsequent studies demonstrated that the PVN might be the primary site of action in AgRP-mediated stimulation of feeding behavior since much lower doses of AgRP are needed to induce food intake when directly injected into the PVN compared to other area (Wirth and Giraudo, 2000).

It should be noted that the important role of leptin-regulated melanocortin circuit in energy homeostasis in rodents and humans is also highlighted by the fact that defects in multiple molecules in this circuit lead to obesity, as evidenced by the phenotypes manifested in multiple rodent models including *ob/ob* mice, *db/db* mice and Zucker *fatty* rats, *Pomc* knockout mice, *fat/fat* mice, *Agrp*-overexpressing mice, and *Mc4r* knockout mice, as well as phenotypes observed in humans harboring *leptin*, *leptin receptor*, *POMC*, *PC1*, and *MC4R* mutations (reviewed in (Tao, 2010)).

1.4.3 *MC4R* mutations in obesity pathogenesis

Since the first two frameshift mutations in the *MC4R* were independently reported by Vaisse *et al.* and Yeo *et al.* (Vaisse et al., 1998; Yeo et al., 1998), extensive clinical studies have

been performed attempting to identify novel *MC4R* mutations in different obese patient cohorts. To date, mutation in the *MC4R* is the most prevalent form of monogenic obesity, with more than 170 naturally occurring mutations been identified. These mutations include at least 142 non-synonymous, 13 frameshift, 3 deletions, 8 nonsense mutations (Hinney et al., 2013), which are scattered throughout the MC4R. More than 118 residues are mutated, covering 36% of the whole receptor.

In vitro functional characterization is crucial and a prerequisite to determine whether a mutation causes the disease or not. Depending on the functional defects, mutants can be divided into five classes according to a classification scheme we proposed earlier (Tao, 2005, 2006; Tao and Segaloff, 2003). Class I mutants are defective in receptor biosynthesis and/or have accelerated protein degradation; Class II mutants are synthesized but trapped intracellularly, primarily by endoplasmic reticulum quality control system, although some mutants may be trapped in the Golgi apparatus; Class III mutants are defective in ligand binding; Class IV mutants are signaling defective; and Class V mutants display normal function.

Extensive functional studies have demonstrated that the majority of loss of function *MC4R* mutations belong to Class II (reviewed in (Hinney et al., 2013; Tao, 2009)). As summarized in Tables 1-3, a total of 79 Class II mutations have been reported, accounting for almost 45% of all naturally occurring human *MC4R* mutations identified to date. Different dysfunctional severity is observed, with some mutants exhibiting total loss of function (Table 1), some severely dysfunctional (Table 2), and some mildly dysfunctional or normal (Table 3).

1.4.3.1 Class II MC4R mutants that are nonfunctional

Nonsense and frameshift mutations are expected to have catastrophic impact on protein

sequence, likely resulting in a complete dysfunctional protein. Indeed, five nonsense and six frameshift Class II *MC4R* mutations have been reported (Table 1). The first *MC4R* pathogenic mutations, 211del CTCT and 244ins GATT, were reported by two groups simultaneously (Vaisse et al., 1998; Yeo et al., 1998) and later were characterized as producing receptors that are totally intracellularly retained with complete loss of function (Ho and MacKenzie, 1999; Yeo et al., 2003). Mutation 211del CTCT was identified in a four-year-old child with >99th centile BMI and a history of hyperphagia (Yeo et al., 1998). His father heterozygous for this mutation is also extremely obese with a BMI of 41 kg/m^2 (Yeo et al., 1998). The other frameshift mutation, 244ins GATT, was found in a 35-year-old woman with 65% total body fat and a BMI of 30 kg/m^2 at age 20 (Vaisse et al., 1998). Her mother, her sister and one of her nieces have a very similar weight history (Vaisse et al., 1998). The most frequent nonfunctional *MC4R* mutation to date, Y35X, was found to have a frequency as high as 0.6% in severely obese German and Danish populations (Lubrano-Berthelier et al., 2003).

Given the critical role of MC4R in the control of food intake and energy expenditure in humans, it is expected that mutations leading to complete loss of function of MC4R would be associated with a more severe obesity phenotype compared to the WT or partially dysfunctional mutations. Indeed, a systematic mutation-screened study in 500 Caucasians with severe childhood obesity showed that 23 subjects harboring nonfunctional mutant receptors are significantly more obese than the 22 individuals with partially functioning mutant receptors (Farooqi et al., 2003).

1.4.3.2 Class II MC4R mutants that are severely dysfunctional

As shown in Table 2, a total of 32 missense Class II *MC4R* mutations lead to severely

dysfunctional protein that retain some residual ligand binding and signaling capabilities. Since these mutations are scattered throughout the MC4R, the mechanism by which each mutation impairs the folding property and subsequent functionality still calls for further investigation. Up to now, numerous studies have been performed to characterize the functional phenotypes of MC4R mutants. It is clear from these studies that, with several exceptions that are discussed later, the intracellular retention of MC4R mutants is variable but strongly correlates with the impairment of their cAMP signaling. Interestingly, one screening study for novel *MC4R* mutations found that the decrease in cell surface expression of the mutants seems to correlate with the age of obesity onset (Lubrano-Berthelier et al., 2003).

1.4.3.3 Class II MC4R mutants that are mildly dysfunctional or normal

Some Class II MC4R mutants have mildly reduced or even normal function (Table 3). They interrupt the protein folding and stability while do not affect significantly the capability of the protein to bind to the ligand nor to induce the downstream cAMP signaling. For example, L54P and I69T were identified in a large Genetics of Obesity Study consisting of 2000 early-onset severely obese patients. L54P was found in 8 years-old Turkish boy and I69T was detected in two white European boys (one was 9 years old and the other was 13 years old) (Tan et al., 2009). All the carriers have a BMI above the 98th percentile (Tan et al., 2009). Detailed functional analysis demonstrated that both L54P and I69T have decreased cell surface expression but retain normal ligand binding and cAMP generation (Tan et al., 2009). There are two possibilities that may explain why these mutants have reduced plasma density but still retain relatively normal function: i) some mutants have improved ligand binding affinities and/or signaling potencies (*e.g.*, H76R and D146N); ii) spare receptors may exist in the *in vitro* system, in which full

response is elicited by agonists at a concentration that does not require full occupancy of the receptor (Tao, 2005). However, spare receptors identified from *in vitro* system are unlikely to exist *in vivo*, raising caution in the interpretation of *in vitro* data.

The relatively normal functional property of these mutants is not consistent with their potential role in obesity pathogenesis. However, whether these mutations impair other aspects of MC4R function, such as ERK1/2 signaling pathway (He and Tao, 2014), remains to be investigated.

1.5 Therapeutic strategies for rescuing misfolded *MC4R* mutations

1.5.1 Molecular chaperone promotes the folding of the MC4R

In the crowded cellular environment, the newly synthesized polypeptides are marginally stable and are at high risk of misfolding and aggregation, potentially resulting in deleterious consequences to the cell. Therefore, a network of molecular chaperones that promote folding and prevent aggregation are employed by the cell to avoid this undesired outcome. Molecular chaperones, by definition, are proteins that interact with, stabilize or aid another protein to achieve its functionally active conformation, without being present in its final structure (Hartl et al., 2011). They are critical for maintaining protein homeostasis, a process that integrates signals and regulates flux from protein synthesis through protein folding, misfolding, and degradation. Several classes of molecular chaperones have been identified in the cells, such as heat shock proteins (HSP40, HSP60, HSP70, HSP90, HSP100 and the small HSPs), calnexin and calreticulin, protein disulfide isomerase, and other client-specific chaperones (reviewed in (Tao and Conn, 2014)).

Melanocortin-2 receptor (MC2R) accessory proteins (MRAPs), including MRAP and MRAP2, have been demonstrated to be essential for the MC2R trafficking and function (Chan et al., 2009; Metherell et al., 2005; Sebag and Hinkle, 2007), serving as MC2R specific molecular chaperones. Indeed, the identification of MRAPs provides a molecular explanation for the difficulties encountered in the expression of the MC2R in nonadrenal cell lines (Noon et al., 2002). In contrast, MRAPs reduce MC4R surface expression and responsiveness to NDP-MSH in CHO cells cotransfected with MRAPs and MC4R (Chan et al., 2009). The two isoforms of MRAP2 in zebrafish appear to have different effects on MC4R function. Interaction of MRAP2a with MC4R results in reduced affinity of the MC4R to bind with α-MSH whereas interaction of MRAP2b with MC4R leads to inhibited receptor constitutive activity but increased potency of α-MSH (Sebag et al., 2013). Furthermore, the physiological relevance of MRAP2 interaction with MC4R was recently demonstrated. Majzoub, Farooqi and colleagues showed that transgenic mice with whole body deletion and brain-specific targeted deletion of the *Mrap2* gene develop severe obesity at a young age (Asai et al., 2013). In the same study, rare heterozygous mutations in *MRAP2* are associated with early-onset severe obesity in humans (Asai et al., 2013). However, the molecular basis of the interaction between MRAPs and MC4R, as well as the mechanisms by which MRAP2 exerts its effects on body weight regulation remain to be investigated.

An elegant study by Chapple and colleagues demonstrated that cytosolic chaperone system can functionally rescue intracellularly retained mutant MC4Rs by promoting their folding (Meimaridou et al., 2011). In that study, three naturally occurring *MC4R* mutations, S58C, P78L, and D90N, are demonstrated to have decreased cell surface expression and to be retained in the ER due to misfolding (Meimaridou et al., 2011). Cytosolic cognate 70-kDa heat-shock protein (Hsc70) interacts with MC4R and promotes the anterograde trafficking of mutant receptors,

resulting in increased NDP-MSH-stimulated cAMP production (Meimaridou et al., 2011). Hsc70 also increases the folding of ER-retained MC4Rs with enhanced diffusional mobility in ER membranes, whereas coexpression with HSJ1b, a cochaperone that increases the degradation of Hsc70 clients, decreases the cellular expression levels of MC4R (Meimaridou et al., 2011). In addition, Hsp90 is shown to collaborate with Hsp70 in the cellular processing of MC4Rs, as evidenced by the observation that inhibition of endogenous Hsp90 by geldanamycin reduces cellular levels of MC4R whereas stimulation of the ATPase activity of Hsp90 by enhancing the expression of cochaperone Aha1 increases the cellular levels of MC4R (Meimaridou et al., 2011). It should be noted that in addition to the intracellularly retained *MC4R* mutants, the cytosolic Hsp70/Hsp90 chaperone system can also increase the cell surface expression and function of WT MC4R (Meimaridou et al., 2011), consistent with previous findings that WT MC4R is not optimally folded (Fan and Tao, 2009). Therefore, this chaperone system might represent a potential therapeutic strategy for treating obese patients without *MC4R* mutations.

1.5.2 Chemical chaperone rescues misfolded MC4Rs

Chemical chaperones are small and low molecular weight molecules that non-selectively enhance protein stability and folding. Multiple chemical chaperones have been identified and broadly divided into two groups, osmolytes and hydrophobic chaperones (reviewed in (Cortez and Sim, 2014; Papp and Csermely, 2006)). The mechanisms by which they promote protein folding vary. Osmolytes such as glycerol can indirectly protect the partially folded intermediates from aggregation by sequestering the hydrophobic residues from polar solvent (Vagenende et al., 2009), whereas hydrophobic chaperones such as sodium 4-phenylbutyrate (4-PBA) are able to aid protein folding by binding to the exposed hydrophobic segments of the unfolded or misfolded

protein and/or inducing the synthesis of endogenous molecular chaperones (Papp and Csermely, 2006).

Following the demonstration that chemical chaperones can rescue mutant proteins from aggregation or facilitate them to escape from quality control and subsequent degradation (Burrows et al., 2000; Cheong et al., 2007; Robben et al., 2006; Rubenstein et al., 1997; Uversky et al., 2001), the group of Baldini reported the first chemical chaperone with potential rescuing effect on the MC4R (Granell et al., 2010). In that study, PBA partially increases the cell surface expression of WT and three intracellularly retained mutant MC4Rs (P78L, I316S, and I317T) and the rescued I316S MC4R at the cell surface responds to α-MSH stimulation with increased cAMP production (Granell et al., 2010). These rescuing effects are achieved by decreasing the misfolding of mutant receptors, as evidenced by increased proportion of cell surface I316S MC4R, reduced levels of ubiquitinated I316S MC4R, and suppressed mutant-induced ER stress (Granell et al., 2010). In another study performed by the same group, PBA exhibits similar rescuing effects on P272L MC4R, an intracellularly retained mutant that is associated with severe early-onset obesity (Granell et al., 2012). However, treatment with a ubiquitin activating enzyme inhibitor, UBE-41, that suppresses MC4R ubiquitination, rescues the cell surface expression of MC4R P272L more efficiently compared to the treatment with PBA that promotes MC4R folding (Granell et al., 2012). Moreover, the effects of PBA and UBE-41 are additive (Granell et al., 2012), indicating that PBA and UBE-41 affect MC4R exit from the ER by targeting steps that are, at least in part, independent of each other. These results suggest that strategies aiming at the folding and/or ubiquitination step of intracellularly trapped MC4Rs by using chemical chaperones and/or by E1 inhibitor might represent a novel approach for personalized treatment of specific form of obesity.

However, despite encouraging results in some disease models (Inden et al., 2007; Wiley et al., 2011), the clinical utility of chemical chaperones is still questionable due to their lack of specificity, high concentration required, and issues related to the intolerable toxicity.

1.5.3 Pharmacoperone stabilizes misfolded MC4Rs

1.5.3.1 Pharmacoperones for protein misfolding diseases

After the discovery of chemical chaperones that nonspecifically stabilize misfolded proteins, Loo and Clarke initially found that substrates or modulators of P-glycoprotein specifically rescue mutant P-glycoproteins within a few hours after addition of the substrate but do not rescue the ΔF508 cystic fibrosis transmembrane conductance regulator (CFTR) (Loo and Clarke, 1997). These substrates or modulators are now known as pharmacoperones, which are small hydrophobic compounds that enter the cell and specifically correct the folding and routing of misfolded proteins. Pharmacoperones stabilize the intramolecular structure and/or quaternary structure of multimeric proteins and the rescue may occur cotranslationally or, in most cases, posttranslationally (Arakawa et al., 2006; Leidenheimer and Ryder, 2014). Pharmacoperones are commonly identified from substrates and inhibitors of enzymes or ligands of receptors and ion channels. They may rescue misfolded proteins in most cellular compartments, especially in the mitochondrion, lysosome, and ER where proteins suffer unusual stress (Loo and Clarke, 2007; Ringe and Petsko, 2009).

Up to now, diverse pharmacoperones have been developed and pharmacoperone therapy has been proposed as a potential treatment for many human protein misfolding diseases. These include pharmacoperones of P53 (Bykov et al., 2002; Foster et al., 1999) and human telomerase reverse transcriptase (Kang et al., 2016) to treat cancer, pharmacoperones of HERG potassium

channel to treat long QT syndrome (Zhou et al., 1999), pharmacoperones of CFTR to treat cystic fibrosis (Sampson et al., 2011; Wainwright et al., 2015), pharmacoperones of phosphomannomutase 2 to treat congenital disorder of glycosylation (Yuste-Checa et al., 2017), and pharmacoperones of α-galactosidase A, β-glucosidase, and aspartylglucosaminidase to treat Fabry disease (Khanna et al., 2010; Yam et al., 2006), Gaucher disease (de la Mata et al., 2015; Lieberman et al., 2007), and aspartylglucosaminuria (Banning et al., 2016), respectively. Most importantly, clinical trials of several pharmacoperones have been successfully conducted and pharmacoperone therapy is now considered as a promising alternative to gene therapy and enzyme replacement therapy (Clancy et al., 2012; Giugliani et al., 2013; Hughes et al., 2017; Warnock et al., 2015; Zimran et al., 2013).

In the case of GPCRs, Morello *et al.* were the first to use nonpeptidic antagonists to restore the expression of mutant arginine vasopressin V_2 receptors (AVPR2) (Morello et al., 2000). The first clinical trial of pharmacoperones for GPCRs was also done on this receptor in nephrogenic diabetes insipidus (NDI) patients (Bernier et al., 2006). Five NDI patients each bearing one type of *AVPR2* mutations were treated with SR49059 for a short-term and their 24-hour urine volume and water intake are significantly decreased and urine osmolalities are increased (Bernier et al., 2006). Unfortunately, the trial of SR49059 was discontinued due to side effects (Los et al., 2010). Another AVPR2 antagonist OPC41061 (Tolvaptan) has been approved in the USA and Europe to treat hyponatraemia and heart failure with little side effects (Farmakis et al., 2008; Schrier et al., 2006). OPC41061 is a promising candidate as a pharmacoperone to be tested clinically for the treatment of NDI (Los et al., 2010).

A number of ligands have been identified as pharmacoperones for several other GPCRs, such as δ-opioid receptor (Petaja-Repo et al., 2002), rhodopsin (Noorwez et al., 2003),

gonadotropin-releasing hormone receptor (GnRHR) (Conn and Janovick, 2011), and LH receptor (Newton et al., 2011). While most pharmacoperones of GPCRs have been tested in cellular studies, one antagonist pharmacoperone therapy of IN3 has been successfully performed in knock-in mouse expressing a trafficking defective GnRHR mutant (Janovick et al., 2013). Pulsatile IN3 therapy rescues mutant GnRHR to the cell surface and restores spermatogenesis, proteins associated with steroid transport and steroidogenesis, and androgen levels (Janovick et al., 2013). Successful trials of pharmacoperones in humans and in animals demonstrate the therapeutic feasibility of pharmacoperones of GPCRs *in vivo*.

1.5.3.2 Antagonist pharmacoperones for the MC4R

We identified the first pharmacoperone for the MC4R, ML00253764, in 2009 (Fan and Tao, 2009; Tao, 2010). ML00253764 is a small molecule antagonist (Vos et al., 2004) and partial inverse agonist (Huang and Tao, 2012; Nicholson et al., 2006) of the MC4R that can cross the blood-brain barrier and act on MC4R *in vivo* after intraperitoneal injection (Nicholson et al., 2006; Vos et al., 2004). Since then, seven more antagonists have been developed as pharmacoperones for the MC4R, including MTHP, PPPone, MPCI, DCPMP, NBP, Ipsen 5i, and Ipsen 17 (Rene et al., 2010; Tao and Huang, 2014; Wang et al., 2014) (Fig. 1.2). In addition, four more compounds (identities not disclosed) have also been reported to have chaperoning activity on the MC4R (Ward et al., 2012), although the details have not been reported.

Antagonist-rescued proteins arrive at the plasma membrane in an antagonist-bound state, potentially preventing the receptor being activated by endogenous agonists. In general, it is relatively difficult for high-affinity antagonist pharmacoperones to dissociate from the target receptor whereas it is easier for low-affinity antagonist pharmacoperones to dissociate from the

target receptor. However, low-affinity antagonist pharmacoperones require a higher effective concentration, which is not practical for potential therapeutic applications. For example, NBP (*K*i, 2.4 nM) rescues several misfolded MC4R mutants but cannot restore their NDP-MSH responsiveness, possibly because of prolonged binding (Rene et al., 2010). DCPMP (*K*i, 0.02 μM) (Rene et al., 2010) can rescue most of the tested mutants but have a rescue EC_{50} around 10 μM whereas Ipsen 5i (*K*i, 2.0 nM) (Tao and Huang, 2014) and Ipsen 17 (*K*i, 0.96 nM) (Wang et al., 2014) have a rescue EC_{50} around 10 nM. In addition, Ipsen 5i and Ipsen 17 have relatively low functional antagonist potencies (77 nM and 44 nM respectively) (Poitout et al., 2007) and the signaling potency of α-MSH on Ipsen 17-treated MC4R is only 2-fold higher than that of the untreated WT (Wang et al., 2014). This indicates that Ipsen 5i and Ipsen 17 have a relatively rapid dissociation rate, allowing the binding of endogenous ligands.

Ipsen 5i (Tao and Huang, 2014) and Ipsen 17 (Wang et al., 2014) have broad rescue spectra rescuing 10 of 11 and 11 of 12 studied mutants, respectively. The signaling of fourteen rescued mutants are proportional to or greater than the increase in cell surface expression, suggesting that the primary defect of these mutants is misfolding resulting in detection by the cellular quality control system and intracellular retention but not ligand binding or signaling. These mutants retain intrinsic function and can become functional when coaxed to the cell surface.

1.5.3.3 One agonist pharmacoperone for the MC4R

In contrast to antagonist pharmacoperones, agonist pharmacoperones do not need to dissociate from the target receptor. THIQ is a small molecule potent agonist of the MC4R (EC_{50}, 2.1 nM) which shares part of the binding pocket with NDP-MSH (IC_{50}, 1.2 nM) and has several unique interaction determinants (Chen et al., 2007; Tao, 2010). THIQ shows good oral

bioavailability and can penetrate the blood-brain barrier (Chen et al., 2007). We show that THIQ is also a pharmacoperone of the MC4R promoting the proper folding and subsequent signaling of intracellularly retained mutant MC4Rs (Huang and Tao, 2014b). THIQ rescues the cell surface expression and signaling of 7 of 10 mutants studied in two physiologically relevant neuronal cell lines, Neuro2a and NIE-115, with a rescue EC_{50} varying from 10 nM to 1 μM depending on the mutants (Huang and Tao, 2014b). THIQ only rescues 3 mutants in the HEK293 cells, suggesting a more efficient chaperoning activity of THIQ in neuronal cells than in HEK293 cells (Huang and Tao, 2014b). However, such a difference between different cell lines is not obvious for Ipsen 5i (Tao and Huang, 2014) and ML00253764 (unpublished data). THIQ also increases the signaling of two mutants, P78L and P260Q, without increasing their cell surface expression (Huang and Tao, 2014b). The increased signaling might be due to signal amplification or THIQ might induce intracellular signaling. A similar observation has been reported on AVPR2: three cell-permeable agonists initiate intracellular signaling without promoting cell surface expression of mutant AVPR2s (Petaja-Repo et al., 2002).

Many GPCR agonists promote receptor desensitization, internalization, and/or block the recycling of internalized receptor (Lefkowitz, 2013; McDaniel et al., 2012; Mohammad et al., 2007). Indeed, prolonged treatment (24 h) of THIQ decreases the cell surface expression and signaling of WT MC4R by approximately 50% (Huang and Tao, 2014b). To avoid receptor desensitization and internalization, screening of allosteric modulators but not agonists or antagonists with better therapeutic potentials and less side effects will be particularly important (Huang and Tao, 2014b; Jaffe et al., 2013; Noorwez et al., 2008; Tao, 2014; Yang et al., 2015a).

1.5.3.4 Pharmacoperones for WT MC4R

It is well known that various WT GPCRs are not efficiently folded (see (Tao and Conn, 2014) for a comprehensive review). Pharmacoperones may promote the folding and trafficking of WT receptors and such observations have been reported in several GPCRs, such as δ-opioid receptor (Petaja-Repo et al., 2002) and GnRHR (Conn et al., 2007; Janovick et al., 2002). All the eight antagonist pharmacoperones of the MC4R described above increase the cell surface expression of the WT MC4R (Fan and Tao, 2009; Rene et al., 2010; Tao, 2010; Tao and Huang, 2014; Wang et al., 2014). Therefore, in addition to being a therapeutic avenue for obese patients harboring *MC4R* mutations, pharmacoperone therapy may also be used to treat obese patients without any *MC4R* mutation.

1.5.4 ER-targeted α-MSH stabilizes an active conformation of the MC4R

Recently, an interesting study has proposed an alternative approach to stabilize the active conformation of MC4R and rescue the cell surface targeting of misfolded mutants through intracellular delivery of the melanocortin peptide, α-MSH (Granell et al., 2013). A designed ER-targeted α-MSH interacts with MC4R in the ER and traffic together to the cell surface where it induces constant cAMP and AMP kinase signaling (Granell et al., 2013). MC4R in a complex with intracellular α-MSH exists in an active conformation that is resistant to desensitization, lysosome degradation, and AgRP antagonism (Granell et al., 2013). Binding of intracellular α-MSH changes the conformation of one misfolded MC4R mutant, I316S, and promote its cell surface expression and constant signaling (Granell et al., 2013). Chronic administration of MTII and other agonists of the MC4R causes tachyphylaxis possibly because of desensitization of the receptor and/or upregulation of anorexigenic hormones such as AgRP (Bluher et al., 2004;

Pierroz et al., 2002). Thus, development of novel small molecule or peptide agonists for intracellular targeting may constitute a therapeutic approach to promote persistent receptor signaling with resistance to desensitization.

Table 1.1 Functional properties of Class II MC4R mutants that are nonfunctional with no detectable ligand binding and/or signaling.

Class II mutation	Cell surface expression	Total expression	Binding	Signaling	Cell type	Reference
'G' ins at codon 16	ND	NA	NA	ND	HEK293	(Lubrano-Berthelier et al., 2006)
'A' ins at codon 112	ND[a]	NA	ND	ND	COS-7 &HEK293	(Yeo et al., 2003)
	NA	NA	NA	ND	HEK293	(Farooqi et al., 2003)
'CTCT' del at codon 211	ND[a]	—[a]	ND	ND	COS-7 &HEK293T	(Ho and MacKenzie, 1999)
	ND[a]	NA	ND	ND	COS-7 &HEK293	(Yeo et al., 2003)
	NA	NA	NA	ND	HEK293	(Farooqi et al., 2003)
'GATT' ins at codon 244	ND[a]	—[a]	ND	ND	COS-7 &HEK293T	(Ho and MacKenzie, 1999)
	ND	NA	NA	ND	HEK293	(Lubrano-Berthelier et al., 2006)
'GA' del at codon 251	~40%	—	ND	ND	HEK293	(Xiang et al., 2010)
	NA	NA	NA	ND	COS-7	(Hinney et al., 2003)
'GT' ins at codon 279	NA	NA	NA	ND	HEK293	(Farooqi et al., 2003)
Del170	~15%	~70%	ND	ND	HEK293T	(Wang and Tao, 2011)
W16X	ND[a]	NA	NA	ND	HEK293	(Bolze et al., 2013)
Y35X	~5%	—	>1[b]	ND	HEK293	(Xiang et al., 2006)
	NA	NA	ND	NA	HEK293	(Larsen et al., 2005)
I69M	~31%	NA	NA	ND	HEK293	(Lubrano-Berthelier et al., 2006)
I69R	~10%	—	ND	ND	HEK293T	(Wang and Tao, 2011)
P78L	~18%	—	>1[b]	ND	HEK293	(Xiang et al., 2006)
	~31%	NA	NA	ND	HEK293	(Lubrano-Berthelier et al., 2003)
	~0.9%	NA	ND	ND	HEK293	(Nijenhuis et al., 2003)
	↓[a]	—	ND	ND	HEK293	(Tao and Segaloff, 2003)
Y80X	ND	NA	NA	ND	HEK293	(Lubrano-Berthelier et al., 2006)
C84R	~10%	40%	ND	↓Rmax, ↑EC_{50}	HEK293	(Fan and Tao, 2009)
	NA	NA	NA	ND	COS-7	(Hainerova et al., 2007)
S94R	~45%	—	>1[b]	ND	HEK293	(Xiang et al., 2010)
	NA	NA	NA	ND	COS-7	(Hinney et al., 2003)
V95I	~2%	—	>1[b]	ND	HEK293	(Xiang et al., 2006)
	NA	NA	NA	ND	COS-7	(Hinney et al., 2003)
N97D	↓[a]	NA	↓B_{max}, ↑IC_{50}	ND	COS-7 &HEK293	(Yeo et al., 2003)
	NA	NA	NA	ND	HEK293	(Farooqi et al., 2003)
	~20%	—	↑IC_{50}	↑EC_{50}	HEK293	(Xiang et al., 2006)
G98R	~70%	—	>1[b]	ND	HEK293	(Xiang et al., 2010)

	↓[a]	—	NA	NA	HEK293	(Tao and Segaloff, 2003)
L106P	↓[a]	NA	↓B_{max}, ↑IC_{50}	ND	COS-7 &HEK293	(Yeo et al., 2003)
	NA	NA	NA	ND	HEK293	(Farooqi et al., 2003)
	~30%	—	—	↑EC_{50}	HEK293	(Xiang et al., 2006)
I125K	↓[a]	NA	↓B_{max}, ↑IC_{50}	ND	COS-7 &HEK293	(Yeo et al., 2003)
	2%	~60%	>1[b]	ND	HEK293	(Xiang et al., 2006)
S136P	~15%	~37%	↓B_{max}, ↑IC_{50}	ND	HEK293	(Tan et al., 2009)
C172R	ND	NA	ND	↓Rmax, ↑EC_{50}	HEK293	(Hohenadel et al., 2014)
W174C	~30%	—	>1[b]	ND	HEK293	(Xiang et al., 2010)
	~10%	40%	ND	↓Rmax, ↑EC_{50}	HEK293	(Fan and Tao, 2009)
G181D	~30%	—	>1[b]	ND	HEK293	(Xiang et al., 2010)
	NA	NA	NA	ND	COS-7	(Hinney et al., 2003)
	NA	NA	ND	NA	HEK293	(Larsen et al., 2005)
I194T	~15%	—	ND	ND	HEK293T	(Wang and Tao, 2011)
P260Q	~25%	—	ND	ND	HEK293T	(Wang and Tao, 2011)
	↓[a]	NA	NA	↓Rmax	COS-7	(Beckers et al., 2010)
	NA	NA	NA	↓Rmax	HEK293	(Stutzmann et al., 2008)
I269N	~50%	70%	↓B_{max}	ND	HEK293	(Tan et al., 2009)
	~40%	NA	↓B_{max}	—	HEK293	(Hohenadel et al., 2014)
C271Y	ND[a]	NA	ND	ND	COS-7 &HEK293	(Yeo et al., 2003)
	~20%	—	—	↑EC_{50}	HEK293	(Xiang et al., 2006)
	~38%	NA	NA	NA	HEK293	(Lubrano-Berthelier et al., 2003)
	↓[a]	—	ND	ND	HEK293	(Tao and Segaloff, 2003)
	NA	NA	NA	ND	HEK293	(Farooqi et al., 2003)
Y287X	ND	NA	ND	ND	COS-7 &HEK293	(Yeo et al., 2003)
	~25%	—	>1[b]	↑EC_{50}	HEK293	(Xiang et al., 2006)
	NA	NA	NA	ND	HEK293	(Farooqi et al., 2003)
P299H	~25%	—	>1[b]	ND	HEK293	(Xiang et al., 2006)
	~18%	NA	NA	ND	HEK293	(Lubrano-Berthelier et al., 2003)
	NA	NA	ND	ND	CHO	(Roubert et al., 2010)
P299L	~30%	—	>1[b]	ND	HEK293	(Xiang et al., 2010)
Q307X	~20%	—	ND	ND	HEK293T	(Wang and Tao, 2011)
	~31%	—	ND	ND	HEK293	(Santoro et al., 2009)

↓: denotes significantly decreased, ↑: denotes significantly increased, —: denotes no significant change, ND: not detectable, NA: not assessed.

[a] Indicates that the receptor expression was measured by confocal microscopy or surface enzyme-linked immunosorbent assay.

[b] Indicates that the IC_{50} could not be determined up to 1 μM concentrations or no competitive displacement binding of NDP-MSH was observed.

Table 1.2 Functional properties of Class II MC4R mutants that are severely dysfunctional but retain some residual ligand binding and signaling capabilities.

Class II mutation	Cell surface expression	Total expression	Binding	Signaling	Cell type	Reference
R7C	~40%	~70%	—	↑EC_{50}	HEK293	(Fan and Tao, 2009)
S58C	~30%	—	—	↑EC_{50}	HEK293	(Xiang et al., 2006)
	~50%	NA	NA	↓Rmax, ↑EC_{50}	HEK293	(Lubrano-Berthelier et al., 2003)
	↓[a]	—	↓B_{max}	—	HEK293	(Tao and Segaloff, 2003)
	NA	NA	—	↓Rmax, ↑EC_{50}	CHO	(Roubert et al., 2010)
E61K	~50%	—	>1[b]	↓Rmax, ↑EC_{50}	HEK293	(Xiang et al., 2010)
	~25%	~72%	↓B_{max}, ↑IC_{50}	↓Rmax	HEK293	(Tan et al., 2009)
	NA	NA	NA	↓Rmax	HEK293	(Calton et al., 2009)
N62S	↓[a]	NA	↓B_{max}, ↑IC_{50}	↓Rmax, ↑EC_{50}	COS-7 &HEK293	(Yeo et al., 2003)
	~10%	—	>1[b]	↑EC_{50}	HEK293	(Xiang et al., 2006)
	ND[a]	—	↓B_{max}	↓Rmax	HEK293	(Tao and Segaloff, 2003)
N72K	~3%	—	NA	↓Rmax, ↑EC_{50}	HEK293	(Delhanty et al., 2014)
D90N	~78%	—	NA	ND	COS-7	(Biebermann et al., 2003)
	~60%	—	—	↓Rmax, ↑EC_{50}	HEK293	(Xiang et al., 2010)
S94N	~50%	~70%	↓B_{max}	—	HEK293T	(Wang and Tao, 2011)
	NA	NA	NA	↓Rmax	HEK293	(Stutzmann et al., 2008)
I102S	~57%	NA	NA	ND	HEK293	(Lubrano-Berthelier et al., 2003)
	~8%	—	—	↑EC_{50}	HEK293	(Xiang et al., 2006)
	—[a]	NA	ND	↓Rmax, ↑EC_{50}	HEK293	(Tao and Segaloff, 2005)
	NA	NA	↓B_{max}, ↑IC_{50}	↓Rmax, ↑EC_{50}	CHO	(Roubert et al., 2010)
I121T	~45%	—	↑IC_{50}	↑EC_{50}	HEK293	(Xiang et al., 2010)
	NA	NA	NA	↑EC_{50}	COS-7	(Hinney et al., 2003)
S127L	~45%	—	↓B_{max}	↓Rmax	HEK293	(Fan and Tao, 2009)
	—	NA	NA	↑EC_{50}	HEK293	(Lubrano-Berthelier et al., 2003)
	—[a]	NA	NA	↓Rmax, ↑EC_{50}	HEK293T	(Valli-Jaakola et al., 2004)
	NA	NA	↑IC_{50}	↑EC_{50}	CHO	(Roubert et al., 2010)
I137T	~30%	NA	↓B_{max}	↑EC_{50}	HEK293	(Nijenhuis et al., 2003)
	NA	NA	—	↑EC_{50}	HEK293	(Xiang et al., 2006)
T150I	~60%	—	—	↑EC_{50}	HEK293	(Xiang et al., 2006)
	—	NA	—	↓Rmax, ↑EC_{50}	HEK293	(Lubrano-Berthelier et al., 2006)
	—	—	↓B_{max}	↓Rmax, ↑EC_{50}	HEK293	(Vaisse et al., 2000)
Y157S	~30%	—	—	↓Rmax, ↑EC_{50}	HEK293	(Xiang et al., 2010)

	↓[a]	—	↓B_{max}	↓Rmax	HEK293	(Tao and Segaloff, 2003)
	NA	NA	NA	↓Rmax, ↑EC_{50}	HEK293	(Lee et al., 2008)
M161T	~35%	~95%	↓B_{max}, ↑IC_{50}	↓Rmax	HEK293	(Tan et al., 2009)
	~20%	—	ND	↓Rmax, ↑EC_{50}	HEK293	Unpublished data
T162I	~20%	67%	—	↓Rmax	HEK293	(Tan et al., 2009)
R165G	~10%	NA	↓B_{max}	—	HEK293	(Hohenadel et al., 2014)
R165Q	~25%	—	—	↑EC_{50}	HEK293	(Xiang et al., 2006)
	~7.5%	NA	↓B_{max}	↓Rmax	HEK293	(Nijenhuis et al., 2003)
	~7%	NA	↓B_{max}	—	HEK293	(Hohenadel et al., 2014)
	NA	NA	NA	↓Rmax, ↑EC_{50}	HEK293	(Farooqi et al., 2003)
R165W	~26%	NA	NA	ND	HEK293	(Lubrano-Berthelier et al., 2006)
	~20%	—	—	↑EC_{50}	HEK293	(Xiang et al., 2006)
	~9.4%	NA	↓B_{max}	↓Rmax	HEK293	(Nijenhuis et al., 2003)
I170V	~45%	NA	↓B_{max}	↓Rmax	HEK293	(Nijenhuis et al., 2003)
	~84%	NA	NA	↑EC_{50}	HEK293	(Lubrano-Berthelier et al., 2006)
P230L	~40%	—	↓B_{max}	↑EC_{50}	HEK293	(Fan and Tao, 2009)
L250Q	~65%	NA	NA	↓Rmax	HEK293	(Lubrano-Berthelier et al., 2006)
	~50%	—	↓IC_{50}	↑EC_{50}	HEK293	(Xiang et al., 2006)
	~16%	NA	↓B_{max}, ↓IC_{50}	↓Rmax	HEK293	(Nijenhuis et al., 2003)
G252S	~60%	—	—	↑EC_{50}	HEK293	(Xiang et al., 2006)
	~96%	NA	NA	↑EC_{50}	HEK293	(Lubrano-Berthelier et al., 2006)
	NA	NA	↓B_{max}, ↑IC_{50}	↑EC_{50}	CHO	(Roubert et al., 2010)
F261S	~20%	—	↓B_{max}	↓Rmax	HEK293	(Fan and Tao, 2009)
	↓[a]	NA	NA	↓Rmax	COS-7 &HEK293	(Fang et al., 2008)
C271R	~30%	—	—	↓Rmax, ↑EC_{50}	HEK293	(Xiang et al., 2010)
	~41%	NA	ND	↓Rmax, ↑EC_{50}	COS-7	(Tarnow et al., 2003)
P272L	~30%	NA	NA	↓Rmax	N2A	(Granell et al., 2012)
I301T	<10%	NA	↓B_{max}, ↓IC_{50}	↓Rmax	HEK293	(Nijenhuis et al., 2003)
	~25%	—	—	↑EC_{50}	HEK293	(Xiang et al., 2006)
	~37%	NA	NA	↑EC_{50}	HEK293	(Lubrano-Berthelier et al., 2006)
Y302F	~53%	—	—	↑EC_{50}	HEK293	(Roth et al., 2009)
A303P	~10%	NA	↓B_{max}	—	HEK293	(Hohenadel et al., 2014)
	NA	NA	NA	↓Rmax, ↑EC_{50}	HEK293	(Thearle et al., 2012)
R305W	~69%	NA	NA	↑EC_{50}	HEK293	(Lubrano-Berthelier et al., 2006)
R310K	~47%	—	↓B_{max}	—	HEK293	Unpublished data
I316S	~40%	—	↓B_{max}	↓Rmax	HEK293	Unpublished data
	NA	NA	NA	↓Rmax, ↑EC_{50}	HEK293	(Farooqi et al., 2003)
	~45%	—	—	—	HEK293	(Xiang et al., 2006)

L325F	~72%	—	—	↑ EC_{50}	HEK293	(Fan and Tao, 2009)
	~70%	—	↑IC_{50}	—	HEK293	(Xiang et al., 2010)
	NA	NA	ND	NA	HEK293	(Larsen et al., 2005)

↓: denotes significantly decreased, ↑: denotes significantly increased, —: denotes no significant change, ND: not detectable, NA: not assessed.

[a] Indicates that the receptor expression was measured by confocal microscopy or surface enzyme-linked immunosorbent assay.

[b] Indicates that the IC_{50} could not be determined up to 1 μM concentrations or no competitive displacement binding of NDP-MSH was observed.

Table 1.3 Functional properties of Class II MC4R mutants that are only mildly dysfunctional or relatively normal.

Class II mutation	Cell surface expression	Total expression	Binding	Signaling	Cell type	Reference
V50M	~69%	NA	NA	—	HEK293	(Lubrano-Berthelier et al., 2003)
	NA	NA	—	—	CHO	(Roubert et al., 2010)
L54P	~21%	~44%	—	—	HEK293	(Tan et al., 2009)
I69T	~44%	—	—	—	HEK293	(Tan et al., 2009)
H76R	~55%	—	$\downarrow IC_{50}$	—	HEK293T	(Wang and Tao, 2011)
T112M	~41%	NA	$\downarrow IC_{50}$	—	HEK293	(Nijenhuis et al., 2003)
	—[a]	NA	—	—	HEK293	(Tao and Segaloff, 2005)
	—[a]	NA	NA	—	HEK293T	(Valli-Jaakola et al., 2004)
D146N	~20%	75%	$\downarrow IC_{50}$	—	HEK293T	(Wang and Tao, 2011)
I195S	~30%	—	$\downarrow IC_{50}$	—	HEK293T	(Wang and Tao, 2011)
M215L	~73%	—	—	—	HEK293	Unpublished data
A244E	~60%	—	—	$\downarrow EC_{50}$	HEK293	(Xiang et al., 2006)
	NA	NA	NA	$\uparrow EC_{50}$	COS-7	(Hinney et al., 2003)
I251L	~25%	—	—	—	HEK293	(Xiang et al., 2006)
V253I	~76%	NA	—	—	HEK293	(Nijenhuis et al., 2003)
	NA	NA	—	—	HEK293	(Xiang et al., 2006)
F280L	~55%	—	$\downarrow IC_{50}$	—	HEK293T	(Wang and Tao, 2011)
	↓[a]	NA	NA	NA	COS-7	(Beckers et al., 2010)
L300P	~25%	—	$\downarrow IC_{50}$	—	HEK293T	(Wang and Tao, 2011)
I317T	~60%	—	$\downarrow IC_{50}$	—	HEK293	(Xiang et al., 2006)
	~66%	NA	NA	—	HEK293	(Lubrano-Berthelier et al., 2003)
	~42%	NA	$\downarrow B_{max}$	—	HEK293	(Nijenhuis et al., 2003)
I317V	~80%	—	—	$\uparrow EC_{50}$	HEK293	(Fan and Tao, 2009)
	~60%	—	—	—	HEK293	(Xiang et al., 2010)

↓: denotes significantly decreased. ↑: denotes significantly increased. —: denotes no significant change. NA: not assessed.

[a] Indicates that the receptor expression was measured by confocal microscopy or surface enzyme-linked immunosorbent assay.

Figure 1.1 Schematic representation of the MC4R.

Mutation sites of Class II MC4R are highlighted with black background with those that are nonfunctional with no detectable ligand binding or signaling in pink font, those that are severely dysfunctional but retain some residual ligand binding and signaling capabilities in light blue font, and those that are mildly dysfunctional in light green font. Residues that have multiple mutations classified into different classes are highlighted in white font.

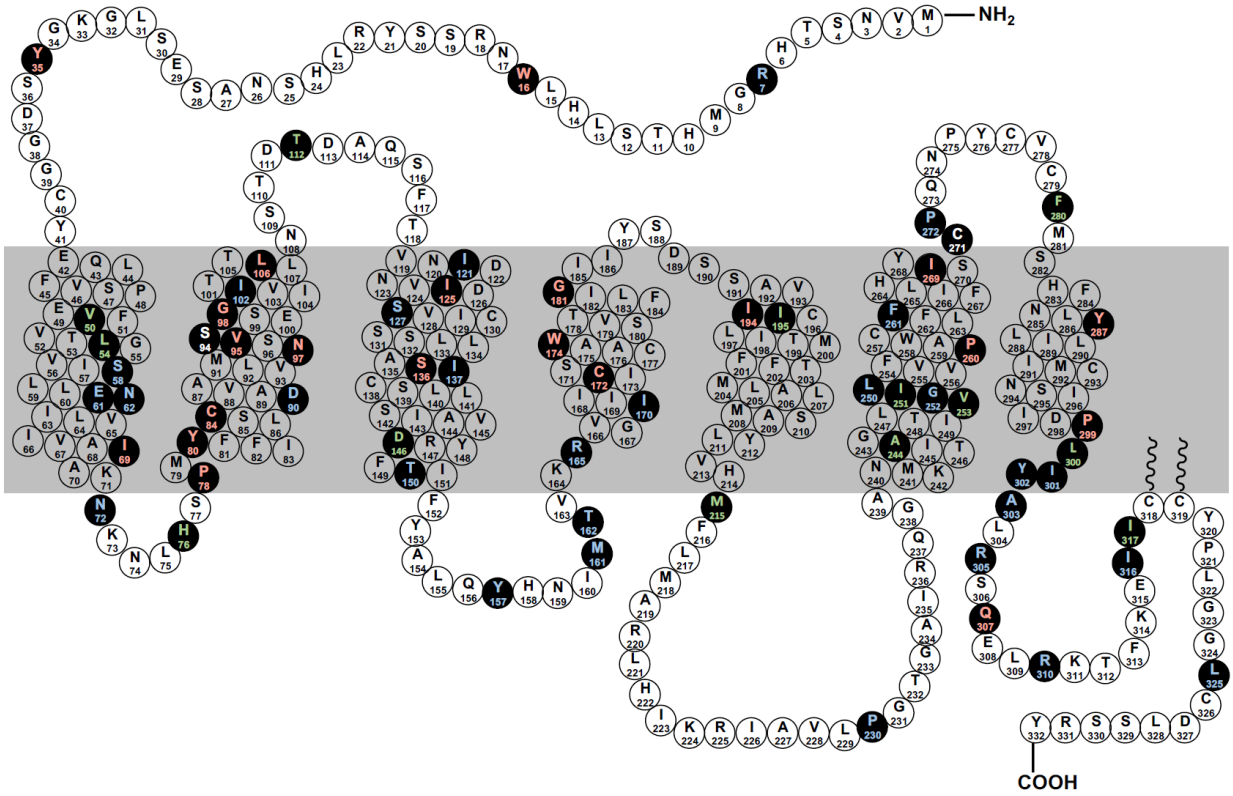

Figure 1.2 Structures of small molecule chemical chaperone (A), agonist (B), and antagonists (C) that promote the proper folding of intracellularly retained mutant MC4Rs.

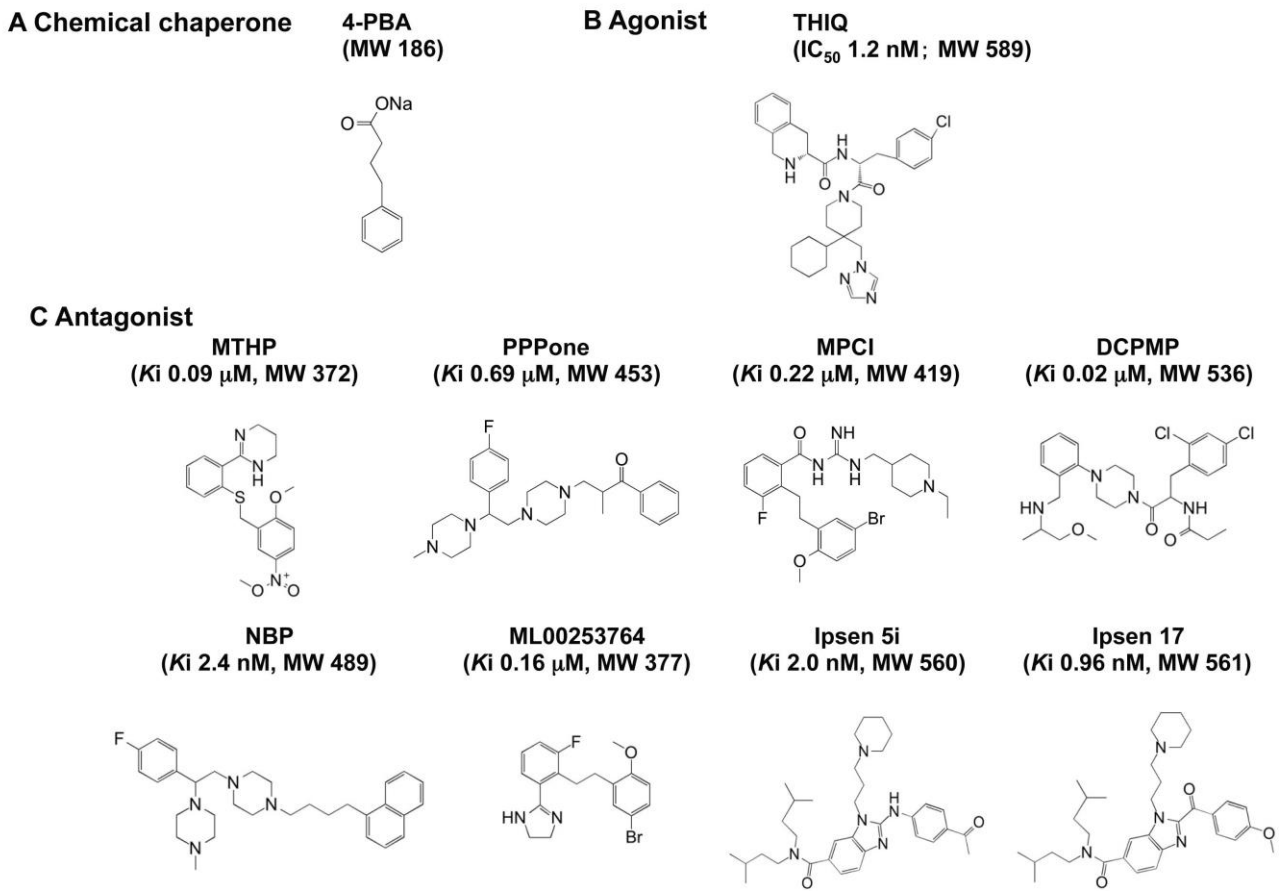

Chapter 2

2.1 Introduction

The melanocortin-4 receptor (MC4R) belongs to the superfamily of G protein-coupled receptors (GPCRs) consisting of the hallmark seven transmembrane domains (TMs) connected by alternating extracellular and intracellular loops, with an extracellular N-terminus and intracellular C-terminus (Gantz et al., 1993). The endogenous agonist of MC4R, α-melanocyte stimulating hormone (MSH), is a small peptide derived from post-translational processing of pro-opiomelanocortin (reviewed in (Smith and Funder, 1988)). Agouti-related protein is the endogenous antagonist of the MC4R. Upon agonist stimulation, MC4R couples to the heterotrimeric stimulatory G protein and then activates adenylyl cyclase to promote the intracellular accumulation of cAMP (Gantz et al., 1993). Other signaling pathways, including calcium and mitogen-activated protein kinase, are also activated by the MC4R (Mountjoy et al., 2001; Vongs et al., 2004), although the relevance of these signaling pathways in mediating the diverse functions of the MC4R are not fully elucidated yet (reviewed in (Huang and Tao, 2014b)).

Since the cloning of human MC4R (hMC4R) in 1993 (Gantz et al., 1993), MC4R have been cloned from a number of other mammals, including rat (Mountjoy et al., 1994), pig (Kim et al., 2000), cattle (Haegeman et al., 2001), and dog (Skorczyk et al., 2007). In recent years, with increasing interests in role of MC4R in energy homeostasis of lower vertebrates, MC4Rs of some nonmammalian species including trout (Haitina et al., 2004), flouder (Kobayashi et al.,

2008), goldfish (Cerda-Reverter et al., 2003), spiny dogfish (Ringholm et al., 2003), and cavefish (Aspiras et al., 2015), among others, were also cloned.

During the past decade, anatomical, pharmacological and rodent genetic studies have shown that MC4R plays a critical role in regulating food intake and energy expenditure (reviewed in (Cone, 2005; Tao, 2005)). It regulates both energy intake and expenditure (Huszar et al., 1997), with the effect of food intake accounting for 60% of the effect on body weight (Balthasar et al., 2005). Human genetic studies provided further supporting evidence that the MC4R is important in maintaining energy homeostasis in humans, playing major roles in the development of both monogenic and polygenic obesity (reviewed in (Hinney et al., 2013; Tao, 2009)). Mutations in *MC4R* are the most common cause of early onset obesity, with up to 6% of obese Caucasian kids harboring *MC4R* mutations (Farooqi et al., 2003). Mutations in cavefish *mc4r* have been shown to contribute to the adaptation to nutrient availability (Aspiras et al., 2015).

Giant panda (*Ailuropoda melanoleuca*), famous as the "living fossil", is an ancient species with a history of about 7 million years and an endangered species endemic to China (Lindburg and Baragona, 2004). Due to its highly specialized feeding habits and reproductive capability, giant panda typically has a low fertility and high neonatal mortality, contributing to the endangered status of giant panda. There are only about 1600 giant pandas surviving in the wild. Previous studies suggested that there is a close relationship between the nutritional status and reproduction of the mammals (reviewed in (Tena-Sempere, 2013)). The MC4R participates in the control of energy homeostasis as well some reproductive function (reviewed in (Tao, 2010)). Hence cloning MC4R is important for understanding nutritional problems and field starvation of giant panda. So far there are few studies on the giant panda at the molecular level.

As the central melanocortin system has been suggested to play an important role in regulation of energy balance in a variety of species from fish to human, we propose that it is also critical for energy homeostasis of giant panda. To begin to understand the roles MC4R might play in regulating energy homeostasis and other physiological processes in the giant panda, we report herein the molecular cloning and pharmacology of the giant panda MC4R (amMC4R). Based on the sequence deposited at NCBI (reference sequence number XM002924679.1), we designed the primers and successfully cloned amMC4R cDNA and inserted it into pcDNA 3.1, a mammalian expression vector. We also analyzed the sequence characteristics of the protein encoded by the cDNA and compared it with those of human and other species reported. With hMC4R as a control, the binding and signaling properties of amMC4R were investigated using several agonists of the MC4R, including [Nle^4, D-Phe^7]-α-MSH (NDP-MSH), α- and β-MSH, and a small molecule agonist of the MC4R, THIQ ([(N-[(3R)-1,2,3,4-tetrahydroisoquinolinium-3-ylcarbonyl]-(1R)-1-(4-chlorobenzyl)-2-[4-cyclohexyl-4-(1H-1,2,4-triazol-1-ylmethyl)piperidin-1-yl]-2-oxoethylamine) (Sebhat et al., 2002). This study provides data for inquiring into the hereditary traits of the gene from giant panda and basis for formulating protective strategy for the giant panda.

2.2 Materials and Methods

2.2.1 Hormones and supplies

NDP-MSH was purchased from Peptides International (Louisville, KY). α-MSH was purchased from Pi Proteomics (Huntsville, AL). β-MSH was purchased from CHI Scientific (Maynard, MA). THIQ was purchased from Tocris Bioscience (Ellisville, MO). ^{125}I-NDP-MSH was iodinated as previously described (Mo et al., 2012). ^{125}I-cAMP was iodinated with

chloramine T method (Steiner et al., 1969). Tissue culture plastic wares were purchased from Corning (Corning, NY). Cell culture media, newborn calf serum, and other reagents for cell culture were obtained from SunShine (Nanjing SunShine Biotechnology Co., LTD., Nanjing, China).

2.2.2 Materials and DNA preparation

Genomic DNA was isolated from about 200 μl of blood collected and donated by colleagues at Yangzhou Zoo (Yangzhou, China) using the Genomic DNA Preparation Kit according to the manufacturer's instructions (TransGen Biotech, Beijing, China). The genomic DNA extracted were dissolved in water, and kept at -70 ^{o}C.

2.2.3 Molecular cloning of amMC4R

The amMC4R coding region was amplified directly from giant panda genomic DNA using a primer pair (sense primer 5'-AAGAATTCATGAACTCGACGCTCCACCATGGGATG-3' and anti-sense primer 5'-CCTCTAGATTAATATCTGCTAGACAAGTCACAAAGGCC-3') designed based on the published nucleotide sequence of amMC4R (NCBI reference sequence number: XM002924679.1) incorporating *EcoR*I and *Xba*I restriction sites in sense and anti-sense primers (underlined), respectively. PCR amplification was performed in a 25 μl mixture containing 100 ng of the giant panda genomic DNA, 0.4 μM of each primer, 12.0 μl 2× Easy Taq PCR Supper Mix (TransGen Biotech) with the following cycling parameters: 2 min at 95 ^{o}C for one cycle and 1 min at 95 ^{o}C, 60s at 56 ^{o}C, and 90 s at 72 ^{o}C for 35 cycles followed by a final cycle of extension at 72 ^{o}C for 10 min.

After amplification, PCR products were separated by electrophoresis in 1.5% agarose gel with 1× TAE buffer, stained with ethidium bromide and visualized under UV light. The expected size fragments of PCR products were harvested and purified from gel using Axygen PCR purification kit (Axygen, Beijing, China), and then double digested with *EcoR*I and *Xba*I (Promega, Shanghai, China). The double digested PCR fragment was ligated into the expression vector pcDNA3.1(+) using T4 DNA ligase (TransGen Biotech) at 16 ^{o}C for 12 hours. The recombinant molecules were transformed into *Escherichia coli* competent cells (DH5α), and then spread on the LB-plate containing 50 μg/mL ampicillin. Plasmid DNA was extracted with Axygen mini-prepare kit (Axygen) to screen clones with the insert of expected size after digestion with *EcoR*I and *Xba*I. The nucleotide sequence of the cloned amMC4R was determined by sequencing three independent plasmids performed at Sangon Biotech Co. Ltd (Shanghai, China). After verifying that the entire coding region was achieved by automated DNA sequencing, amMC4R tagged at its N terminus (after the initiating Met) with myc tag was generated by Sangon Biotech (Shanghai) Co. Ltd. Plasmid DNA containing a myc epitope tag and the amMC4R of correct sequence (myc-amMC4R-pcDNA3.1) was prepared with Axygen Plasmid Maxi kit for transfection as described below.

2.2.4 Homology and phylogenetic analysis of amMC4R

Homology and phylogenetic analyses at nucleotide and amino acid levels were performed between different species including giant panda (*Ailuropoda melanoleuca*), human (*Homo sapiens*), mouse (*Mus musculus*), rat (*Rattus norvegicus*), pig (*Sus scrofa*), cattle (*Bos taurus*), dog (*Canis lupus*), cat (*Felis catus*), chicken (*Gallus gallus*) and zebrafish (*Danio rerio*) using DNASTAR Lasergene v7.1.0 program, according to the manufacturer's protocols.

2.2.5 Cells and transfections

Human embryonic kidney (HEK) 293T cells, purchased from American Type Culture Collection (Manassas, VA, USA), were grown at 5% CO_2 in Dulbecco's modified Eagle's medium containing 10 mM HEPES, 10% newborn calf serum, 50 μg/ml gentamicin, and 100 units/ml of penicillin and 100 μg/ml streptomycin. For transient expression of the amMC4Rs, cells were plated on gelatin-coated 35 mm six-well clusters. When the cells reached 50-70% confluency, they were transfected using calcium phosphate precipitation method (Chen and Okayama, 1987). Ligand binding and signaling studies were performed approximately 48 h later after transient transfection.

2.2.6 Western blot analysis

Protein for western blot was extracted from cells transfected with amMC4R by ultrasonic lysis. Protein samples were prepared with SDS loading buffer. After removal of cell debris by centrifugation, aliquots of the samples (70 μg per lane) were separated by 12% SDS-PAGE and transferred to nitrocellulose membrane (SunShine, Nanjing, China), and then blocked with TBS-T (25 mM Tris-HCl, pH 7.5, 150 mM NaCl, 50 mM KCl, 0.05% (w/v) Tween 20) containing 5% skim milk. After incubation in blocking solution, the filters were reacted overnight with mouse anti-myc antibody (Invitrogen, Carlsbad. CA) in 1% bovine serum albumin (BSA) (1:5000) at 4°C. Then, the membranes were treated with horseradish peroxidase-conjugated goat anti-mouse antibody (SunShine) in 1% BSA (1:15,000) for 1 h at room temperature, developed with an ECL kit, and visualized using and ECL Chemiluminescence Imaging System (Bio-Rad, Hercules, CA).

2.2.7 Radioligand binding assay

The method for ligand binding has been described in detail before (Tao and Segaloff, 2003). Briefly, 48 h after transfection, cells were washed twice with warm Waymouth's MN752/1 media (Sigma-Aldrich, St. Louis, MO) containing 1 mg/ml BSA (referred herein as Waymouth/BSA). Then fresh Waymouth/BSA with or without different concentrations of unlabeled ligands (NDP-, α- or β-MSH, THIQ) and 100,000 cpm of ^{125}I-NDP-MSH (50 μl) was added to each well. The final concentrations of unlabeled ligands ranged from 10^{-11} to 10^{-6} M for NDP-MSH or THIQ, and from 10^{-10} to 10^{-5} M for α- or β-MSH. The total volume is 1 ml in each well. After incubation at 37 ºC for 1 h, plates were placed directly on ice, washed twice with cold Hanks' balanced salt solution contain 1 mg/ml BSA. Then 100 μl of 0.5 N NaOH was added to each well. Cell lysates were then collected from each well using cotton swabs to plastic tubes, and counted in a gamma counter. All determinations were performed in duplicates and three independent experiments were performed. B_{max} (maximal binding) and IC_{50} (concentration of unlabeled ligand that resulted in 50% displacement) were calculated using GraphPad Prism 4.0 software (San Diego, CA).

2.2.8 Intracellular cAMP generation

Forty-eight hours after transfection, HEK293T cells were washed twice with warm Waymouth/BSA and incubated with fresh Waymouth/BSA containing 0.5 mM isobutylmethylxanthine (Sigma-Aldrich) at 37 °C for 15 min. Then different concentrations of NDP, α- or β-MSH, or THIQ were added into each well to make a final volume of 1 ml and incubated at 37 °C for another 1 h. The reaction was terminated on ice and the cells were lysed by 0.5 M perchloric acid containing 180 μg/ml theophylline and neutralized by 0.72 M KOH/0.6 M $KHCO_3$. cAMP levels were measured using RIA. All determinations were performed in triplicate and the experiment was repeated three times. Maximal response (R_{max}) and EC_{50}

(concentration of agonist that cause 50% maximal cAMP production) values were calculated using Prism 4.0 software.

2.2.9 Statistic analysis

GraphPad Prism 4.0 Software (San Diego, CA, USA) was used to calculate ligand binding and signaling parameters including IC_{50}, EC_{50}, B_{max}, and R_{max}. The significance of differences in binding and signaling parameters between the human and giant panda WT MC4Rs were analyzed using Student's *t*-test with Prism 4.0.

2.3 Results

2.3.1 Nucleotide and deduced amino acid sequences of the putative amMC4R

Rompler and colleagues first reported the partial CDS sequence of the amMC4R (GenBank accession number: EF384251.1) in 2007. The predicted complete sequence of the amMC4R was published in 2010 (NCBI Reference Sequence: XM002924679.1) based on the shotgun genome sequence of giant panda (Li et al., 2010). In the present study, the amMC4R we cloned matched the predicted sequence perfectly.

We performed nucleotide sequence alignment among the obtained nucleotide sequence of amMC4R gene and nucleotide sequences of human, mouse, rat, pig, cattle, dog, cat, chicken and zebrafish MC4Rs (GenBank accession number or NCBI reference sequence number: AY236539.1, NM_016977.3, NM013099.2, AB021664, NM_174110.1, DQ084210.2, XM_003995231.2, AB012211, and AY078989.1, respectively). The sequence analysis revealed that the giant panda MC4R gene was intronless and contained an open reading frame of 999 bp predicted to encode a protein of 332 amino acids (Fig. 2.1A). Comparison of the amMC4R sequence with that of the MC4Rs from other species showed that amMC4R is 93.6%, 88.7%,

88.6%, 92.2%, 89.3%, 92.2%, 94.5%, 79.9%, and 68.0% homologous at nucleotide level (Fig. 2.1B). At the amino acid level, the homology of giant panda MC4R was over 96% to human, pig, dog, and cat, 95% to 90% to mouse, rat, and cattle, 87.3% to chicken and 71.1% to zebrafish MC4Rs (Fig. 2.2B), with the highest homology in the TMDs, extracellular, and intracellular loops and lower homology at the amino and carboxyl termini. Giant panda MC4R had the same length as other mammalian (human, mouse, rat, pig, cattle, dog, and cat) MC4Rs. The chicken MC4R is one amino acid shorter at N-terminus than mammalian MC4Rs. The zebrafish MC4R is three amino acids shorter at the C- and N-termini than mammalian MC4Rs, respectively (Fig. 2.2A). Phylogenetic analysis indicates that amMC4R clustered together with MC4Rs from other species at nucleotide level (Fig. 2.1C) but was significantly convergent from dog and cat MC4R and to a less degree from chicken and zebrafish MC4Rs at amino acid level (Fig. 2.2C).

2.3.2 Western blot analyses of amMC4R protein

The recombinant myc-amMC4R was transfected into HEK293T cells. Twenty-four hours after transfection, total cellular protein was extracted and the expression of amMC4R was examined using western blot. The sequence analysis revealed that the giant panda MC4R encoded a receptor protein of 332 amino acids and protein molecular weight was 36.9 kDa. Molecular weight of myc tag was about 1.2 kDa. The putative molecular weight of amMC4R protein (with the myc tag) should be about 38 kDa. In present study, western blot analysis revealed a protein band with a molecular weight of approximately 38 kDa (Fig. 2.3). There was no protein band in empty vector group or un-transfected group. The result showed that expression vector myc-amMC4R-pcDNA3.1 was successfully constructed and the recombinant could be expressed in HEK293T cells.

2.3.3 Ligand binding properties of the amMC4R to four MC4R agonists

To investigate the binding properties of amMC4R and hMC4R, we performed competitive binding assay using ^{125}I-NDP-MSH as the iodinated ligand and four agonists as competitors. NDP-MSH is a superpotent long-lasting analog of the natural agonist (α-MSH) widely used in melanocortin receptor studies. The endogenous ligands, α- and β-MSHs, and a small molecule agonist of the MC4R (THIQ) were also used. Fig. 2.4 showed the results from a typical experiment (from a total of 3 independent experiments) of ligand binding of amMC4R and hMC4R to ^{125}I-NDP-MSH, displaced by unlabeled NDP-MSH (Fig. 2.4A), α-MSH (Fig. 2.4B), β-MSH (Fig. 2.4C), or THIQ (Fig. 2.4D). The ligand-binding assays revealed that amMC4R bound NDP-MSH with the highest affinity, followed by THIQ, α-MSH and β-MSH, the same ranking order as hMC4R (Fig. 2.4 and Table 2.1). As shown in Fig. 2.4 and Table 2.1, amMC4R and hMC4R bound to the same agonist with similar IC_{50}s. B_{max} of amMC4R was 59% of that of hMC4R, indicating decreased expression level compared to hMC4R.

2.3.4 Signaling properties of amMC4R to four MC4R agonists

To demonstrate whether the cloned amMC4R is capable of producing a biologically active receptor protein, we transfected the amMC4R construct obtained into HEK293T cells and analyzed its signaling property using four agonists, NDP-, α-, or β-MSH, or THIQ. As shown in Fig. 2.5, four agonists induced dose-dependent accumulations of intracellular cAMP for the cloned amMC4R and hMC4R. amMC4R responded to NDP-, α-, or β-MSH, or THIQ stimulation with similar R_{max}s as hMC4R. The EC_{50}s of amMC4R to α-MSH, β-MSH, or THIQ were similar to hMC4R, whereas that of NDP-MSH was slightly decreased. The basal activity of amMC4R was similar to that of hMC4R (Fig. 2.5 and Table 2.2). The data from the signaling

assays demonstrated that NDP-MSH was the most potent agonist to stimulate dose-dependent cAMP generation with an EC_{50} of 1.07 nM.

2.4 Discussion

In the present study, as the first step towards elucidating the role(s) of the MC4R in giant panda energy homeostasis, we described the molecular cloning and pharmacological characterization of the giant panda MC4R. Through bioinformatics analysis and progress in giant panda genome sequencing, the putative full-length coding region of amMC4R was identified. Primers designed based on this sequence were used to amplify the coding region from giant panda genomic DNA by taking advantage of the fact that the mammalian MC4Rs, including the putative amMC4R, are intronless. This amplified fragment was inserted into pcDNA3.1 and the sequence verified.

Our results herein showed that mammalian MC4Rs all share the same gene structure and have the coding region of the same size compared to that of hMC4R. The amino acid sequences are highly conserved among the mammalian MC4Rs reported. The phylogenetic analysis clearly separated the mammalian and nonmammalian MC4Rs. Homology and phylogenetic analysis of nucleotide sequence for MC4R of several species were in line with previous studies (Ringholm et al., 2002; Schioth et al., 2003; Staubert et al., 2007). Western blot analysis showed that amMC4R protein was expressed in HEK293T cells after transient transfection of myc-amMC4R-pcDNA3.1 with a molecular weight of about 38 kDa.

For future *in vivo* investigation of the role that amMC4R plays in giant panda energy homeostasis, the most potent and selective agonist for amMC4R must be selected from the pool of known MC4R agonists. Herein, we tested the pharmacological properties of several MC4R

agonists on the cloned amMC4R. Four ligands were used, and hMC4R was included in all experiments for comparison. We were interested in whether amMC4R had similar pharmacology as hMC4R. From ligand binding studies, we showed that of the four agonists tested, the rank order in terms of affinity was: NDP-MSH, THIQ, α-MSH, and β-MSH. Human MC4R had the same rank order for these ligands. Our data for amMC4R (IC_{50} of 16.57 nM) was very close to the numbers reported for human and dog MC4Rs (Schioth et al., 1996; Yan and Tao, 2011).

The classical signaling pathway for the MC4R is by coupling to the heterotrimeric stimulatory G protein, with receptor activation leads to increased cAMP production, and consequently protein kinase A activation (Gantz et al., 1993). In the present study, signal transduction properties were analyzed by intracellular cAMP assays after transient transfection of amMC4R into HEK293T cells. NDP-MSH is a superpotent long-lasting analog of the natural agonist derived from proopionmelanocortin, α-MSH. As a commonly used analog for MCR studies, NDP-MSH is more potent than the endogenous ligands α- and β-MSHs and therefore is better for *in vitro* studies to elucidate the signaling property of MC4R (Fan et al., 2008; Sawyer et al., 1980; Yan and Tao, 2011). Treatment of HEK293T cells expressing amMC4R with different concentration NDP-MSH resulted in the dose-dependent increase of intracellular cAMP level. Of the four agonists, NDP-MSH was the most potent agonist, therefore would suited for further *in vivo* studies to elucidate the functional importance of MC4R in energy homeostasis in giant panda.

Here, our data obtained from β-MSH were similar to the data obtained when α-MSH was used as the agonist, suggesting that amMC4R bound α-MSH with similar affinity and responded with similar potency compared with β-MSH. Similar results were also obtained in chicken MC4R (Wang et al., 2016). We concluded that α- and β-MSHs might be both important in

activating amMC4R. Therefore β-MSH might also be an important endogenous ligand for activation of MC4R and regulation of energy homeostasis in different animals. Additionally, THIQ is a highly selective nonpeptidic MC4R agonist. Recently, studies have also been performed on the ligand binding and signaling properties of MC4R for THIQ (Hogan et al., 2006; Pogozheva et al., 2005; Yang et al., 2009). Xiang *et al.* reported that THIQ might bind to residues on the MC4R different from endogenous ligand (Xiang et al., 2007). For amMC4R and hMC4R, our data obtained in binding and signaling assasy from THIQ were close to NDP-MSH, suggesting that THIQ was a superpotent agonist for the two MC4Rs.

In summary, we have cloned the amMC4R. Expression of the cloned amMC4R in HEK293T cells revealed that indeed amMC4R was fully functional upon stimulation with agonists *in vitro*. Pharmacological characterizations using four agonists revealed that the amMC4R and hMC4R have the same rank orders in binding affinity for these ligands. The results will lay a foundation for further study of amMC4R on giant panda physiology.

Table 2.1 Ligand binding properties of hMC4R and amMC4R.

MC4R	n	B_{max} (%)	IC_{50} (nM)			
			NDP-MSH	α-MSH	β-MSH	THIQ
hMC4R	3	100	20.08 ± 2.03	410.77 ± 84.54	568.55 ± 95.78	55.69 ± 15.80
amMC4R	3	59 ± 1[a]	16.57 ± 2.53	382.73 ± 14.81	556.27 ± 162.58	40.02 ± 7.76

The data were expressed as the mean ± SEM of three independent experiments. IC_{50} was the concentration of ligand that was needed to cause 50% inhibition in the binding assay.

[a] Significantly different from hMC4R, $p < 0.001$.

Table 2.2 Agonist-stimulated cAMP responses of hMC4R and amMC4R.

MC4R	n	NDP-MSH		α-MSH		β-MSH		THIQ	
		EC_{50} (nM)	R_{max}	EC_{50} (nM)	R_{max}	EC_{50} (nM)	R_{max}	EC_{50} (nM)	R_{max}
hMC4R	3	2.38 ± 0.13	100	3.68 ± 0.53	100	2.37 ± 0.55	100	4.35 ± 0.20	100
amMC4R	3	1.07 ± 0.23[a]	104 ± 7	3.14 ± 0.15	105 ± 8	2.02 ± 0.19	106 ± 8	3.12 ± 0.99	117 ± 12

The data were expressed as the mean ± SEM of three independent experiments. EC_{50} was the concentration of agonist that results in 50% stimulation of the maximal response. The maximal response (R_{max}) was 3382 ± 743 pmol cAMP/10^6 cells for hMC4R under NDP-MSH stimulation, 2791 ± 578 pmol under α-MSH stimulation, 2536 ± 578 pmol under β-MSH stimulation, and 3147 ± 410 pmol under THIQ stimulation.

[a] Significantly different from hMC4R, $p < 0.001$.

Figure 2.1 Deduced nucleotide and amino acid sequences of amMC4R and comparison with MC4Rs from other species.

(A) Sequence of the full-length amMC4R cDNA with in silico translation is shown. Underlined sequence indicates restriction sites of the primers used for amplification of the cDNA by PCR. The sequence of myc tag is shaded in gray. (B) Homology and (C) phylogenetic analysis of MC4R nucleotide sequences from several species.

A

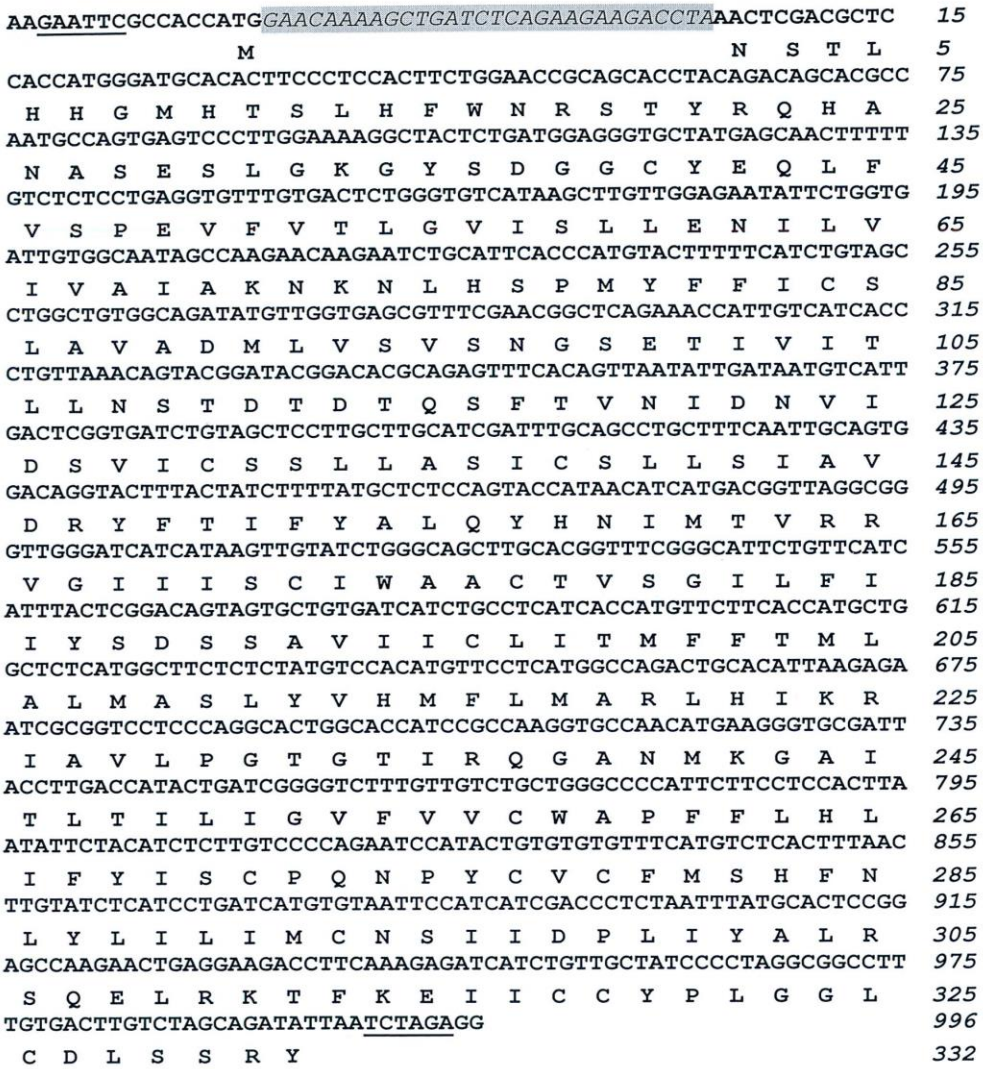

B

	Giant panda	Human	Mouse	Rat	Pig	Cattle	Dog	Cat	Chicken	Zebrafish
Giant panda	100.0	93.6	88.7	88.6	92.2	89.3	92.2	94.5	79.9	68.0
Human		100.0	88.9	88.5	92.1	87.0	89.5	92.9	80.9	68.1
Mouse			100.0	95.0	88.3	85.3	87.5	88.2	78.4	68.7
Rat				100.0	88.2	85.4	87.1	88.1	78.6	69.4
Pig					100.0	89.1	90.1	91.9	80.0	69.7
Cattle						100.0	88.1	89.0	78.5	70.1
Dog							100.0	91.4	79.7	69.2
Cat								100.0	81.1	69.1
Chicken									100.0	67.2
Zebrafish										100.0

C

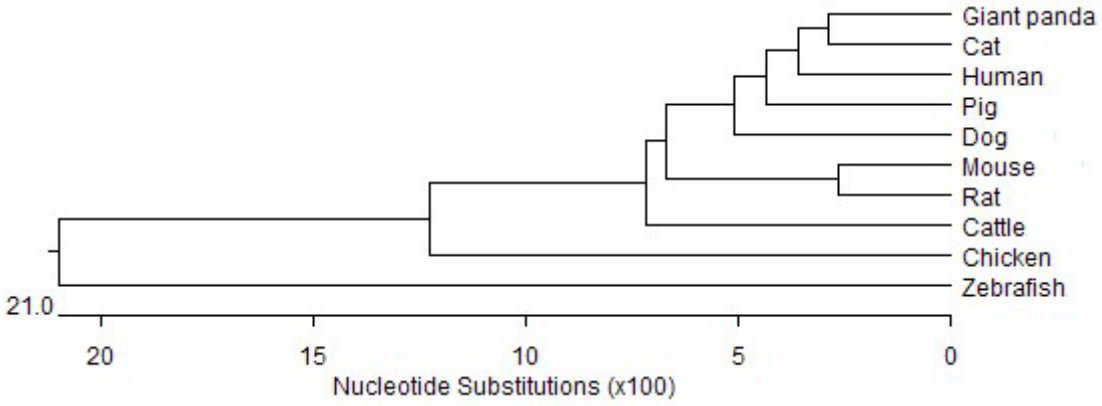

Figure 2.2 Comparison of amino acid sequences between amMC4R and MC4Rs from other species.

(A) Alignment of the amino acid sequences between giant panda (amMC4R) and human (hMC4R), mouse (mMC4R), rat (rMC4R), pig (sMC4R), cattle (bMC4R), dog (cMC4R), cat (fMC4R), chicken (gMC4R) and zebrafish (dMC4R) MC4Rs. Positions of different regions of the receptor are indicated above the sequences and labeled as follows: transmembrane domains as TMD 1–7, extracellular loops as EL 1–3, intracellular loops as IL 1–3, amino and carboxyl termini as extracellular amino terminus and cytoplasmic tail respectively. The conserved residues are indicated with stars below (*). The transmembrane domains are shaded in gray. (B) Homology and (C) phylogenetic analysis of MC4R amino acid sequences from several species.

A

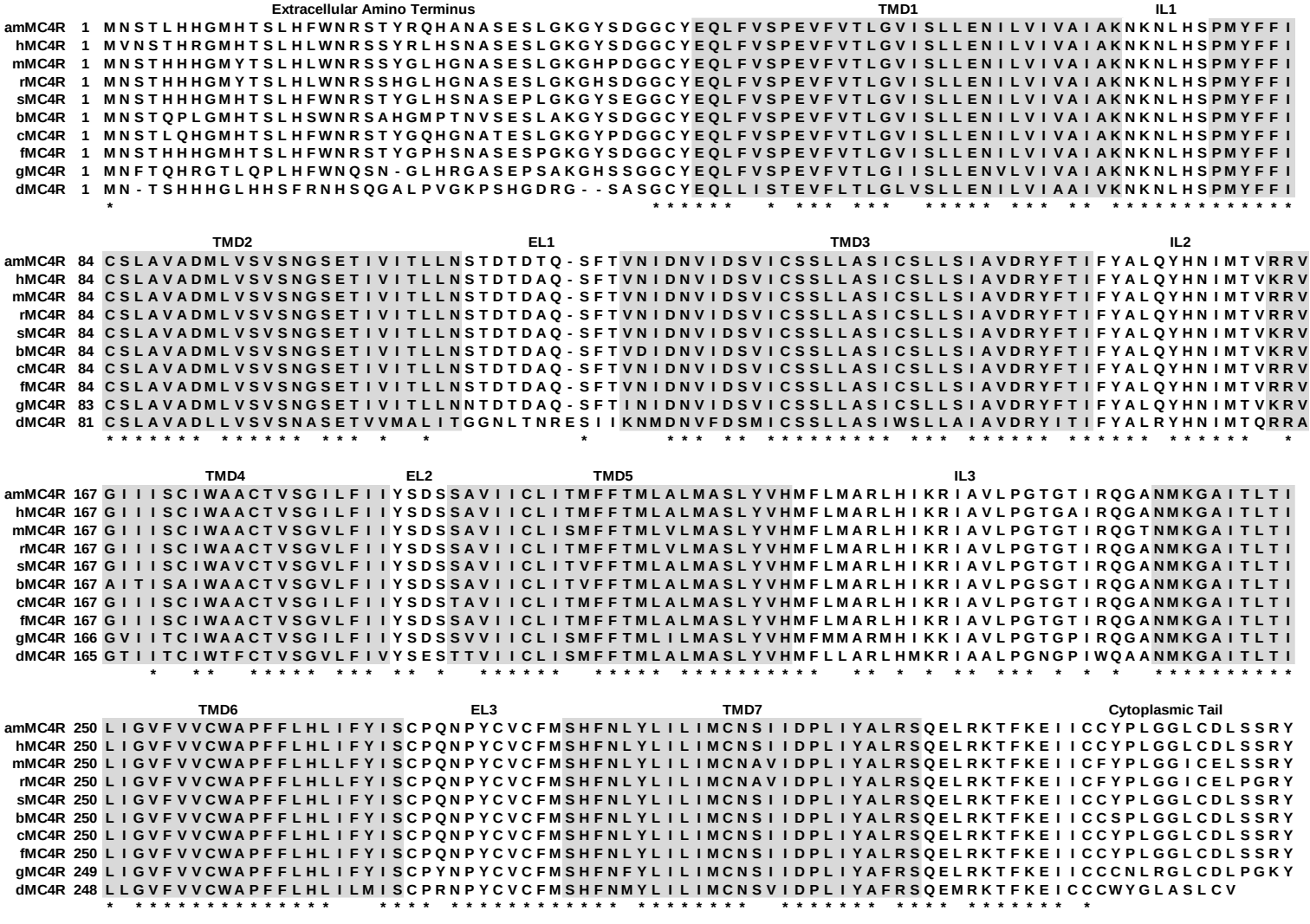
Extracellular Amino Terminus
TMD1
IL1
amMC4R 1 MNSTLHHGMHTSLHFWNRSTYRQHANASESLGKGYSDGGCYEQLFVSPEVFVTLGVISLLENILVIVAIAKNKNLHSPMYFFI
hMC4R 1 MVNSTHRGMHTSLHLWNRSSYRLHSNASESLGKGYSDGGCYEQLFVSPEVFVTLGVISLLENILVIVAIAKNKNLHSPMYFFI
mMC4R 1 MNSTHHHGMYTSLHLWNRSSYGLHGNASESLGKGHPDGGCYEQLFVSPEVFVTLGVISLLENILVIVAIAKNKNLHSPMYFFI
rMC4R 1 MNSTHHHGMYTSLHLWNRSSHGLHGNASESLGKGHSDGGCYEQLFVSPEVFVTLGVISLLENILVIVAIAKNKNLHSPMYFFI
sMC4R 1 MNSTHHHGMHTSLHFWNRSTYGLHSNASEPLGKGYSEGGCYEQLFVSPEVFVTLGVISLLENILVIVAIAKNKNLHSPMYFFI
bMC4R 1 MNSTQPLGMHTSLHSWNRSAHGMPTNVSESLAKGYSDGGCYEQLFVSPEVFVTLGVISLLENILVIVAIAKNKNLHSPMYFFI
cMC4R 1 MNSTLQHGMHTSLHFWNRSTYGQHGNATESLGKGYPDGGCYEQLFVSPEVFVTLGVISLLENILVIVAIAKNKNLHSPMYFFI
fMC4R 1 MNSTHHHGMHTSLHFWNRSTYGPHSNASESPGKGYSDGGCYEQLFVSPEVFVTLGVISLLENILVIVAIAKNKNLHSPMYFFI
gMC4R 1 MNFTQHRGTLQPLHFWNQSN-GLHRGASEPSAKGHSSGGCYEQLFVSPEVFVTLGIISLLENVLVIVAIAKNKNLHSPMYFFI
dMC4R 1 MN-TSHHHGLHHSFRNHSQGALPVGKPSHGDRG--SASGCYEQLLISTEVFLTLGLVSLLENILVIAAIVKNKNLHSPMYFFI
TMD2
EL1
TMD3
IL2
amMC4R 84 CSLAVADMLVSVSNGSETIVITLLNSTDTDTQ-SFTVNIDNVIDSVICSSLLASICSLLSIAVDRYFTIFYALQYHNIMTVRRV
hMC4R 84 CSLAVADMLVSVSNGSETIVITLLNSTDTDAQ-SFTVNIDNVIDSVICSSLLASICSLLSIAVDRYFTIFYALQYHNIMTVKRV
mMC4R 84 CSLAVADMLVSVSNGSETIVITLLNSTDTDAQ-SFTVNIDNVIDSVICSSLLASICSLLSIAVDRYFTIFYALQYHNIMTVRRV
rMC4R 84 CSLAVADMLVSVSNGSETIVITLLNSTDTDAQ-SFTVNIDNVIDSVICSSLLASICSLLSIAVDRYFTIFYALQYHNIMTVRRV
sMC4R 84 CSLAVADMLVSVSNGSETIVITLLNSTDTDAQ-SFTVNIDNVIDSVICSSLLASICSLLSIAVDRYFTIFYALQYHNIMTVKRV
bMC4R 84 CSLAVADMLVSVSNGSETIVITLLNSTDTDAQ-SFTVDIDNVIDSVICSSLLASICSLLSIAVDRYFTIFYALQYHNIMTVKRV
cMC4R 84 CSLAVADMLVSVSNGSETIVITLLNSTDTDAQ-SFTVNIDNVIDSVICSSLLASICSLLSIAVDRYFTIFYALQYHNIMTVRRV
fMC4R 84 CSLAVADMLVSVSNGSETIVITLLNSTDTDAQ-SFTVNIDNVIDSVICSSLLASICSLLSIAVDRYFTIFYALQYHNIMTVRRV
gMC4R 83 CSLAVADMLVSVSNGSETIVITLLNNTDTDAQ-SFTINIDNVIDSVICSSLLASICSLLSIAVDRYFTIFYALQYHNIMTVKRV
dMC4R 81 CSLAVADLLVSVSNASETVVMALITGGNLTNRESIIKNMDNVFDSMICSSLLASIWSLLAIAVDRYITIFYALRYHNIMTQRRA
TMD4
EL2
TMD5
IL3
amMC4R 167 GIIISCIWAACTVSGILFIIYSDSSAVIICLITMFFTMLALMASLYVHMFLMARLHIKRIAVLPGTGTIRQGANMKGAITLTI
hMC4R 167 GIIISCIWAACTVSGILFIIYSDSSAVIICLITMFFTMLALMASLYVHMFLMARLHIKRIAVLPGTGAIRQGANMKGAITLTI
mMC4R 167 GIIISCIWAACTVSGVLFIIYSDSSAVIICLISMFFTMLVLMASLYVHMFLMARLHIKRIAVLPGTGTIRQGTNMKGAITLTI
rMC4R 167 GIIISCIWAACTVSGVLFIIYSDSSAVIICLITMFFTMLVLMASLYVHMFLMARLHIKRIAVLPGTGTIRQGANMKGAITLTI
sMC4R 167 GIIISCIWAVCTVSGVLFIIYSDSSAVIICLITVFFTMLALMASLYVHMFLMARLHIKRIAVLPGTGTIRQGANMKGAITLTI
bMC4R 167 AITISAIWAACTVSGVLFIIYSDSSAVIICLITVFFTMLALMASLYVHMFLMARLHIKRIAVLPGSGTIRQGANMKGAITLTI
cMC4R 167 GIIISCIWAACTVSGILFIIYSDSTAVIICLITMFFTMLALMASLYVHMFLMARLHIKRIAVLPGTGTIRQGANMKGAITLTI
fMC4R 167 GIIISCIWAACTVSGVLFIIYSDSSAVIICLITMFFTMLALMASLYVHMFLMARLHIKRIAVLPGTGTIRQGANMKGAITLTI
gMC4R 166 GVIITCIWAACTVSGILFIIYSDSSVVIICLISMFFTMLILMASLYVHMFMMARMHIKKIAVLPGTGPIRQGANMKGAITLTI
dMC4R 165 GTIITCIWTFCTVSGVLFIVYSESTTVIICLISMFFTMLALMASLYVHMFLLARLHMKRIAALPGNGPIWQAANMKGAITLTI
TMD6
EL3
TMD7
Cytoplasmic Tail
amMC4R 250 LIGVFVVCWAPFFLHLIFYISCPQNPYCVCFMSHFNLYLILIMCNSIIDPLIYALRSQELRKTFKEIICCYPLGGLCDLSSRY
hMC4R 250 LIGVFVVCWAPFFLHLIFYISCPQNPYCVCFMSHFNLYLILIMCNSIIDPLIYALRSQELRKTFKEIICCYPLGGLCDLSSRY
mMC4R 250 LIGVFVVCWAPFFLHLLFYISCPQNPYCVCFMSHFNLYLILIMCNAVIDPLIYALRSQELRKTFKEIICFYPLGGICELSSRY
rMC4R 250 LIGVFVVCWAPFFLHLLFYISCPQNPYCVCFMSHFNLYLILIMCNAVIDPLIYALRSQELRKTFKEIICFYPLGGICELPGRY
sMC4R 250 LIGVFVVCWAPFFLHLIFYISCPQNPYCVCFMSHFNLYLILIMCNSIIDPLIYALRSQELRKTFKEIICCYPLGGLCDLSSRY
bMC4R 250 LIGVFVVCWAPFFLHLIFYISCPQNPYCVCFMSHFNLYLILIMCNSIIDPLIYALRSQELRKTFKEIICCSPLGGLCDLSSRY
cMC4R 250 LIGVFVVCWAPFFLHLIFYISCPQNPYCVCFMSHFNLYLILIMCNSIIDPLIYALRSQELRKTFKEIICCYPLGGLCDLSSRY
fMC4R 250 LIGVFVVCWAPFFLHLIFYISCPQNPYCVCFMSHFNLYLILIMCNSIIDPLIYALRSQELRKTFKEIICCYPLGGLCDLSSRY
gMC4R 249 LIGVFVVCWAPFFLHLIFYISCPYNPYCVCFMSHFNFYLILIMCNSIIDPLIYAFRSQELRKTFKEIICCCNLRGLCDLPGKY
dMC4R 248 LLGVFVVCWAPFFLHLILMISCPRNPYCVCFMSHFNMYLILIMCNSVIDPLIYAFRSQEMRKTFKEICCCWYGLASLCV

B

	Giant panda	Human	Mouse	Rat	Pig	Cattle	Dog	Cat	Chicken	Zebrafish
Giant panda	100.0	96.4	94.0	94.0	96.7	93.4	97.9	97.9	87.3	71.1
Human		100.0	93.4	93.4	95.8	92.8	95.2	96.1	87.7	70.8
Mouse			100.0	98.2	94.0	90.7	94.3	94.9	85.8	70.5
Rat				100.0	94.0	91.3	93.7	94.9	86.7	70.5
Pig					100.0	94.0	96.1	97.9	88.0	71.4
Cattle						100.0	93.1	94.0	85.5	69.2
Dog							100.0	97.3	86.7	71.1
Cat								100.0	87.7	71.7
Chicken									100.0	70.8
Zebrafish										100.0

C

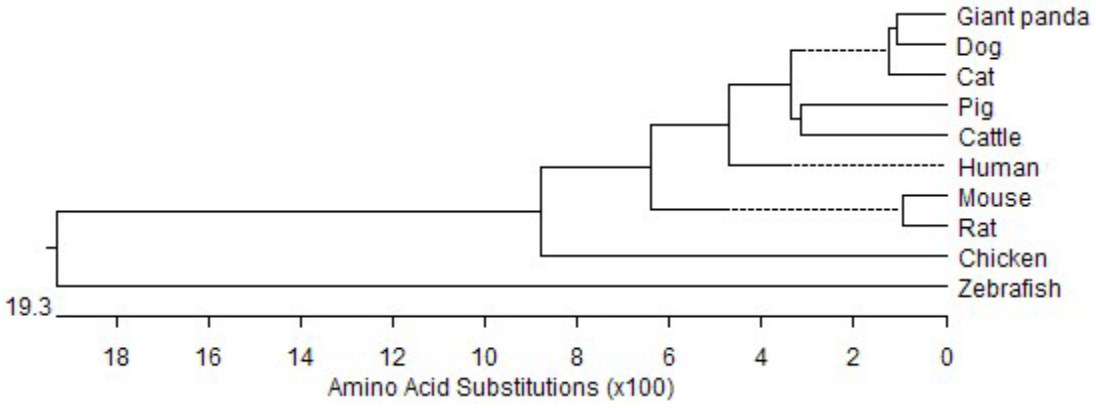

Figure 2.3 Western blot analysis of the expression of the cloned amMC4R.

Protein samples were extracted from cells transfected with the cloned amMC4R (lane A), cells transfected with empty vector (lane B), and non-transfected cells (lane C). Seventy micrograms of protein was loaded in each lane. The molecular weights of standard marker proteins are indicated at the left.

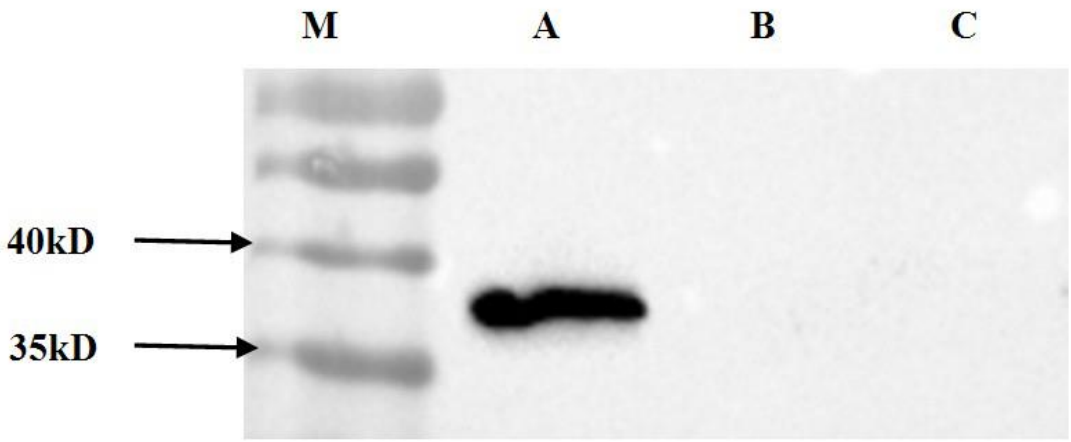

Figure 2.4 Ligand binding properties of the cloned amMC4R in HEK293T cells.

HEK293T cells were transiently transfected with the cloned amMC4R (hMC4R was used as a control), and binding properties of the MC4Rs were measured as described in Section 2. Different concentrations of unlabeled agonists were used to displace the binding of ^{125}I-NDP-MSH to MC4Rs on intact cells (A, NDP-MSH; B, α-MSH; C, β-MSH; D, THIQ). Results shown were expressed as mean % of hMC4R binding ± range from duplicate determinations within one experiment. All experiments were performed three times.

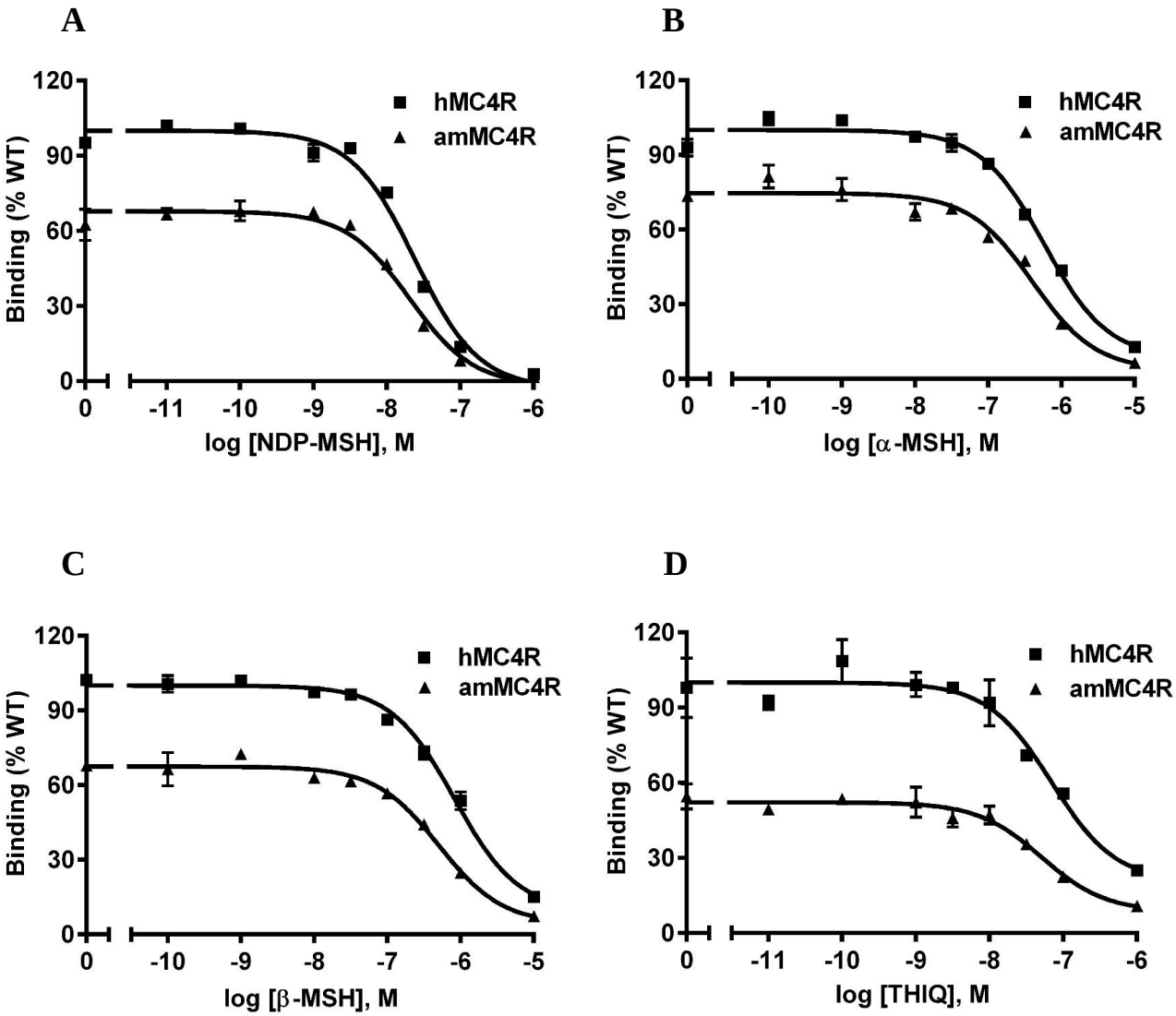

Figure 2.5 Signaling properties of the cloned amMC4R in HEK293T cells.

HEK293T cells were transiently transfected with the cloned amMC4R (hMC4R was used as a control), and signaling assays were performed as described in Section 2. For measurement of cAMP accumulation, the transfected cells were stimulated with various concentrations of agonists (A, NDP-MSH; B, α-MSH; C, β-MSH; D, THIQ). Intracellular cAMP levels were measured by RIA. Results were expressed as the mean ± SEM of triplicate determinations within one experiment, and all experiments were performed three times.

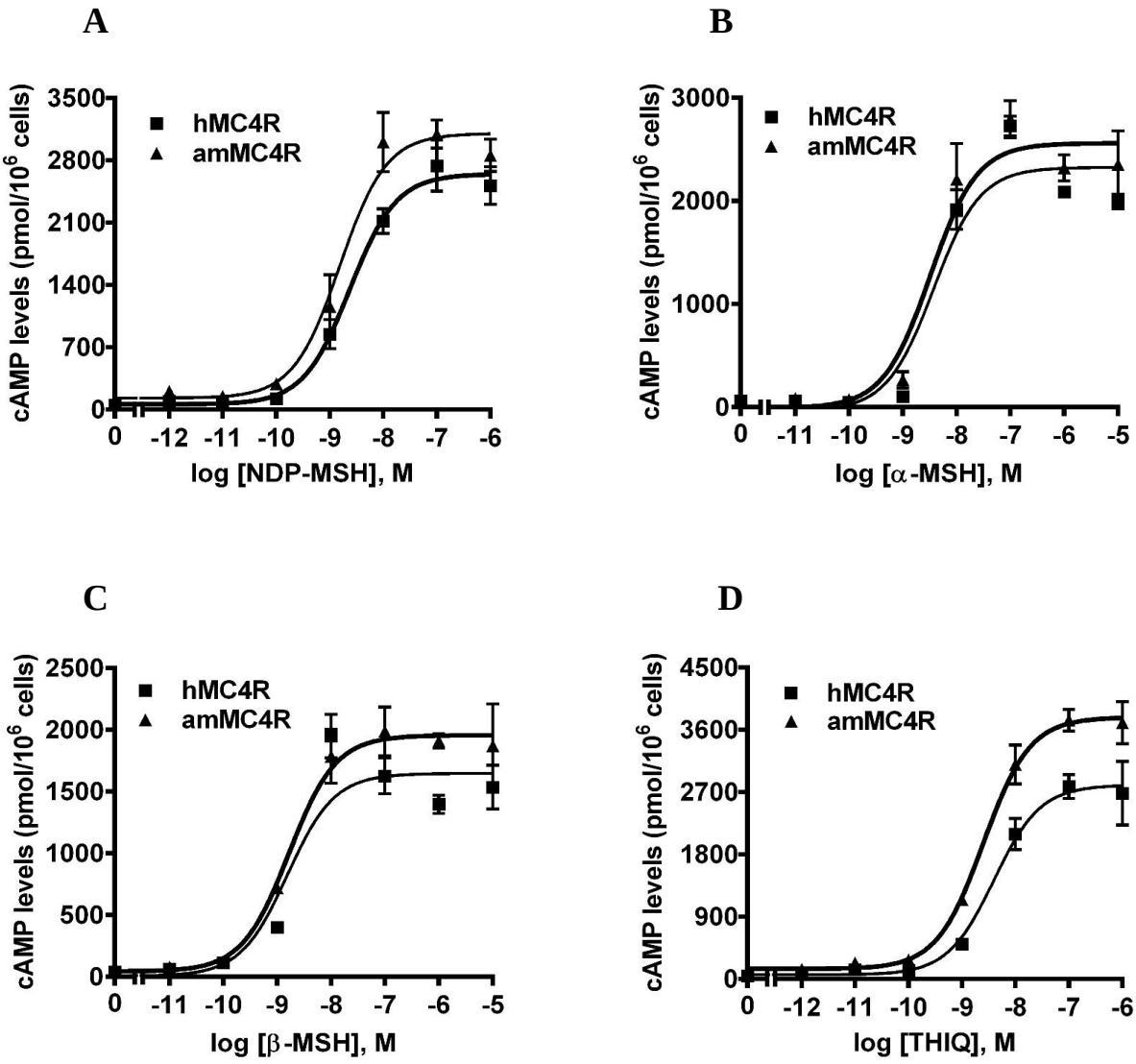

Chapter 3

3.1 Introduction

Obesity is a complex metabolic disorder caused by an imbalance of food intake and energy expenditure. Human obesity has reached epidemic levels worldwide and caused substantial public health crisis due to its close association with several medical conditions, including type 2 diabetes mellitus, hypertension, and cardiovascular disease as well as certain types of cancer (reviewed in (Haslam and James, 2005; Tao et al., 2013)). In the past two decades, several genes have been identified to be associated with obesity, and mutations in the melanocortin-4 receptor (*MC4R*) gene have been characterized as the most common cause of monogenic obesity in human, with a prevalence of up to 6% in some populations with early-onset morbid obesity (Hinney et al., 2003).

The MC4R belongs to family A rhodopsin-like G protein-coupled receptors (GPCRs) with the hallmark structure of seven transmembrane (TM) domains. The MC4R is primarily expressed in central nervous system (Gantz et al., 1993; Mountjoy et al., 1994) and plays a vital role in regulating both food intake and energy expenditure (Huszar et al., 1997). The endogenous ligands for MC4R include agonistic peptides derived from processing of proopiomelanocortin and the antagonist agouti-related peptide (reviewed in (Tao, 2010)). Since MC4R primarily couples to the stimulatory G protein, receptor activation enhances the adenylyl cyclase activity, which results in increased intracellular cAMP production and subsequent activation of protein kinase A. MC4R activation by α-melanocyte stimulating hormone (α-MSH) leads to decreased

food intake and increased energy expenditure whereas antagonism of MC4R by agouti-related peptide results in positive energy balance (Fan et al., 1997; Ollmann et al., 1997).

Since two groups of O'Rahilly and Froguel independently reported that frameshift mutations in the *MC4R* are associated with severe early-onset obesity (Vaisse et al., 1998; Yeo et al., 1998), more than 170 distinct mutations in the coding region of the *MC4R* gene have been identified from different patient cohorts (Hinney et al., 2013; Tao, 2009). These mutations are divided into five classes according to a classification scheme based on the life cycle of GPCRs (Tao, 2005; Tao and Segaloff, 2003). Class I mutants have decreased receptor biosynthesis and/or increased receptor degradation; Class II mutants are synthesized but trapped intracellularly; Class III mutants are expressed on the cell membrane but have defects in binding to the ligand; Class IV mutants exhibit normal cell surface expression and ligand binding but are defective in cAMP signaling; Class V mutants behave normally in all the parameters mentioned above, therefore their potential pathogenic role in obesity remains elusive.

Previously, several groups reported the identification of nine *MC4R* mutations in various patient cohorts. They are L23R (Wang et al., 2006) in the N-terminus, K73R (Nowacka-Woszuk et al., 2011) in intracellular loop (IL) 1, T101N (Buchbinder et al., 2011) in TM2, T112K (Hinney et al., 2006) in extracellular loop 1, M161T (Tan et al., 2009) in IL2, L207V (Rouskas et al., 2012) in TM5, M215L (Nowacka-Woszuk et al., 2011) in IL3, R310K (Wang et al., 2006) and I316S (Yeo et al., 2003) in the C-terminus (shown schematically in Fig. 3.1). The clinical characteristics of the patients harboring these mutant MC4Rs are listed in Table 3.1. However, these mutants were either not characterized or characterized incompletely. In the current study, we investigated the total and cell surface expression, ligand binding, and cAMP signaling properties of these mutant receptors.

MC4R also activates ERK1/2 signaling pathway (Chai et al., 2006; Mo and Tao, 2013), which has been suggested to be related to MC4R function of energy homeostasis *in vivo* (Daniels et al., 2003; Sutton et al., 2005). We previously showed that defects in the basal or ligand-stimulated ERK1/2 signaling might be associated with the obesity pathogenesis in patients harboring Class V *MC4R* mutations (He and Tao, 2014). We and others also reported unbalanced cAMP and ERK1/2 signaling in the MC4R (He and Tao, 2014; Mo and Tao, 2013; Patten et al., 2007). Therefore, the ERK1/2 signaling pathway of naturally occurring *MC4R* mutations might be important to unravel the MC4R functions and was also investigated.

Extensive functional studies of obesity-associated *MC4R* mutations have shown that the majority of inactivating mutants are trapped intracellularly (Hinney et al., 2013; Tao, 2009). However, some mislocalized mutant receptors with minor defects might still retain the potential to function normally if they were escorted to the plasma membrane. Pharmacological chaperone (pharmacoperone) has emerged as a promising therapeutic approach for correcting the dysfunctional misfolded receptors by selectively stabilizing the proteins and facilitating their trafficking to their sites of action. A number of small molecules, including agonists, antagonists, and allosteric modulators, have been identified as pharmacoperones for a diverse array of GPCRs using *in vitro* system (Chen et al., 2006; Huang and Tao, 2014b; Janovick et al., 2002; Morello et al., 2000; Newton et al., 2011; Noorwez et al., 2004). Several *in vivo* studies demonstrated high efficacy of pharmacoperones in transgenic animals and clinical trials (Bernier et al., 2006; Janovick et al., 2013; Los et al., 2010). We previously reported that two MC4R inverse agonists, Ipsen 5i and ML00253764, promote proper folding and trafficking of some Class II mutant MC4Rs (Fan and Tao, 2009; Tao and Huang, 2014). Here the general effects of these two small molecules on Class II mutant MC4Rs were also investigated.

3.2 Materials and Methods

3.2.1 Materials

[Nle^4, D-Phe^7]-α-melanocyte stimulating hormone (NDP-MSH) was purchased from Peptides International (Louisville, KY) and iodinated as described previously (Mo et al., 2012). α-MSH was purchased from Phoenix Pharmaceuticals (Belmont, CA). Melanotan II (MTII) (Al-Obeidi et al., 1989) and THIQ (Sebhat et al., 2002) were purchased from Tocris Bioscience (Ellisville, MO). Ipsen 5i (Poitout et al., 2007) and ML00253764 (Vos et al., 2004) were custom synthesized by Enzo Life Science (Plymouth Meeting, PA).

3.2.2 Site-directed mutagenesis

Mutant hMC4Rs were generated by QuickChange site-directed mutagenesis kit (Stratagene, La Jolla, CA) using the (wild-type) WT receptor as the template (Tao and Segaloff, 2003). Automated DNA sequencing was performed by DNA Sequencing Facility of University of Chicago Cancer Research Center (Chicago, IL) to verify the presence of desired mutations and the absence of errors in the coding sequences.

3.2.3 Cell culture and transfection

HEK293 and 293T cells were purchased from American Type Culture Collection (Manassas, VA) and were cultured in DMEM with 10% newborn calf serum, 10 mM HEPES, 100 units/ml penicillin, 100 μg/ml streptomycin, 0.25 μg/ml amphotericin B, and 50 μg/ml gentamicin. HEK293T cells were plated into gelatin-coated 35 mm six-well clusters, transfected with the WT or mutant constructs at 50-70% confluency using calcium phosphate precipitation method (Chen and Okayama, 1987), and were assayed for binding and signaling 48 h later. For

Western blot, HEK293T cells were seeded into gelatin-coated 100 mm dishes and were transfected using the same method. For confocal microscopy and flow cytometry, stable cells were established after transfection of HEK293 cells and selection with G418 as described previously (Tao and Segaloff, 2003).

3.2.4 Confocal microscopy

The method for confocal microscopy has been described earlier (Tao and Segaloff, 2003). On the day of experiment, stably transfected HEK293 cells were washed three times with filtered PBS-IH, fixed with 4% paraformaldehyde for 30 min, and blocked with 5% bovine serum albumin (BSA) for 1 h. Cells were then incubated with 9E10 monoclonal anti-myc antibody (1:100; Developmental Studies Hybridoma Bank, the University of Iowa, Iowa City, IA) for 1 h, and this was followed by incubation with Alexa Fluor 488-conjugated goat anti-mouse IgG (1:1000; Invitrogen, Carlsbad, CA) for 1 h. After being washed for 5 times, cells were covered by VectaShield Mounting Media (Vector Laboratories, Burlingame, CA) and a glass coverslip. Fluorescent images were taken using a Bio-Rad laser scanning confocal microscope.

3.2.5 Flow cytometry

Flow cytometry was performed as described previously (Wang and Tao, 2011). On the day of experiment, cells were rinsed once with ice-cold PBS-IH and collected. The antibodies used and dilutions of antibodies were the same as described above for confocal microscopy. Fluorescence signals were measured with a C6 Accuri Cytometer (Accuri Cytometers, Inc, Ann Arbor, MI). All the steps were performed at room temperature. Fluorescence from cells stably transfected with pcDNA3.1 empty vector was used to measure background staining. The

expression levels of each mutant were calculated as a percentage of WT MC4R expression using the formula: (mutant fluorescence – pcDNA3.1 fluorescence)/(WT fluorescence – pcDNA3.1 fluorescence) ×100%.

3.2.6 Radioligand binding assay

Forty-eight hours after transfection, cells were washed twice with warm Waymouth's MB752/1 media (Sigma-Aldrich, St. Louis, MO) containing 1 mg/ml BSA (Waymouth/BSA). Then cells were incubated with 1 ml Waymouth/BSA containing 50 μl, 100,000 cpm of ^{125}I-NDP-MSH, and with or without different concentrations of NDP- or α-MSH at 37 °C for 1 h. Cells were then washed twice with cold Hank's balanced salt solution to terminate the reactions, lysed by 100 μl 0.5 N NaOH, collected with cotton swabs, and counted in a gamma counter.

3.2.7 cAMP assay

Forty-eight hours after transfection, cells were washed twice with warm Waymouth/BSA and then incubated with fresh Waymouth/BSA containing 0.5 mM isobutylmethylxanthine (Sigma-Aldrich) at 37 °C for 15 min. Then either buffer alone or different concentrations of NDP- or α-MSH were added and the incubation was continued for 1 h. The reaction was terminated on ice and the intracellular cAMP was extracted by the addition of 0.5 N perchloric acid containing 180 μg/ml theophylline and 0.72 M KOH/0.6 M $KHCO_3$ into each well. cAMP concentrations were determined by radioimmunoassay as described in detail before (Steiner et al., 1969).

3.2.8 ERK1/2 phosphorylation assay

Twenty-four hours after transfection, cells were starved in Waymouth/BSA at 37 °C for another 24 h. Upon treatment with or without 1 μM NDP-MSH or 10 μM α-MSH at 37 °C for 5 min, cells were collected after being washed with cold 0G (150 mM NaCl and 20 mM Hepes, pH 7.4). Total protein concentrations were determined by Bradford protein assay, and 30 μg protein samples were separated by 10% SDS–PAGE and blotted onto pre-wetted PVDF membranes. After blocking in 10% nonfat dry milk for at least 4 h at room temperature with agitation, the membranes were then immunoblotted with the primary antibodies, rabbit anti-pERK1/2 antibody (1:2000; Cell Signaling, Billerica, MA) and mouse anti-β-tubulin antibody (1:5000; Developmental Studies Hybridoma Bank, the University of Iowa) overnight at 4 °C. This was followed by the incubation of the HRP-conjugated secondary antibodies, donkey anti-rabbit IgG (1:2000; Jackson ImmunoResearch, West Grove, PA) and donkey anti-mouse IgG (1:5000; Jackson ImmunoResearch) for at least 1 h at room temperature. Specific bands were visualized with ECL reagent (Thermo Scientific, Rockford, IL) and were analyzed and quantified by Image J Software (NIH, Bethesda, MD).

3.2.9 Antagonist treatment of the HEK293 cells

This method was performed as described before (Fan and Tao, 2009). Briefly, HEK293 cells stably expressing WT, M161T, or I316S MC4Rs were plated on gelatin-coated six-well plates. Then cells were incubated in the presence of 0.1% DMSO, 1 μM Ipsen 5i, or 10 μM ML00253764 at 37 °C for 24 h. On the day of experiment, cells were either immunostained at non-permeabilized status for flow cytometry study or stimulated with 1 μM NDP-MSH for 1 h for cAMP signaling assay.

3.2.10 Statistical analysis

Ligand binding and signaling data were analyzed using GraphPad Prism 4.0 to calculate maximal binding (B_{max}), 50% inhibition concentration (IC_{50}), maximal response (R_{max}), and 50% maximal response concentration (EC_{50}). The significance of differences in cell surface and total expression levels, pEKR1/2 levels, as well as binding and signaling parameters between the WT and mutant hMC4Rs were analyzed using Student's *t*-test with Prism 4.0.

3.3 Results

3.3.1 Localization of WT and mutant hMC4Rs by confocal microscopy

Previous studies suggested intracellular retention is the predominant defect in naturally occurring mutant hMC4Rs. Therefore, we performed confocal microscopy to study the localization of these hMC4Rs. The monoclonal antibody 9E10, which selectively binds to the myc epitope tag at the N-terminus of hMC4R, revealed the localization of hMC4R. As shown in Fig. 3.2, T112K, M161T, M215L, R310K, and I316S had significantly reduced or even absent cell surface expression whereas the rest of mutants were expressed at the cell surface as good as WT hMC4R.

3.3.2 Quantification of WT and mutant hMC4R expression by flow cytometry

To quantitate the expression of mutant hMC4Rs, flow cytometry was performed. Consistent with the confocal microscopy results, the data from non-permeabilized cells showed that T112K, M161T, M215L, R310K, and I316S had significantly reduced cell surface expression compared to WT control (Fig. 3.3A). The results from permeabilized cells showed that all the mutants had

similar total expression levels as those of WT hMC4R except that T112K had a small but statistically significant decrease in total expression levels (Fig. 3.3B).

3.3.3 Ligand binding of WT and mutant hMC4Rs

To investigate whether the *MC4R* mutations cause alterations in the ligand binding properties of the receptor, competitive ligand binding assays were performed using NDP- or α-MSH as the competitor. NDP-MSH is a synthetic superpotent agonist and α-MSH is a natural agonist for MCRs except MC2R. Both agonists are widely used in MC4R functional studies.

When NDP-MSH was used as the ligand, M161T had no detectable binding whereas R310K and I316S showed increased affinity compared to the WT hMC4R (Fig. 3.4A and Table 3.2). When α-MSH was employed as the competitor, similar results were observed except that R310K had normal IC_{50} (Fig. 3.4B and Table 3.2). Maximal binding values were also calculated from the binding assays. In addition to M161T with no measurable binding, three mutants, T101N, R310K, and I316S, had significantly reduced B_{max} compared to the WT hMC4R (Fig. 3.4 and Table 3.2).

3.3.4 cAMP signaling of WT and mutant hMC4Rs

To investigate whether the missense *MC4R* mutations alter the signaling properties, the agonist-induced intracellular cAMP production was measured. As shown in Fig. 3.5A-B and Table 3.3, WT hMC4R showed a dose-dependent increase in intracellular cAMP accumulation in stimulation with NDP- and α-MSHs, with EC_{50}s of 0.34 and 2.64 nM, respectively. When NDP-MSH was used as the ligand, all the mutants showed similar R_{max} and EC_{50} values as those of WT hMC4R except that L207V and R310K had significantly decreased EC_{50}s (Fig. 3.5A and

Table 3.3). When α-MSH was used as the ligand, M161T only responded to > 1 μM α-MSH stimulation (Fig. 5B). T101N had increased EC_{50} and I316S displayed decreased R_{max}, whereas the other mutants could signal similarly as the WT hMC4R (Fig. 3.5B and Table 3.3).

Since it has been suggested that constitutive activity of MC4R might be important for maintaining long-term energy homeostasis in human (Srinivasan et al., 2004), we also measured the basal activity. The basal cAMP levels of the WT receptor were 24.30 ± 4.85 pmol/10^6 cells. Four mutants, L207V, M215L, R310K, and I316S, displayed significant elevation in basal activity whereas M161T had lower basal cAMP levels compared to WT hMC4R. The other mutants exhibited normal basal signaling (Fig. 3.5C).

3.3.5 ERK1/2 signaling of WT and mutant hMC4Rs

Both *in vitro* and *in vivo* studies have demonstrated that MC4R activation leads to ERK1/2 phosphorylation and defective ERK1/2 signaling might be involved in obesity pathogenesis. Therefore, the ERK1/2 signaling of mutant hMC4Rs were also investigated.

Upon stimulation with 1 μM NDP-MSH, WT and five mutant hMC4Rs (L23R, T112K, M161T, M215L, and R310K) showed significantly increased pERK1/2 levels compared to basal condition whereas K73R, T101N, L207V, and I316S failed to respond to NDP-MSH stimulation in ERK1/2 activation (Fig. 6A-B). Upon stimulation with 10 μM α-MSH, WT and six mutant hMC4Rs (K73R, T112K, M161T, L207V, M215L, and R310K) showed significantly elevated ERK1/2 phosphorylation whereas L23R, T101N, and I316S did not respond to α-MSH stimulation in the ERK1/2 activation (Fig. 6C-D).

In addition, we showed that all the mutants, including the L207V, M215L, R310K, and I316S that were constitutively active in the cAMP pathway as well as M161T that exhibited

decreased basal cAMP levels, had similar basal pERK1/2 levels as those of WT hMC4R (Fig. 3.6E).

3.3.6 MTII or THIQ-induced cAMP signaling of M161T hMC4R

Interestingly, our data showed that M161T exhibited severely impaired cAMP signaling in response to α-MSH but had normal NDP-MSH-stimulated cAMP production (Fig. 3.5A-B). To test whether other MC4R agonists could also induce normal cAMP signaling of M161T, MTII and THIQ, two potent synthetic MC4R agonists with nanomolar potency, were employed (Al-Obeidi et al., 1989; Sebhat et al., 2002). Our results showed that the EC_{50}s of MTII and THIQ for the WT MC4R was 0.58 and 2.36 nM, respectively (data not shown). In addition, M161T failed to respond to MTII (Fig. 3.7A) and only had a modest increase in the cAMP levels upon 1 μM THIQ stimulation (Fig. 3.7B).

3.3.7 Functional rescue of thirteen Class II hMC4Rs

Since Ipsen 5i or ML00253764 have been reported as pharmacoperones for MC4R (Fan and Tao, 2009; Tao and Huang, 2014), we measured the effects of these two small molecules on the cell surface expression and function of M161T and I316S, together with other eleven Class II MC4R mutants (including I69T, I102S, T162I, R165Q, R165W, I195S, I269N, Y287X, P299H, A303P, and Q307X).

HEK293 cell stably expressing WT and mutant hMC4Rs were incubated with 1 μM Ipsen 5i or 10 μM ML00253764 for 24 h and assayed for flow cytometry. As shown in Fig. 3.8A, the cell surface expression of eleven mutants (I69T, I102S, M161T, T162I, R165Q, R165W, I195S, I269N, P299H, A303P, and I316S) treated with Ipsen 5i were dramatically increased to a

level that were similar or even higher than that of the vehicle-treated WT hMC4R whereas those of two other mutants (Y287X and Q307X) were not significantly increased. ML00253764 significantly enhanced the cell surface expression of ten mutants (I69T, I102S, M161T, T162I, R165Q, R165W, I195S, I269N, A303P, and I316S) compared to that of the vehicle-treated controls but had no significant effect on that of Y287X, P299H, and Q307X. Notably, WT hMC4R also showed a 1.5-fold increase in the cell surface expression after each antagonist treatment (Fig. 3.8A).

To further investigate whether the rescued mutant hMC4Rs were functional at the cell surface, the cells were stimulated with 1 μM NDP-MSH for 1 h and the intracellular cAMP levels were measured. As shown in Fig. 3.8B, Ipsen 5i treatment significantly increased cAMP signaling of I69T, M161T, T162I, R165Q, R165W, and A303P whereas it had no effect on I195S, I269N, Y287X, P299H, Q307X, and I316S compared to that of the corresponding vehicle-treated controls. In addition, ML00253764 treatment significantly elevated NDP-MSH-stimulated cAMP production of I69T, M161T, T162I, and R165W whereas it did not affect R165Q, I195S, I269N, Y287X, P299H, A303P, Q307X, and I316S. It should be noted that both Ipsen 5i and ML00253764 treatment attenuated NDP-MSH-induced cAMP production in WT and I102S hMC4Rs by approximately 40% and 60%, respectively (Fig. 3.8B).

3.4 Discussion

In the present study, we performed detailed functional analysis of nine novel naturally occurring MC4R mutations with unknown or partially known functional properties. Based on the functional data summarized in Table 3.4, T112K is a Class I mutant, M161T, M215L, R310K,

and I316S are Class II mutants, T101N belongs to Class III, L23R, K73R, and L207V are Class V mutants.

Previous studies showed that T112K has similar cell surface expression and NDP-, α-, or β-MSH-stimulated cAMP production compared to WT hMC4R (Hinney et al., 2006). In this study, despite normal ligand binding and cAMP signaling properties, T112K had significantly impaired total and cell surface expression (Table 3.4). The discrepancy of cell surface expression might be due to the differences in the assays sensitivity and/or the cell types used in two studies. Hence, T112K is a Class I mutant.

Mutants M161T, M215L, R310K, and I316S had normal total expression but significantly decreased cell surface expression compared to the WT hMC4R, and corresponding decreases in maximal binding and/or ligand-stimulated cAMP signaling were also observed (Table 3.2 and 3.3). These data suggested that resides M161, M215L, R310, and I316, located in the intracellular loop or C-terminal tail, were required for MC4R trafficking and targeting onto the cell membrane. Indeed, previous mutagenesis studies of cytoplasmic side of receptor have led to the identification of several conserved motifs that play a critical role in GPCR export from the endoplasmic reticulum (Bermak et al., 2001; Duvernay et al., 2004; Robert et al., 2005). Substitution of residues on or near these motifs might impair receptor anterograde trafficking. Therefore, they are Class II mutants.

T101N was identified from a morbidly obese male but no functional study was reported (Buchbinder et al., 2011). We observed that T101N had normal receptor expression but a significant decrease in B_{max} and a 500-fold increase in EC_{50} in response to α-MSH (Table 3.2 and 3.3). It is well known that TMs and extracellular loops are important for ligand binding and receptor activation in various GPCRs. Residue T101 is located in the extracellular side of TM2, a

region that has been shown to be directly involved in the ligand-receptor interaction (Kalani et al., 2004; Lane et al., 2014; Miura et al., 2003). In addition, by introducing His residues into the MC4R to form metal ion binding sites, Lagerström *et al.* showed that E100 and I104 in TM2 and D122 and I125 in TM3 are involved in the orientation of the helices and activation of the receptor (Lagerstrom et al., 2003). Substitution of T101 might blunt ligand-receptor interaction and lead to defective ligand binding and receptor activation. Therefore, T101N belongs to Class III.

Mutants L23R, K73R and L207V were shown with normal receptor expression, ligand binding, and cAMP signaling compared to WT hMC4R (Table 3.4). Therefore, they are Class V mutants. However, L23R, K73R and L207V failed to respond to either NDP- or α-MSH in the ERK1/2 signaling pathway (Fig. 3.6), suggesting defect in the ERK1/2 signaling pathway might be a cause of obesity in the patients harboring these Class V mutations. Consistently, similar observations were reported previously (He and Tao, 2014).

Unexpectedly, mutant M161T with severely defective α-MSH-stimulated cAMP signaling (Fig. 3.5B) had dose-dependent cAMP production that was similar to WT MC4R upon NDP-MSH stimulation (Fig. 3.5A). Consistent with our observations, Xiang *et al.* demonstrated that synthetic agonists, NDP-MSH, MTII, THIQ, and AMW3-130, restore normal functional response of some mutant hMC4Rs that have decreased endogenous agonist potency (Xiang et al., 2007; Xiang et al., 2010). To further test the potential of other potent synthetic ligands to rescue the cAMP signaling of M161T hMC4R, MTII and THIQ, two potent and widely used MC4R agonists, were also employed for the cAMP assay. Our results demonstrated that M161T was also severely defective in responding to MTII or THIQ stimulation (Fig. 3.7). THIQ- and NDP-MSH-induced divergent cAMP signaling through MC4R have been reported. Yang *et al.*

demonstrated that THIQ-induced cAMP signaling through double MC4R mutant T150H/K242H is blocked by Zn^{2+}, whereas NDP-MSH-initiated signaling is not, suggesting that structurally different MC4R ligands could induce distinct downstream signaling by stabilizing the receptor in different conformations (Yang et al., 2014). Therefore, the difference of cAMP response induced by NDP-MSH and that by α-MSH or MTII might also result from the subtle differences of the MC4R conformations stabilized by these agonists. NDP-MSH but not α-MSH or MTII could stabilize the M161T in a conformation that is similar to that of activated WT hMC4R. Although NDP-MSH shares high structural homology with α-MSH and MTII, previous studies have revealed that subtle changes in the receptor conformation (molecular movements as small as 1 Å) could result in dramatic modification on the activity of receptor and downstream enzymes (Koshland, 1998; Rahmeh et al., 2012). However, the molecular basis responsible for MC4R signaling mediated by different agonists demands further investigation.

The WT MC4R is constitutively active and loss of basal activity in the mutant MC4Rs has been suggested to be one cause of obesity (Srinivasan et al., 2004). We demonstrated that mutants L207V, M215L, R310K, and I316S with normal basal pERK1/2 levels, were constitutively active in the cAMP signaling pathway. Similar results were observed before. We previously reported that two MC4R mutants (A244G and A259G) with normal basal pERK1/2 levels are constitutively active in the cAMP signaling (Huang and Tao, 2012). These findings support the currently accepted dogma that GPCRs exist in multiple active conformations and some mutant GPCRs preferentially stabilize certain active conformations (Reiter et al., 2012).

Collectively, we showed that NDP-MSH selectively elevated cAMP production for K73R, T101N, L207V, and I316S without significant activation of ERK1/2 cascade (Table 3.5), whereas α-MSH selectively elevated cAMP production for L23R, T101N, and I316S without

significant activation of ERK1/2 cascade (Table 3.5). Therefore, these mutants were biased receptors, in which agonist only stabilizes a restricted subset of conformations activating one signaling pathway. Indeed, biased signaling in the cAMP and ERK1/2 signaling pathways has been previously reported in the MC4R (He and Tao, 2014; Huang and Tao, 2012) and melanocortin-3 receptor (Yang et al., 2015a; Yang et al., 2015b). These data confirm the existence of multiple activation states of MC4R with ligand-specific and/or mutant-specific conformations that could couple MC4R to distinct signaling pathways, adding a new layer of complexity to the MC4R signaling.

Interestingly, mutant M161T with no measurable ligand binding responded to both ligands with increased ERK1/2 phosphorylation levels (Fig. 3.4 and 3.6). Though it is uncommon, similar observations have previously been reported in other GPCRs, including melanocortin-3 receptor (Yang et al., 2015b) and gonadotropin-releasing hormone receptor (Bedecarrats et al., 2003). One possible explanation is that these mutant receptors had a lower affinity and underwent a faster dissociation of the ligand, making the binding hard to detect, whereas the ERK1/2 activation could still be achieved by this transient binding (Huang and Tao, 2014a; Yang et al., 2015b).

In tune with previous findings that intracellular retention is the most common defect of inactivating mutant MC4Rs, we showed that four of the nine (44.5%) *MC4R* mutations had defective cell surface expression. The effects of Ipsen 5i and ML00253764 on the cell surface expression and function of intracellularly retained mutant MC4Rs were determined in this study. As shown in Fig. 3.8A, Ipsen 5i and ML00253764 treatment rescued the cell surface expression in 85% and 77%, and the function in 46% and 39% of the thirteen intracellularly retained mutant MC4Rs, respectively. The cell surface expression levels in most mutants were dramatically

increased up to 6 folds compared with the vehicle-treated controls, most of which were even higher than the vehicle-treated WT MC4R, suggesting high rescuing efficiency of Ipsen 5i and ML00253764.

The cell surface expression and function of I69T, M161T, T162I, R165Q, R165W, and A303P hMC4Rs were rescued by Ipsen 5i and those of I69T, M161T, T162I, and R165W hMC4Rs were rescued by ML00253764 (Fig. 3.8), indicating the functionality of these mutants could be restored once they were escorted to the cell membrane. I102S, I195S, I269N, and I316S hMC4Rs treated with Ipsen 5i or ML00253764 had obviously increased cell surface expression but unchanged cAMP production (Fig. 3.8), suggesting that the defects of these mutants were not only due to intracellular retention but also abnormal ligand binding or signaling. Mutants Y287X, P299H, and Q307X were not rescued by Ipsen 5i and ML00253764 in the cell surface expression and cAMP signaling with the exception that P299H only had a small increase in cell surface expression (Fig. 3.8), indicating that these mutants might suffer more severe conformational instability and could not be rescued by these two small molecules.

It should be noted that the cell surface expression of WT hMC4R was also increased by 50% after antagonist treatment (Fig. 3.8A), suggesting a potential therapeutic strategy for treatment of obese patients that do not harbor *MC4R* mutations. We also showed the cAMP production of WT hMC4R treated with ML00253764 or Ipsen 5i was dramatically reduced to ~60% of vehicle-treated control after 1h stimulation of NDP-MSH (Fig. 3.8B), which might be caused by residual Ipsen 5i or ML00253764 that still occupied the receptor, competing with NDP-MSH and blocking its binding with WT hMC4R. This antagonizing effect led to decreased cAMP production.

In summary, a systematic functional study of nine naturally occurring *MC4R* mutations was performed. In agreement with previous studies, four out of nine MC4R mutants were shown to be trapped intracellularly, suggesting that intracellular retention is the most common defect of naturally occurring *MC4R* mutations. We also demonstrated that defect in the ERK1/2 signaling might be a cause of obesity in patients harboring Class V mutants. Five mutant receptors were shown to be biased receptors in the cAMP and ERK1/2 signaling pathways. In addition, we showed that Ipsen 5i and ML00253764 could act as pharmacoperones to rescue the cell surface expression and function of Class II mutant MC4Rs. The data obtained in our study might provide insights into the structure-function relationship of the MC4R, contribute to a better understanding of MC4R pharmacology, and present a potential personalized medicine for treatment of obesity.

Table 3.1 Phenotypes of patients carrying the nine *MC4R* mutations investigated in the current study.

hMC4R	Prevalence (%)	Phenotypes	Age of obesity onset	References
L23R	0.50[b]	BMI 27.6	Before 10.8	(Wang et al., 2006)
K73R	0.99[b]	RBMI 163.6	Unknown	(Nowacka-Woszuk et al., 2011)
T101N	Unknown	BMI 62	10	(Buchbinder et al., 2011)
T112K	0.02[c]	BMI 28.5	Unknown	(Hinney et al., 2006)
M161T	0.05[a]	Unknown	Before 10	(Tan et al., 2009)
L207V	0.20[a]	BMI 42.4	Unknown	(Rouskas et al., 2012)
M215L	0.41[b]	RBMI 166.0	Before 17	(Nowacka-Woszuk et al., 2011)
R310K	0.50[b]	BMI 27.6	Before 10.8	(Wang et al., 2006)
I316S	0.86[b]	Unknown	Before 10	(Yeo et al., 2003)

BMI, body mass index (defined as body weight in kilograms divided by height in meters squared); RBMI, relative body mass index (defined as the BMI of every obese patient divided by the ideal (50th percentile) BMI for their age and gender and multiplying the obtained result by 100).

[a] Data was obtained from population-based samples.

[b] Data was obtained from obese children and adolescents.

[c] Data was obtained from obese adults.

Table 3.2 Ligand binding properties of WT and mutant hMC4Rs.

hMC4R	n	B_{max} (% WT)	IC_{50} (nM)	
			NDP-MSH	α-MSH
WT	10	100	42.94 ± 13.88	1133.16 ± 260.51
L23R	5	95.05 ± 15.23	23.84 ± 7.28	1408.64 ± 321.15
K73R	5	116.47 ± 15.01	21.02 ± 7.28	967.22 ± 183.52
T101N	5	60.25 ± 4.74[b]	39.54 ± 8.86	1512.23 ± 964.90
T112K	5	102.55 ± 5.84	23.98 ± 8.65	1292.52 ± 503.06
M161T	5	ND[c]	ND[c]	ND[c]
L207V	5	121.71 ± 12.31	37.84 ± 10.08	1192.06 ± 484.85
M215L	5	117.39 ± 11.94	24.19 ± 7.78	860.86 ± 137.81
R310K	5	60.58 ± 8.98[b]	10.80 ± 3.23[a]	555.00 ± 111.87
I316S	5	36.98 ± 6.73[b]	7.54 ± 1.87[a]	405.68 ± 149.41[a]

[a] Significantly different from WT hMC4R, $p < 0.05$.

[b] Significantly different from WT hMC4R, $p < 0.001$.

[c] Not detectable.

B_{max} values are mean ± SEM of at least ten independent experiments with NDP- or α-MSH as the ligand, and the values of other parameters are mean ± SEM of at least five independent experiments.

Table 3.3 Agonist-stimulated cAMP signaling of WT and mutant hMC4Rs.

hMC4R	n	NDP-MSH		α-MSH	
		EC_{50} (nM)	R_{max} (% WT)	EC_{50} (nM)	R_{max} (% WT)
WT	8	0.34 ± 0.05	100	2.64 ± 0.69	100
L23R	4	0.43 ± 0.10	115.16 ± 18.07	4.58 ± 1.59	131.88 ± 5.49[c]
K73R	4	0.33 ± 0.11	89.92 ± 16.94	3.79 ± 1.07	117.87 ± 19.41
T101N	4	0.51 ± 0.10	107.06 ± 30.41	931.05 ± 63.46[c]	113.78 ± 11.10
T112K	4	0.34 ± 0.06	127.96 ± 27.36	5.72 ± 1.56	123.65 ± 16.46
M161T	4	1.95 ± 0.77	100.08 ± 13.47	1377.67 ± 194.89[c]	39.13 ± 11.09[b]
L207V	4	0.16 ± 0.01[a]	112.91 ± 17.52	1.27 ± 0.30	107.84 ± 20.21
M215L	4	0.48 ± 0.11	107.44 ± 25.01	3.64 ± 1.22	122.28 ± 24.95
R310K	4	0.10 ± 0.03[b]	129.26 ± 6.96[a]	1.09 ± 0.29	108.54 ± 25.53
I316S	4	0.49 ± 0.13	173.63 ± 34.07	0.45 ± 0.09[a]	51.15 ± 8.96[b]

[a] Significantly different from WT hMC4R, $p < 0.05$.

[b] Significantly different from WT hMC4R, $p < 0.01$.

[c] Significantly different from WT hMC4R, $p < 0.001$.

EC_{50} and R_{max} values are mean ± SEM of at least four independent experiments. The R_{max} of WT hMC4R was 1296.48 ± 260.55 pmol/10^6 cells with NDP-MSH stimulation and was 1543.94 ± 359.22 pmol/10^6 cells with α-MSH stimulation.

Table 3.4 Summary of functional properties of the nine mutant hMC4Rs studied herein.

hMC4R	Total expression	Cell surface expression	Binding	cAMP Signaling		Class[a]
				Basal	Stimulated	
L23R	—	—	—	—	—	V
K73R	—	—	—	—	—	V
T101N	—	—	↓	—	↓	III
T112K	↓	↓	—	—	—	I
M161T	—	↓	↓	↓	↓	II
L207V	—	—	—	↑	—	V
M215L	—	↓	—	↑	—	II
R310K	—	↓	↓	↑	—	II
I316S	—	↓	↓	↑	↓	II

"↓": denotes the particular function is defective.

"—": denotes the particular function is normal.

[a] The classification of the hMC4R mutants is based on the scheme we proposed earlier.

Table 3.5 The effect of ligands on cAMP and ERK1/2 signaling in WT and mutant hMC4Rs.

hMC4R	NDP-MSH-stimulated signaling			α-MSH-stimulated signaling		
	cAMP	ERK1/2	Bias	cAMP	ERK1/2	Bias
WT	↑	↑	No	↑	↑	No
L23R	↑	↑	No	↑	—	Yes
K73R	↑	—	Yes	↑	↑	No
T101N	↑	—	Yes	↑	—	Yes
T112K	↑	↑	No	↑	↑	No
M161T	↑	↑	No	↑	↑	No
L207V	↑	—	Yes	↑	↑	No
M215L	↑	↑	No	↑	↑	No
R310K	↑	↑	No	↑	↑	No
I316S	↑	—	Yes	↑	—	Yes

The column “Bias” is designated for whether the ligand-induced cAMP and ERK1/2 signaling pathways were divergent, in which “No” denotes balanced cAMP and ERK1/2 signaling, whereas “Yes” denotes biased activation of either signaling pathway. “↑”: denotes increased activity compared to the basal level. “—”: denotes no significant changes between basal and maximal signaling levels.

Figure 3.1 Schematic model of hMC4R with the nine novel naturally occurring mutations characterized in this study highlighted with gray background.

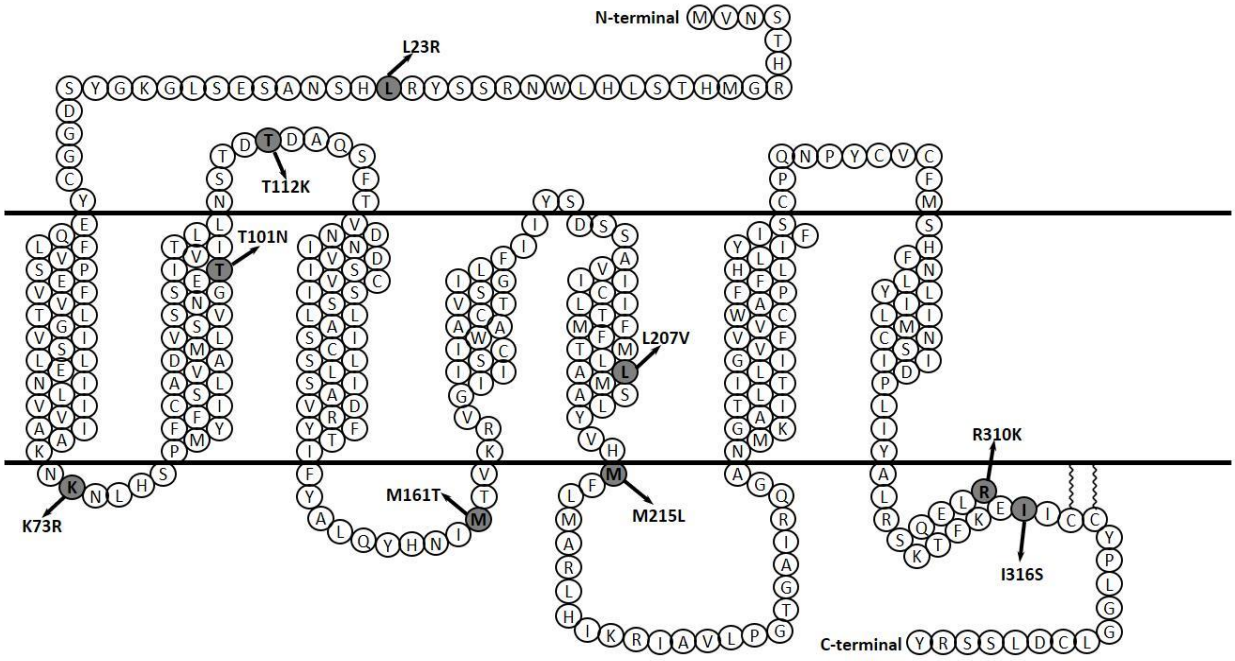

Figure 3.2 Confocal imaging of WT and mutant hMC4Rs.

The HEK293 cells stably transfected with pcDNA3.1, WT, and mutant myc-MC4Rs were stained with Alexa fluorescent 488 antibody and imaged by confocal microscopy. Similar results were observed in at least three independent experiments.

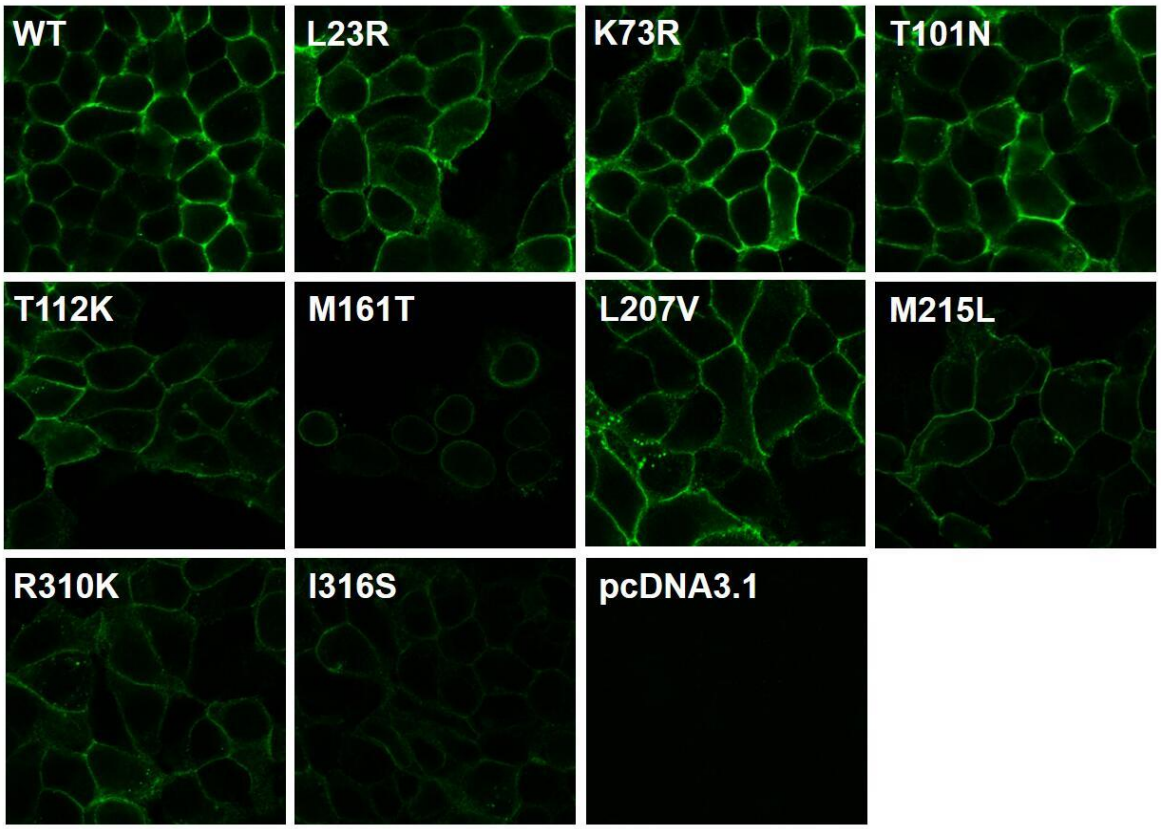

Figure 3.3 Cell surface and total expression of WT and mutant hMC4Rs.

Cell surface expression levels (A) or total expression levels (B) of the WT and mutant hMC4Rs were measured by flow cytometry. The results were expressed as a percentage of cell surface expression levels or total expression levels of the WT hMC4R with correction of the nonspecific staining in cells stably transfected with the empty vector. Data were mean ± SEM of four experiments. Star (*) indicates significantly different from WT hMC4R ($p < 0.05$).

A

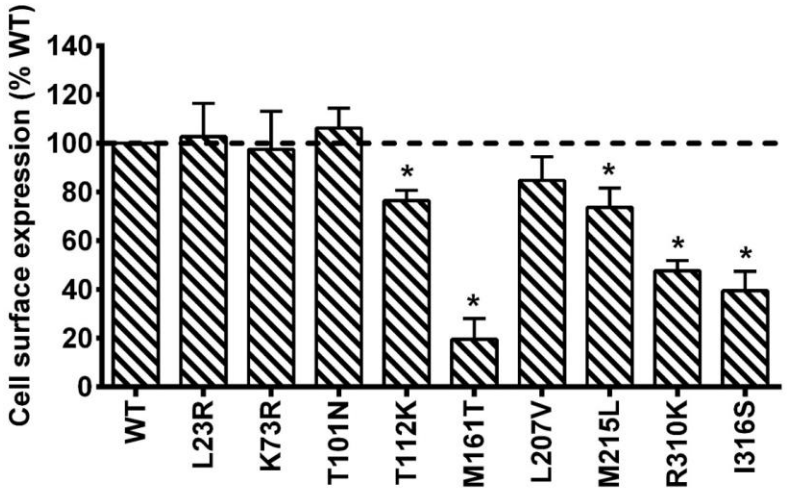

B

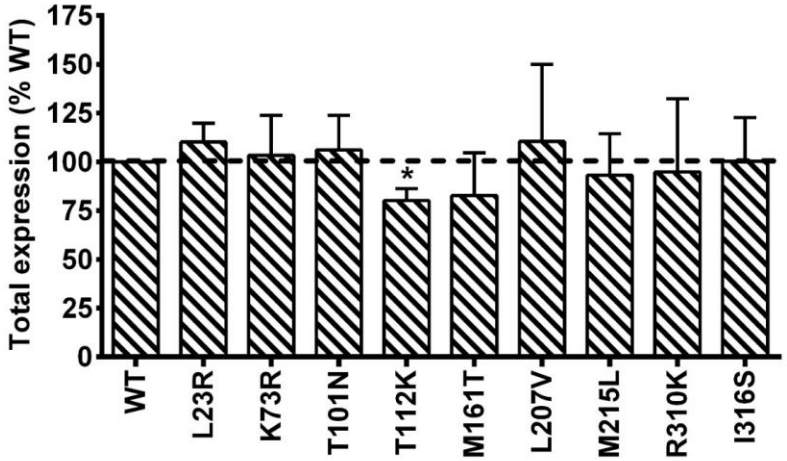

Figure 3.4 Ligand binding properties of WT and mutant hMC4Rs with NDP-MSH or α-MSH as the competitor.

HEK293T cells were transiently transfected with the indicated hMC4R constructs and binding properties of the receptors were measured by displacing the binding of ^{125}I-NDP-MSH with different concentrations of unlabeled NDP-MSH (A) or α-MSH (B) as described in Materials and Methods. Results shown are expressed as % of WT binding ± range from duplicate determinations within one experiment. All experiments were performed at least three times.

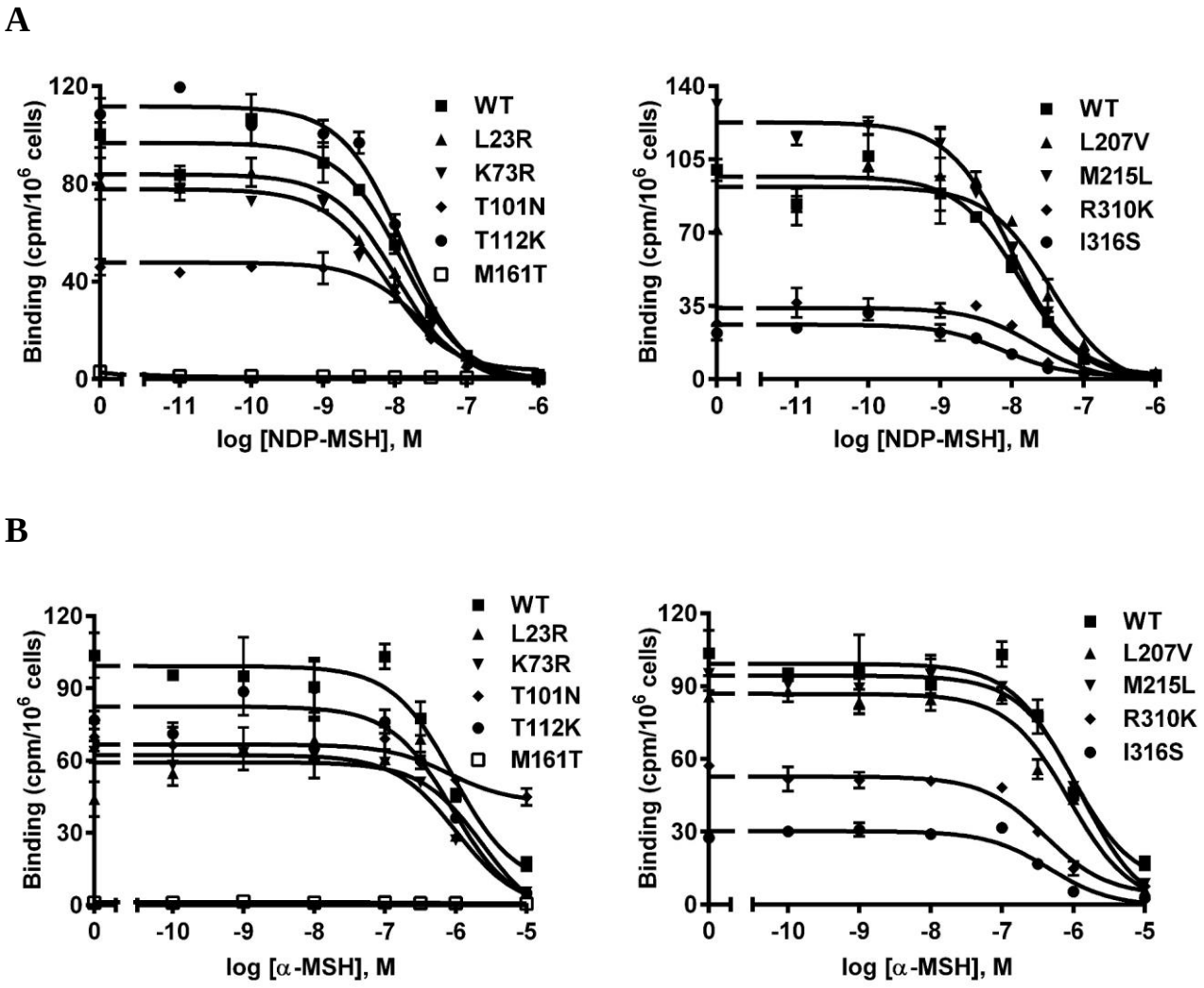

Figure 3.5 cAMP signaling of WT and mutant hMC4Rs with NDP-MSH or α-MSH as the ligand.

HEK293T cells were transiently transfected with the indicated hMC4R constructs were stimulated with different concentrations of NDP-MSH (A) or α-MSH (B). Intracellular cAMP levels were measured as descried in Materials and Methods. The basal cAMP signaling (C) of mutant hMC4Rs are expressed as % of WT basal signaling. Results were expressed as mean ± SEM of at least triplicate determinations within one experiment. All the experiments were performed at least four times. Star (*) indicates significantly different from WT hMC4R ($p < 0.05$).

A

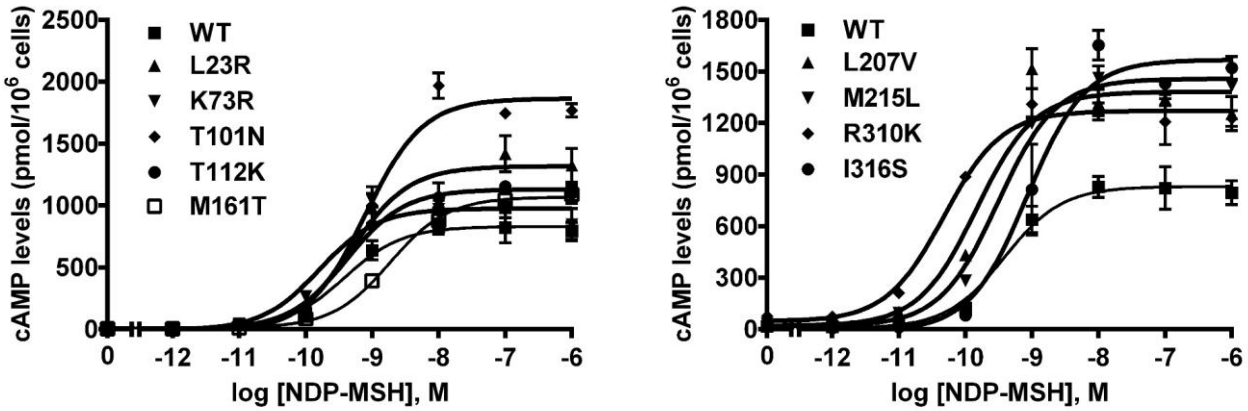

B

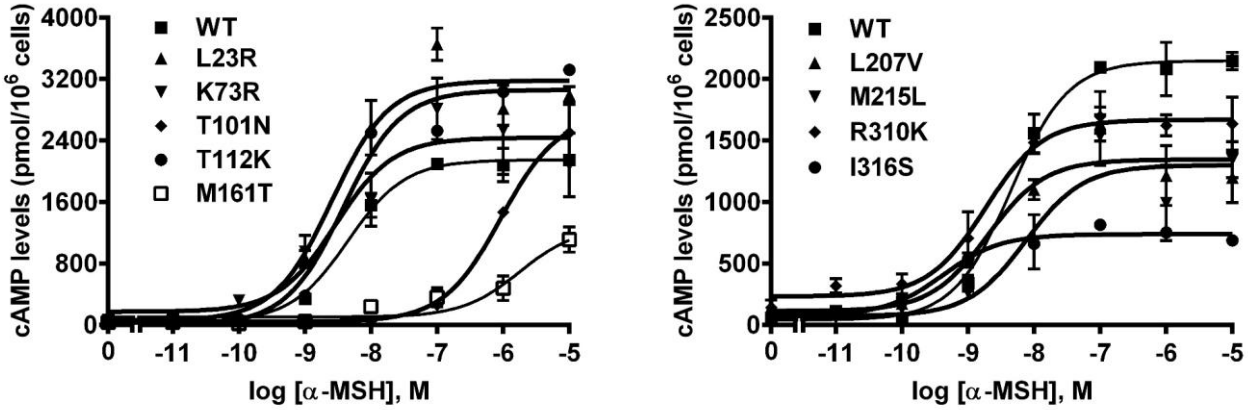

C

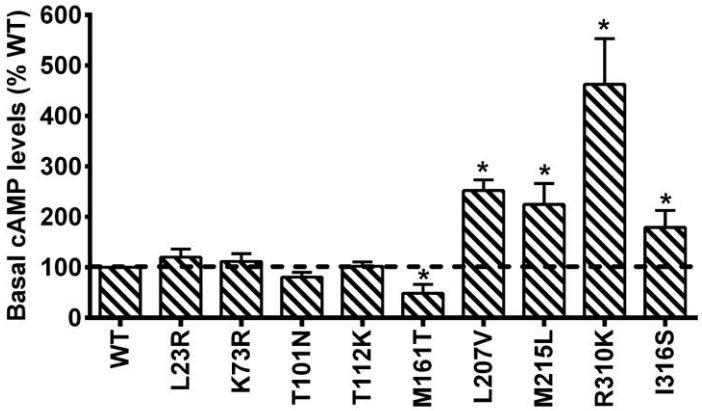
Basal cAMP levels (% WT)
600
500
400
300
200
100
0
WT
L23R
K73R
T101N
T112K
M161T
L207V
M215L
R310K
I316S
*

Figure 3.6 ERK1/2 signaling of WT and mutant hMC4Rs with NDP- or α-MSH as the ligand.

HEK293T cells were stimulated with or without 1 μM NDP-MSH or 10 μM α-MSH for 5 min. ERK1/2 phosphorylation was measured as described in Materials and Methods. Panel A and C showed the representative image of one experiment. Panel B and D showed the densitometry results of ERK1/2 phosphorylation of ligand-stimulated WT and mutant hMC4Rs, expressed as the percentage of the value obtained in non-stimulated cells transfected with corresponding construct. Panel E showed basal pERK1/2 levels of mutant hMC4Rs, expressed as a percentage of WT basal pERK1/2 levels. Shown are mean ± SEM of at least five experiments. Star (*) indicates significantly different from the control group treated with DMSO ($p < 0.05$).

A

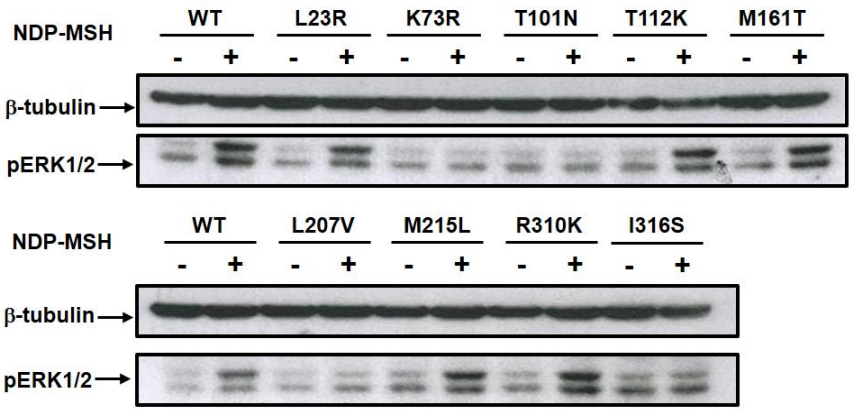
NDP-MSH
WT
L23R
K73R
T101N
T112K
M161T
- + - + - + - + - + - +
β-tubulin
pERK1/2
NDP-MSH
WT
L207V
M215L
R310K
I316S
- + - + - + - + - +
β-tubulin
pERK1/2

B

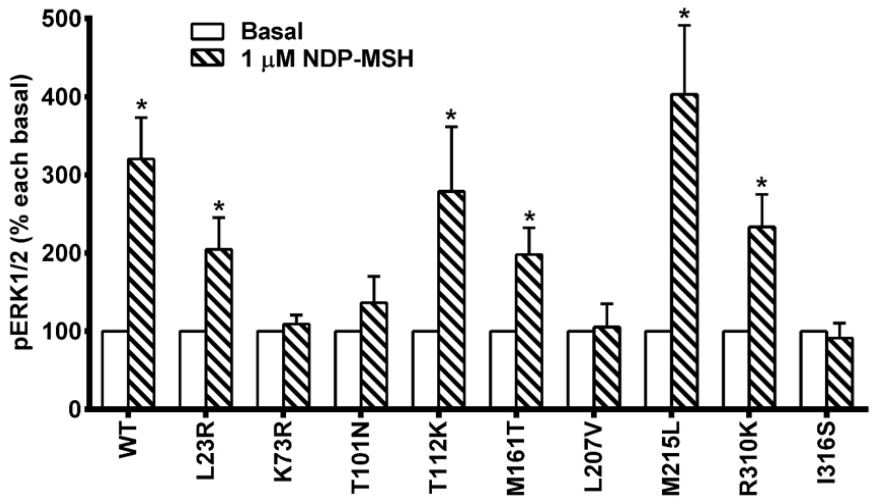
Basal
1 μM NDP-MSH
pERK1/2 (% each basal)
500
400
300
200
100
0
*
WT
L23R
K73R
T101N
T112K
M161T
L207V
M215L
R310K
I316S

C

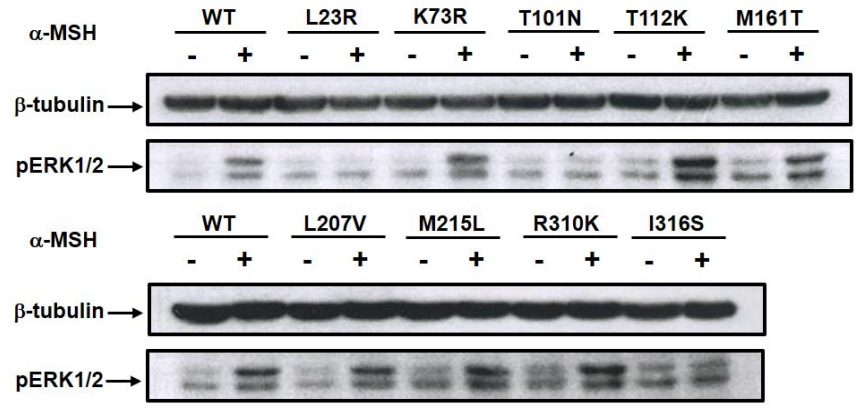
α-MSH
WT
L23R
K73R
T101N
T112K
M161T
- + - + - + - + - + - +
β-tubulin
pERK1/2
α-MSH
WT
L207V
M215L
R310K
I316S
- + - + - + - + - +
β-tubulin
pERK1/2

D

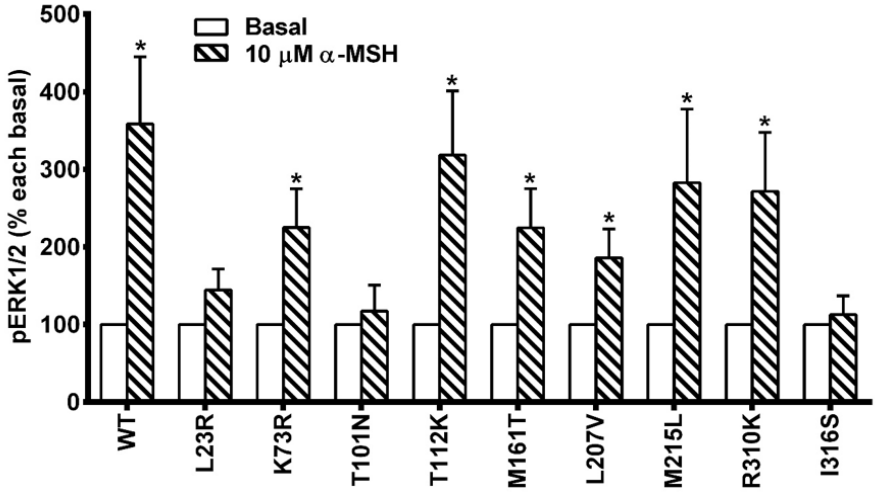
Basal
10 μM α-MSH
pERK1/2 (% each basal)
500
400
300
200
100
0
WT
L23R
K73R
T101N
T112K
M161T
L207V
M215L
R310K
I316S

E

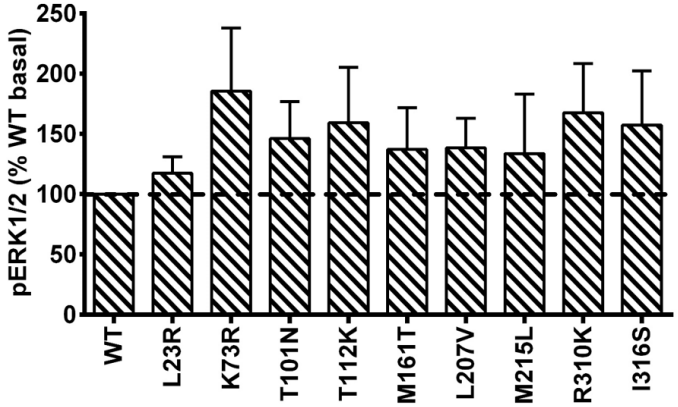
pERK1/2 (% WT basal)
250
200
150
100
50
0
WT
L23R
K73R
T101N
T112K
M161T
L207V
M215L
R310K
I316S

Figure 3.7 cAMP signaling of M161T hMC4R in stimulation with MTII or THIQ. HEK293T cells were transiently transfected with M161T hMC4R were stimulated with different concentrations of MTII (A) or THIQ (B). Intracellular cAMP levels were measured using RIA described in Materials and Methods. Results are expressed as mean ± SEM of at least triplicate determinations within one experiment. All the experiments were performed at least four times.

A

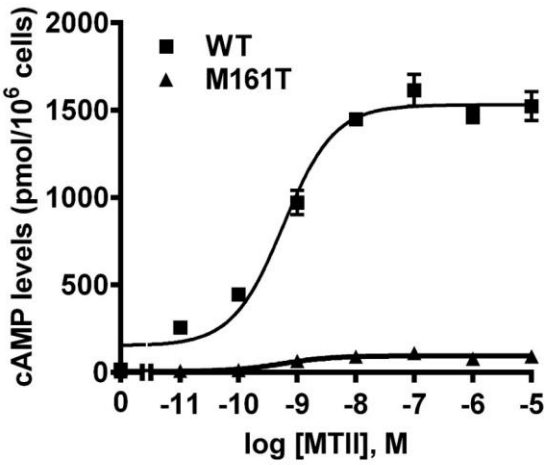

B

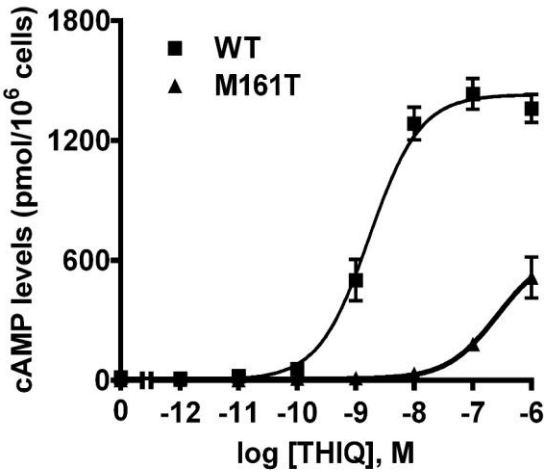

Figure 3.8 Pharmacological rescue of Class II MC4R mutants by Ipsen 5i or ML00253764.

HEK293 cell stably expressing WT and mutant MC4Rs were treated with 0.1% DMSO, 1 μM Ipsen 5i or 10 μM ML00253764 for 24 h, then were sorted with flow cytometry to quantitatively measure the cell surface expression (A) or cAMP assay to measure the cAMP production after 1 h stimulation with 1 μM NDP-MSH (B). Cell surface expression or cAMP levels of WT hMC4R treated with vehicle were set as 100% in each experiment. Shown are mean ± SEM of at least three experiments. Star (*) indicates significantly different from the control group treated with DMSO ($p < 0.05$).

A

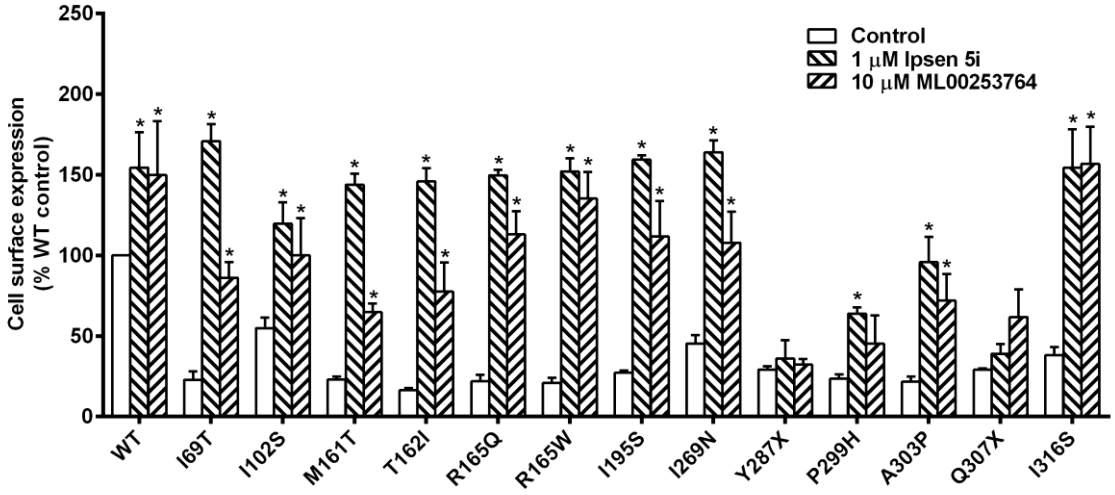
Cell surface expression
(% WT control)
250
200
150
100
50
0
Control
1 μM Ipsen 5i
10 μM ML00253764
WT
I69T
I102S
M161T
T162I
R165Q
R165W
I195S
I269N
Y287X
P299H
A303P
Q307X
I316S

B

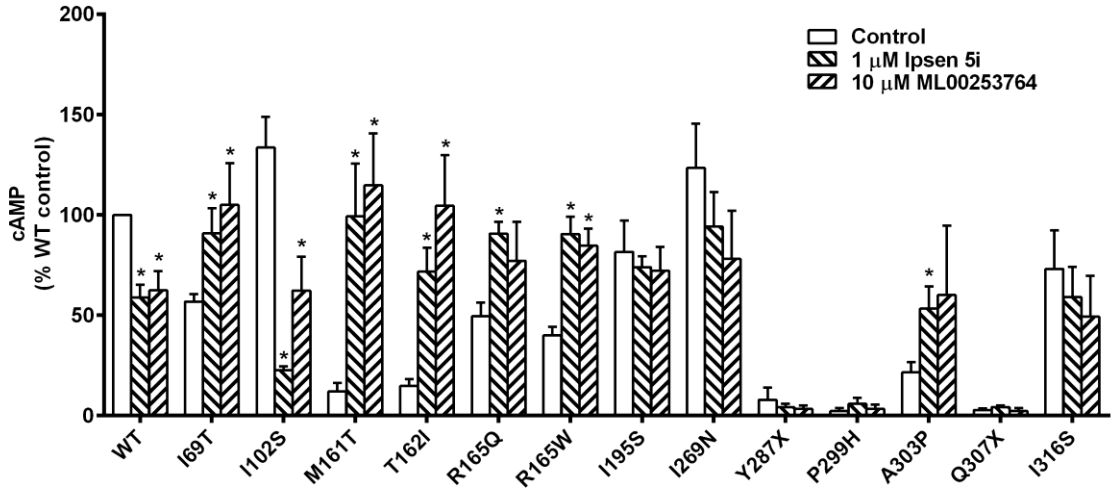
cAMP
(% WT control)
200
150
100
50
0
Control
1 μM Ipsen 5i
10 μM ML00253764
WT
I69T
I102S
M161T
T162I
R165Q
R165W
I195S
I269N
Y287X
P299H
A303P
Q307X
I316S

Conclusions and Future Prospective

Extensive rodent and human studies have suggested the crucial role of MC4R in regulating food intake and energy expenditure. Subsequently, MC4R regulation of energy homeostasis was also demonstrated in other mammals such as rhesus monkeys, dog, cat, pig and sheep. Molecular cloning and pharmacologic characterization of other mammalian MC4Rs are important and necessary to better understand the physiology of MC4R. In addition, mutation in the *MC4R* is the most common monogenic form of obesity. Therefore, unraveling the underlying pathogenic mechanisms of these mutations and seeking therapeutic strategies for treatment of *MC4R* mutation-related obesity are of great importance.

We reported herein the molecular cloning and pharmacology of the amMC4R. Sequence analysis revealed that amMC4R was highly homologous (>88%) at nucleotide and amino acid sequences to several mammalian MC4Rs. We showed that amMC4R bound NDP-MSH with the highest affinity followed by THIQ, α-MSH, and β-MSH, with the same ranking order as hMC4R. Treatment of HEK293T cells expressing amMC4R with different concentrations of agonists resulted in dose-dependent increase of intracellular cAMP levels, with similar EC50s for the four agonists.

Furthermore, the pharmacological study in Chapter 3 demonstrated that four out of nine (44.5%) mutants were defective in targeting onto the cell membrane, suggesting that intracellular retention is the most common defect of naturally occurring *MC4R* mutations. Five mutant receptors were shown to be biased receptors in the cAMP and ERK1/2 signaling pathways and defect in the ERK1/2 signaling might be a cause of obesity in patients harboring Class V mutants. Importantly, two MC4R inverse agonists were shown to act as pharmacoperones to rescue the cell surface expression and function of intracellularly trapped MC4Rs.

The therapeutic feasibility of pharmacoperones has been demonstrated with *in vivo* studies in animals and in humans. Multiple *in vitro* studies have shown that pharmacoperones could rescue many obesity-linked intracellularly retained MC4R mutants with retained intrinsic function. These pharmacoperones are usually orally bioavailable and can cross the blood-brain barrier, opening up the possibility of treating obese patients harboring MC4R mutations. We eagerly await findings from *in vivo* studies of pharmacoperones of the MC4R.

References

Ackroyd, R., Mouiel, J., Chevallier, J.M., Daoud, F., 2006. Cost-effectiveness and budget impact of obesity surgery in patients with type-2 diabetes in three European countries. *Obes Surg* 16, 1488-1503.

Al-Obeidi, F., Hadley, M. E., Pettitt, B. M., & Hruby, V. J., 1989. Design of a new class of superpotent cyclic. alpha-melanotropins based on quenched dynamic simulations. *J Am Chem Soc* 111, 3413-3416.

Arakawa, T., Ejima, D., Kita, Y., Tsumoto, K., 2006. Small molecule pharmacological chaperones: From thermodynamic stabilization to pharmaceutical drugs. *Biochim Biophys Acta* 1764, 1677-1687.

Asai, M., Ramachandrappa, S., Joachim, M., Shen, Y., Zhang, R., Nuthalapati, N., Ramanathan, V., Strochlic, D.E., Ferket, P., Linhart, K., Ho, C., Novoselova, T.V., Garg, S., Ridderstrale, M., Marcus, C., Hirschhorn, J.N., Keogh, J.M., O'Rahilly, S., Chan, L.F., Clark, A.J., Farooqi, I.S., Majzoub, J.A., 2013. Loss of function of the melanocortin 2 receptor accessory protein 2 is associated with mammalian obesity. *Science* 341, 275-278.

Asakawa, A., Inui, A., Kaga, T., Yuzuriha, H., Nagata, T., Ueno, N., Makino, S., Fujimiya, M., Niijima, A., Fujino, M.A., Kasuga, M., 2001. Ghrelin is an appetite-stimulatory signal from stomach with structural resemblance to motilin. *Gastroenterology* 120, 337-345.

Aspiras, A.C., Rohner, N., Martineau, B., Borowsky, R.L., Tabin, C.J., 2015. Melanocortin 4 receptor mutations contribute to the adaptation of cavefish to nutrient-poor conditions. *Proc Natl Acad Sci U S A* 112, 9668-9673.

Balthasar, N., Coppari, R., McMinn, J., Liu, S.M., Lee, C.E., Tang, V., Kenny, C.D., McGovern, R.A., Chua, S.C., Jr., Elmquist, J.K., Lowell, B.B., 2004. Leptin receptor signaling in

POMC neurons is required for normal body weight homeostasis. *Neuron* 42, 983-991.

Balthasar, N., Dalgaard, L.T., Lee, C.E., Yu, J., Funahashi, H., Williams, T., Ferreira, M., Tang, V., McGovern, R.A., Kenny, C.D., Christiansen, L.M., Edelstein, E., Choi, B., Boss, O., Aschkenasi, C., Zhang, C.Y., Mountjoy, K., Kishi, T., Elmquist, J.K., Lowell, B.B., 2005. Divergence of melanocortin pathways in the control of food intake and energy expenditure. *Cell* 123, 493-505.

Banning, A., Gulec, C., Rouvinen, J., Gray, S.J., Tikkanen, R., 2016. Identification of small molecule compounds for pharmacological chaperone therapy of aspartylglucosaminuria. *Sci Rep* 6, 37583.

Barb, C.R., Robertson, A.S., Barrett, J.B., Kraeling, R.R., Houseknecht, K.L., 2004. The role of melanocortin-3 and -4 receptor in regulating appetite, energy homeostasis and neuroendocrine function in the pig. *J Endocrinol* 181, 39-52.

Batterham, R.L., Cohen, M.A., Ellis, S.M., Le Roux, C.W., Withers, D.J., Frost, G.S., Ghatei, M.A., Bloom, S.R., 2003. Inhibition of food intake in obese subjects by peptide YY3-36. *N Engl J Med* 349, 941-948.

Beckers, S., Zegers, D., de Freitas, F., Peeters, A.V., Verhulst, S.L., Massa, G., Van Gaal, L.F., Timmermans, J.P., Desager, K.N., Van Hul, W., 2010. Identification and functional characterization of novel mutations in the melanocortin-4 receptor. *Obes Facts* 3, 304-311.

Bedecarrats, G.Y., Linher, K.D., Janovick, J.A., Beranova, M., Kada, F., Seminara, S.B., Michael Conn, P., Kaiser, U.B., 2003. Four naturally occurring mutations in the human GnRH receptor affect ligand binding and receptor function. *Mol Cell Endocrinol* 205, 51-64.

Benoit, S.C., Air, E.L., Coolen, L.M., Strauss, R., Jackman, A., Clegg, D.J., Seeley, R.J., Woods, S.C., 2002. The catabolic action of insulin in the brain is mediated by melanocortins. *J*

Neurosci 22, 9048-9052.

Bermak, J.C., Li, M., Bullock, C., Zhou, Q.Y., 2001. Regulation of transport of the dopamine D1 receptor by a new membrane-associated ER protein. *Nat Cell Biol* 3, 492-498.

Bernier, V., Morello, J.P., Zarruk, A., Debrand, N., Salahpour, A., Lonergan, M., Arthus, M.F., Laperriere, A., Brouard, R., Bouvier, M., Bichet, D.G., 2006. Pharmacologic chaperones as a potential treatment for X-linked nephrogenic diabetes insipidus. *J Am Soc Nephrol* 17, 232-243.

Biebermann, H., Krude, H., Elsner, A., Chubanov, V., Gudermann, T., Gruters, A., 2003. Autosomal-dominant mode of inheritance of a melanocortin-4 receptor mutation in a patient with severe early-onset obesity is due to a dominant-negative effect caused by receptor dimerization. *Diabetes* 52, 2984-2988.

Bluher, S., Ziotopoulou, M., Bullen, J.W., Jr., Moschos, S.J., Ungsunan, L., Kokkotou, E., Maratos-Flier, E., Mantzoros, C.S., 2004. Responsiveness to peripherally administered melanocortins in lean and obese mice. *Diabetes* 53, 82-90.

Bolze, F., Rink, N., Brumm, H., Kuhn, R., Mocek, S., Schwarz, A.E., Kless, C., Biebermann, H., Wurst, W., Rozman, J., Klingenspor, M., 2013. Characterization of the melanocortin-4-receptor nonsense mutation W16X *in vitro* and *in vivo*. *Pharmacogenomics* J 13, 80-93.

Bottcher, G., Sjoberg, J., Ekman, R., Hakanson, R., Sundler, F., 1993. Peptide YY in the mammalian pancreas: immunocytochemical localization and immunochemical characterization. *Regul Pept* 43, 115-130.

Breit, A., Büch, T.R., Boekhoff, I., Solinski, H.J., Damm, E., Gudermann, T., 2011. Alternative G protein coupling and biased agonism: new insights into melanocortin-4 receptor signalling. *Mol Cell Endocrinol* 331, 232-240.

Buchbinder, S., Bartsch, U., Muller, M., Zorn, M., Nawroth, P.P., Schilling, T., 2011. A novel missense mutation T101N in the melanocortin-4 receptor gene associated with obesity. *Genet Mol Res* 10, 1042-1049.

Burrows, J.A., Willis, L.K., Perlmutter, D.H., 2000. Chemical chaperones mediate increased secretion of mutant α1- antitrypsin (α1-AT) Z: A potential pharmacological strategy for prevention of liver injury and emphysema in α1-AT deficiency. *Proc Natl Acad Sci U S A* 97, 1796-1801.

Bykov, V.J., Issaeva, N., Shilov, A., Hultcrantz, M., Pugacheva, E., Chumakov, P., Bergman, J., Wiman, K.G., Selivanova, G., 2002. Restoration of the tumor suppressor function to mutant p53 by a low-molecular-weight compound. *Nat Med* 8, 282-288.

Calton, M.A., Ersoy, B.A., Zhang, S., Kane, J.P., Malloy, M.J., Pullinger, C.R., Bromberg, Y., Pennacchio, L.A., Dent, R., McPherson, R., Ahituv, N., Vaisse, C., 2009. Association of functionally significant Melanocortin-4 but not Melanocortin-3 receptor mutations with severe adult obesity in a large North American case-control study. *Hum Mol Genet* 18, 1140-1147.

Carlsson, L.M.S., Peltonen, M., Ahlin, S., Anveden, A., Bouchard, C., Carlsson, B., Jacobson, P., Lonroth, H., Maglio, C., Naslund, I., Pirazzi, C., Romeo, S., Sjoholm, K., Sjostrom, E., Wedel, H., Svensson, P.A., Sjostrom, L., 2012. Bariatric surgery and prevention of type 2 diabetes in Swedish obese subjects. *New Engl J Med* 367, 695-704.

Catania, A., Gatti, S., Colombo, G., Lipton, J.M., 2004. Targeting melanocortin receptors as a novel strategy to control inflammation. *Pharmacol Rev* 56, 1-29.

Cerda-Reverter, J.M., Ringholm, A., Schioth, H.B., Peter, R.E., 2003. Molecular cloning, pharmacological characterization, and brain mapping of the melanocortin 4 receptor in the

goldfish: involvement in the control of food intake. *Endocrinology* 144, 2336-2349.

Chai, B., Li, J.Y., Zhang, W., Newman, E., Ammori, J., Mulholland, M.W., 2006. Melanocortin-4 receptor-mediated inhibition of apoptosis in immortalized hypothalamic neurons via mitogen-activated protein kinase. *Peptides* 27, 2846-2857.

Chai, B.X., Neubig, R.R., Millhauser, G.L., Thompson, D.A., Jackson, P.J., Barsh, G.S., Dickinson, C.J., Li, J.Y., Lai, Y.M., Gantz, I., 2003. Inverse agonist activity of agouti and agouti-related protein. *Peptides* 24, 603-609.

Challis, B.G., Pinnock, S.B., Coll, A.P., Carter, R.N., Dickson, S.L., O'Rahilly, S., 2003. Acute effects of PYY3-36 on food intake and hypothalamic neuropeptide expression in the mouse. *Biochem Biophys Res Commun* 311, 915-919.

Chan, L.F., Webb, T.R., Chung, T.T., Meimaridou, E., Cooray, S.N., Guasti, L., Chapple, J.P., Egertova, M., Elphick, M.R., Cheetham, M.E., Metherell, L.A., Clark, A.J., 2009. MRAP and MRAP2 are bidirectional regulators of the melanocortin receptor family. *Proc Natl Acad Sci U S A* 106, 6146-6151.

Chen, C., Okayama, H., 1987. High-efficiency transformation of mammalian cells by plasmid DNA. *Mol Cell Biol* 7, 2745-2752.

Chen, M., Cai, M., Aprahamian, C.J., Georgeson, K.E., Hruby, V., Harmon, C.M., Yang, Y., 2007. Contribution of the conserved amino acids of the melanocortin-4 receptor in D-[Nle^4,Phe^7]-α-melanocyte-stimulating hormone binding and signaling. *J Biol Chem* 282, 21712-21719.

Chen, Y., Chen, C., Wang, Y., Liu-Chen, L.Y., 2006. Ligands regulate cell surface level of the human kappa opioid receptor by activation-induced down-regulation and pharmacological chaperone-mediated enhancement: differential effects of nonpeptide and peptide agonists. *J Pharmacol Exp Ther* 319, 765-775.

Cheong, H.I., Cho, H.Y., Park, H.W., Ha, I.S., Choi, Y., 2007. Molecular genetic study of congenital nephrogenic diabetes insipidus and rescue of mutant vasopressin V2 receptor by chemical chaperones. *Nephrology (Carlton)* 12, 113-117.

Choudhury, A.I., Heffron, H., Smith, M.A., Al-Qassab, H., Xu, A.W., Selman, C., Simmgen, M., Clements, M., Claret, M., Maccoll, G., Bedford, D.C., Hisadome, K., Diakonov, I., Moosajee, V., Bell, J.D., Speakman, J.R., Batterham, R.L., Barsh, G.S., Ashford, M.L., Withers, D.J., 2005. The role of insulin receptor substrate 2 in hypothalamic and beta cell function. *J Clin Invest* 115, 940-950.

Clancy, J.P., Rowe, S.M., Accurso, F.J., Aitken, M.L., Amin, R.S., Ashlock, M.A., Ballmann, M., Boyle, M.P., Bronsveld, I., Campbell, P.W., De Boeck, K., Donaldson, S.H., Dorkin, H.L., Dunitz, J.M., Durie, P.R., Jain, M., Leonard, A., McCoy, K.S., Moss, R.B., Pilewski, J.M., Rosenbluth, D.B., Rubenstein, R.C., Schechter, M.S., Botfield, M., Ordonez, C.L., Spencer-Green, G.T., Vernillet, L., Wisseh, S., Yen, K., Konstan, M.W., 2012. Results of a phase IIa study of VX-809, an investigational CFTR corrector compound, in subjects with cystic fibrosis homozygous for the F508del-CFTR mutation. *Thorax* 67, 12-18.

Cone, R.D., 2005. Anatomy and regulation of the central melanocortin system. *Nat Neurosci* 8, 571-578.

Conn, P.M., Janovick, J.A., 2011. Pharmacoperone identification for therapeutic rescue of misfolded mutant proteins. *Front Neurosci* 2, pii: 00006.

Conn, P.M., Ulloa-Aguirre, A., Ito, J., Janovick, J.A., 2007. G protein-coupled receptor trafficking in health and disease: lessons learned to prepare for therapeutic mutant rescue in vivo. *Pharmacol Rev* 59, 225-250.

Cortez, L., Sim, V., 2014. The therapeutic potential of chemical chaperones in protein folding

diseases. *Prion* 8, 197-202.

Cowley, M.A., Smart, J.L., Rubinstein, M., Cerdan, M.G., Diano, S., Horvath, T.L., Cone, R.D., Low, M.J., 2001. Leptin activates anorexigenic POMC neurons through a neural network in the arcuate nucleus. *Nature* 411, 480-484.

Cowley, M.A., Smith, R.G., Diano, S., Tschop, M., Pronchuk, N., Grove, K.L., Strasburger, C.J., Bidlingmaier, M., Esterman, M., Heiman, M.L., Garcia-Segura, L.M., Nillni, E.A., Mendez, P., Low, M.J., Sotonyi, P., Friedman, J.M., Liu, H., Pinto, S., Colmers, W.F., Cone, R.D., Horvath, T.L., 2003. The distribution and mechanism of action of ghrelin in the CNS demonstrates a novel hypothalamic circuit regulating energy homeostasis. *Neuron* 37, 649-661.

Daniels, D., Patten, C.S., Roth, J.D., Yee, D.K., Fluharty, S.J., 2003. Melanocortin receptor signaling through mitogen-activated protein kinase in vitro and in rat hypothalamus. *Brain Res* 986, 1-11.

de la Mata, M., Cotan, D., Oropesa-Avila, M., Garrido-Maraver, J., Cordero, M.D., Villanueva Paz, M., Delgado Pavon, A., Alcocer-Gomez, E., de Lavera, I., Ybot-Gonzalez, P., Paula Zaderenko, A., Ortiz Mellet, C., Garcia Fernandez, J.M., Sanchez-Alcazar, J.A., 2015. Pharmacological chaperones and coenzyme Q10 teatment improves mutant β-glucocerebrosidase activity and mitochondrial function in neuronopathic forms of Gaucher disease. *Sci Rep* 5, 10903.

de Onis, M., Blossner, M., Borghi, E., 2010. Global prevalence and trends of overweight and obesity among preschool children. *Am J Clin Nutr* 92, 1257-1264.

Delhanty, P.J., Bouw, E., Huisman, M., Vervenne, R.M., Themmen, A.P., van der Lely, A.J., van den Akker, E.L., 2014. Functional characterization of a new human melanocortin-4 receptor

homozygous mutation (N72K) that is associated with early-onset obesity. *Mol Biol Rep* 41, 7967-7972.

Duvernay, M.T., Zhou, F., Wu, G., 2004. A conserved motif for the transport of G protein-coupled receptors from the endoplasmic reticulum to the cell surface. *J Biol Chem* 279, 30741-30750.

Ebihara, K., Ogawa, Y., Katsuura, G., Numata, Y., Masuzaki, H., Satoh, N., Tamaki, M., Yoshioka, T., Hayase, M., Matsuoka, N., Aizawa-Abe, M., Yoshimasa, Y., Nakao, K., 1999. Involvement of agouti-related protein, an endogenous antagonist of hypothalamic melanocortin receptor, in leptin action. *Diabetes* 48, 2028-2033.

Ellacott, K.L., Halatchev, I.G., Cone, R.D., 2006. Interactions between gut peptides and the central melanocortin system in the regulation of energy homeostasis. Peptides 27, 340-349.

Fan, W., Boston, B.A., Kesterson, R.A., Hruby, V.J., Cone, R.D., 1997. Role of melanocortinergic neurons in feeding and the agouti obesity syndrome. *Nature* 385, 165-168.

Fan, W., Ellacott, K.L., Halatchev, I.G., Takahashi, K., Yu, P., Cone, R.D., 2004. Cholecystokinin-mediated suppression of feeding involves the brainstem melanocortin system. *Nat Neurosci* 7, 335-336.

Fan, Z.C., Sartin, J.L., Tao, Y.X., 2008. Pharmacological analyses of two naturally occurring porcine melanocortin-4 receptor mutations in domestic pigs. *Domest Anim Endocrinol* 34, 383-390.

Fan, Z.C., Tao, Y.X., 2009. Functional characterization and pharmacological rescue of melanocortin-4 receptor mutations identified from obese patients. *J Cell Mol Med* 13, 3268-3282.

Fang, Q.C., Jia, W.P., Cai, S.B., Shao, X.Y., Zhang, R., Wang, C.R., Bao, Y.Q., Xiang, K.S., 2008. Intracellular retention of human melanocortin-4 receptor: a molecular mechanism underlying early-onset obesity in F261S pedigree of Chinese. *Biomed Environ Sci* 21, 280-285.

Farmakis, D., Filippatos, G., Kremastinos, D.T., Gheorghiade, M., 2008. Vasopressin and vasopressin antagonists in heart failure and hyponatremia. *Curr Heart Fail Rep* 5, 91-96.

Farooqi, I.S., Keogh, J.M., Yeo, G.S., Lank, E.J., Cheetham, T., O'Rahilly, S., 2003. Clinical spectrum of obesity and mutations in the melanocortin 4 receptor gene. *New Engl J Med* 348, 1085-1095.

Finkelstein, E.A., Fiebelkorn, I.C., Wang, G., 2003. National medical spending attributable to overweight and obesity: how much, and who's paying? *Health Aff (Millwood)*, W3-219-226.

Finkelstein, E.A., Trogdon, J.G., Cohen, J.W., Dietz, W., 2009. Annual medical spending attributable to obesity: payer-and service-specific estimates. *Health Aff (Millwood)* 28, w822-831.

Fong, T.M., Mao, C., MacNeil, T., Kalyani, R., Smith, T., Weinberg, D., Tota, M.R., Van der Ploeg, L.H., 1997. ART (protein product of agouti-related transcript) as an antagonist of MC-3 and MC-4 receptors. *Biochem Biophys Res Commun* 237, 629-631.

Fontaine, K.R., Redden, D.T., Wang, C., Westfall, A.O., Allison, D.B., 2003. Years of life lost due to obesity. *JAMA* 289, 187-193.

Foster, B.A., Coffey, H.A., Morin, M.J., Rastinejad, F., 1999. Pharmacological rescue of mutant p53 conformation and function. *Science* 286, 2507-2510.

Gantz, I., Fong, T.M., 2003. The melanocortin system. *Am J Physiol Endocrinol Metab* 284, E468-474.

Gantz, I., Miwa, H., Konda, Y., Shimoto, Y., Tashiro, T., Watson, S.J., DelValle, J., Yamada, T., 1993. Molecular cloning, expression, and gene localization of a fourth melanocortin receptor. *J Biol Chem* 268, 15174-15179.

Gil-Campos, M., Aguilera, C.M., Canete, R., Gil, A., 2006. Ghrelin: a hormone regulating food intake and energy homeostasis. *Br J Nutr* 96, 201-226.

Giraudo, S.Q., Billington, C.J., Levine, A.S., 1998. Feeding effects of hypothalamic injection of melanocortin 4 receptor ligands. *Brain Res* 809, 302-306.

Giugliani, R., Waldek, S., Germain, D.P., Nicholls, K., Bichet, D.G., Simosky, J.K., Bragat, A.C., Castelli, J.P., Benjamin, E.R., Boudes, P.F., 2013. A Phase 2 study of migalastat hydrochloride in females with Fabry disease: selection of population, safety and pharmacodynamic effects. *Mol Genet Metab* 109, 86-92.

Gong, L., Yao, F., Hockman, K., Heng, H.H., Morton, G.J., Takeda, K., Akira, S., Low, M.J., Rubinstein, M., MacKenzie, R.G., 2008. Signal transducer and activator of transcription-3 is required in hypothalamic agouti-related protein/neuropeptide Y neurons for normal energy homeostasis. *Endocrinology* 149, 3346-3354.

Graham, M., Shutter, J.R., Sarmiento, U., Sarosi, I., Stark, K.L., 1997. Overexpression of Agrt leads to obesity in transgenic mice. *Nat Genet* 17, 273-274.

Grandt, D., Schimiczek, M., Beglinger, C., Layer, P., Goebell, H., Eysselein, V.E., Reeve, J.R., Jr., 1994. Two molecular forms of peptide YY (PYY) are abundant in human blood: characterization of a radioimmunoassay recognizing PYY 1-36 and PYY 3-36. *Regul Pept* 51, 151-159.

Granell, S., Mohammad, S., Ramanagoudr-Bhojappa, R., Baldini, G., 2010. Obesity-linked variants of melanocortin-4 receptor are misfolded in the endoplasmic reticulum and can be

rescued to the cell surface by a chemical chaperone. *Mol Endocrinol* 24, 1805-1821.

Granell, S., Molden, B.M., Baldini, G., 2013. Exposure of MC4R to agonist in the endoplasmic reticulum stabilizes an active conformation of the receptor that does not desensitize. *Proc Natl Acad Sci U S A* 110, E4733-E4742.

Granell, S., Serra-Juhe, C., Martos-Moreno, G.A., Diaz, F., Perez-Jurado, L.A., Baldini, G., Argente, J., 2012. A novel melanocortin-4 receptor mutation MC4R-P272L associated with severe obesity has increased propensity to be ubiquitinated in the ER in the face of correct folding. *PloS ONE* 7, e50894.

Gray, S.M., Meijer, R.I., Barrett, E.J., 2014. Insulin regulates brain function, but how does it get there? *Diabetes* 63, 3992-3997.

Guyenet, S.J., Schwartz, M.W., 2012. Clinical review: Regulation of food intake, energy balance, and body fat mass: implications for the pathogenesis and treatment of obesity. *J Clin Endocrinol Metab* 97, 745-755.

Haegeman, A., Coopman, F., Jacobs, K., Mattheeuws, M., Van Zeveren, A., Peelman, L., 2001. Bovine melanocortin receptor 4: cDNA sequence, polymorphisms and mapping. *Anim Genet* 32, 189-192.

Hainerova, I., Larsen, L.H., Holst, B., Finkova, M., Hainer, V., Lebl, J., Hansen, T., Pedersen, O., 2007. Melanocortin 4 receptor mutations in obese Czech children: studies of prevalence, phenotype development, weight reduction response, and functional analysis. *J Clin Endocr Metab* 92, 3689-3696.

Haitina, T., Klovins, J., Andersson, J., Fredriksson, R., Lagerstrom, M.C., Larhammar, D., Larson, E.T., Schioth, H.B., 2004. Cloning, tissue distribution, pharmacology and three-dimensional modelling of melanocortin receptors 4 and 5 in rainbow trout suggest close

evolutionary relationship of these subtypes. *Biochem J* 380, 475-486.

Hartl, F.U., Bracher, A., Hayer-Hartl, M., 2011. Molecular chaperones in protein folding and proteostasis. *Nature* 475, 324-332.

Haskell-Luevano, C., Monck, E.K., 2001. Agouti-related protein functions as an inverse agonist at a constitutively active brain melanocortin-4 receptor. *Regul Pept* 99, 1-7.

Haslam, D.W., James, W.P., 2005. Obesity. *Lancet* 366, 1197-1209.

Hassan, Y., Head, V., Jacob, D., Bachmann, M.O., Diu, S., Ford, J., 2016. Lifestyle interventions for weight loss in adults with severe obesity: a systematic review. *Clin Obes* 6, 395-403.

He, S., Tao, Y.X., 2014. Defect in MAPK signaling as a cause for monogenic obesity caused by inactivating mutations in the melanocortin-4 receptor gene. *Int J Biol Sci* 10, 1128-1137.

Hewson, G., Leighton, G.E., Hill, R.G., Hughes, J., 1988. The cholecystokinin receptor antagonist L364,718 increases food intake in the rat by attenuation of the action of endogenous cholecystokinin. *Br J Pharmacol* 93, 79-84.

Hinney, A., Bettecken, T., Tarnow, P., Brumm, H., Reichwald, K., Lichtner, P., Scherag, A., Nguyen, T.T., Schlumberger, P., Rief, W., Vollmert, C., Illig, T., Wichmann, H.E., Schafer, H., Platzer, M., Biebermann, H., Meitinger, T., Hebebrand, J., 2006. Prevalence, spectrum, and functional characterization of melanocortin-4 receptor gene mutations in a representative population-based sample and obese adults from Germany. *J Clin Endocrinol Metab* 91, 1761-1769.

Hinney, A., Hohmann, S., Geller, F., Vogel, C., Hess, C., Wermter, A.K., Brokamp, B., Goldschmidt, H., Siegfried, W., Remschmidt, H., Schafer, H., Gudermann, T., Hebebrand, J., 2003. Melanocortin-4 receptor gene: case-control study and transmission disequilibrium test confirm that functionally relevant mutations are compatible with a major gene effect for

extreme obesity. *J Clin Endocr Metab* 88, 4258-4267.

Hinney, A., Volckmar, A.L., Knoll, N., 2013. Melanocortin-4 receptor in energy homeostasis and obesity pathogenesis. *Prog Mol Biol Transl Sci* 114, 147-191.

Ho, G., MacKenzie, R.G., 1999. Functional characterization of mutations in melanocortin-4 receptor associated with human obesity. *J Biol Chem* 274, 35816-35822.

Hogan, K., Peluso, S., Gould, S., Parsons, I., Ryan, D., Wu, L., Visiers, I., 2006. Mapping the binding site of melanocortin 4 receptor agonists: a hydrophobic pocket formed by I3.28(125), I3.32(129), and I7.42(291) is critical for receptor activation. *J Med Chem* 49, 911-922.

Hohenadel, M.G., Thearle, M.S., Grice, B.A., Huang, H., Dai, M.H., Tao, Y.X., Hunter, L.A., Palaguachi, G.I., Mou, Z., Kim, R.C., Tsang, M.M., Haack, K., Voruganti, V.S., Cole, S.A., Butte, N.F., Comuzzie, A.G., Muller, Y.L., Baier, L.J., Krakoff, J., Knowler, W.C., Yanovski, J.A., Han, J.C., 2014. Brain-derived neurotrophic factor in human subjects with function-altering melanocortin-4 receptor variants. *Int J Obes (Lond)* 38, 1068-1074.

Howard, A.D., Feighner, S.D., Cully, D.F., Arena, J.P., Liberator, P.A., Rosenblum, C.I., Hamelin, M., Hreniuk, D.L., Palyha, O.C., Anderson, J., Paress, P.S., Diaz, C., Chou, M., Liu, K.K., McKee, K.K., Pong, S.S., Chaung, L.Y., Elbrecht, A., Dashkevicz, M., Heavens, R., Rigby, M., Sirinathsinghji, D.J., Dean, D.C., Melillo, D.G., Patchett, A.A., Nargund, R., Griffin, P.R., DeMartino, J.A., Gupta, S.K., Schaeffer, J.M., Smith, R.G., Van der Ploeg, L.H., 1996. A receptor in pituitary and hypothalamus that functions in growth hormone release. *Science* 273, 974-977.

Huang, H., Tao, Y.X., 2012. Pleiotropic functions of the transmembrane domain 6 of human melanocortin-4 receptor. *J Mol Endocrinol* 49, 237-248.

Huang, H., Tao, Y.X., 2014a. Functions of the DRY motif and intracellular loop 2 of human melanocortin 3 receptor. *J Mol Endocrinol* 53, 319-330.

Huang, H., Tao, Y.X., 2014b. A small molecule agonist THIQ as a novel pharmacoperone for intracellularly retained melanocortin-4 receptor mutants. *Int J Biol Sci* 10, 817-824.

Hughes, D.A., Nicholls, K., Shankar, S.P., Sunder-Plassmann, G., Koeller, D., Nedd, K., Vockley, G., Hamazaki, T., Lachmann, R., Ohashi, T., 2017. Oral pharmacological chaperone migalastat compared with enzyme replacement therapy in Fabry disease: 18-month results from the randomised phase III ATTRACT study. *J Med Genet* 54, 288-296.

Huszar, D., Lynch, C.A., Fairchild-Huntress, V., Dunmore, J.H., Fang, Q., Berkemeier, L.R., Gu, W., Kesterson, R.A., Boston, B.A., Cone, R.D., Smith, F.J., Campfield, L.A., Burn, P., Lee, F., 1997. Targeted disruption of the melanocortin-4 receptor results in obesity in mice. *Cell* 88, 131-141.

Ilnytska, O., Argyropoulos, G., 2008. The role of the Agouti-Related Protein in energy balance regulation. *Cell Mol Life Sci* 65, 2721-2731.

Inden, M., Kitamura, Y., Takeuchi, H., Yanagida, T., Takata, K., Kobayashi, Y., Taniguchi, T., Yoshimoto, K., Kaneko, M., Okuma, Y., Taira, T., Ariga, H., Shimohama, S., 2007. Neurodegeneration of mouse nigrostriatal dopaminergic system induced by repeated oral administration of rotenone is prevented by 4-phenylbutyrate, a chemical chaperone. *J Neurochem* 101, 1491-1504.

Jaffe, E.K., Stith, L., Lawrence, S.H., Andrake, M., Dunbrack, R.L., Jr., 2013. A new model for allosteric regulation of phenylalanine hydroxylase: implications for disease and therapeutics. *Arch Biochem Biophys* 530, 73-82.

James, W.P., Caterson, I.D., Coutinho, W., Finer, N., Van Gaal, L.F., Maggioni, A.P., Torp-

Pedersen, C., Sharma, A.M., Shepherd, G.M., Rode, R.A., Renz, C.L., Investigators, S., 2010. Effect of sibutramine on cardiovascular outcomes in overweight and obese subjects. *N Engl J Med* 363, 905-917.

Janovick, J.A., Maya-Nunez, G., Conn, P.M., 2002. Rescue of hypogonadotropic hypogonadism-causing and manufactured GnRH receptor mutants by a specific protein-folding template: misrouted proteins as a novel disease etiology and therapeutic target. *J Clin Endocr Metab* 87, 3255-3262.

Janovick, J.A., Stewart, M.D., Jacob, D., Martin, L.D., Deng, J.M., Stewart, C.A., Wang, Y., Cornea, A., Chavali, L., Lopez, S., Mitalipov, S., Kang, E., Lee, H.S., Manna, P.R., Stocco, D.M., Behringer, R.R., Conn, P.M., 2013. Restoration of testis function in hypogonadotropic hypogonadal mice harboring a misfolded GnRHR mutant by pharmacoperone drug therapy. *Proc Natl Acad Sci U S A* 110, 21030-21035.

Jensen, M.D., Ryan, D.H., Apovian, C.M., Ard, J.D., Comuzzie, A.G., Donato, K.A., Hu, F.B., Hubbard, V.S., Jakicic, J.M., Kushner, R.F., Loria, C.M., Millen, B.E., Nonas, C.A., Pi-Sunyer, F.X., Stevens, J., Stevens, V.J., Wadden, T.A., Wolfe, B.M., Yanovski, S.Z., Guidelines, A.C.o.C.A.H.A.T.F.o.P., Society, O., 2014. 2013 AHA/ACC/TOS guideline for the management of overweight and obesity in adults: a report of the American College of Cardiology/American Heart Association Task Force on Practice Guidelines and The Obesity Society. *J Am Coll Cardiol* 63, 2985-3023.

Juonala, M., Magnussen, C.G., Berenson, G.S., Venn, A., Burns, T.L., Sabin, M.A., Srinivasan, S.R., Daniels, S.R., Davis, P.H., Chen, W., Sun, C., Cheung, M., Viikari, J.S., Dwyer, T., Raitakari, O.T., 2011. Childhood adiposity, adult adiposity, and cardiovascular risk factors. *N Engl J Med* 365, 1876-1885.

Kalani, M.Y., Vaidehi, N., Hall, S.E., Trabanino, R.J., Freddolino, P.L., Kalani, M.A., Floriano, W.B., Kam, V.W., Goddard, W.A., 3rd, 2004. The predicted 3D structure of the human D2 dopamine receptor and the binding site and binding affinities for agonists and antagonists. *Proc Natl Acad Sci U S A* 101, 3815-3820.

Kamegai, J., Tamura, H., Shimizu, T., Ishii, S., Sugihara, H., Wakabayashi, I., 2001. Chronic central infusion of ghrelin increases hypothalamic neuropeptide Y and Agouti-related protein mRNA levels and body weight in rats. *Diabetes* 50, 2438-2443.

Kang, H.J., Cui, Y., Yin, H., Scheid, A., Hendricks, W.P., Schmidt, J., Sekulic, A., Kong, D., Trent, J.M., Gokhale, V., Mao, H., Hurley, L.H., 2016. A pharmacological chaperone molecule induces cancer cell death by restoring tertiary DNA structures in mutant hTERT promoters. *J Am Chem Soc* 138, 13673-13692.

Kask, A., Rago, L., Mutulis, F., Pahkla, R., Wikberg, J.E., Schioth, H.B., 1998. Selective antagonist for the melanocortin 4 receptor (HS014) increases food intake in free-feeding rats. *Biochem Biophys Res Commun* 245, 90-93.

Kato, I., Nomura, A., Stemmermann, G.N., Chyou, P.H., 1992. Prospective study of clinical gallbladder disease and its association with obesity, physical activity, and other factors. *Dig Dis Sci* 37, 784-790.

Keire, D.A., Mannon, P., Kobayashi, M., Walsh, J.H., Solomon, T.E., Reeve, J.R., Jr., 2000. Primary structures of PYY, [Pro(34)]PYY, and PYY-(3-36) confer different conformations and receptor selectivity. *Am J Physiol Gastrointest Liver Physiol* 279, G126-131.

Kelly, T., Yang, W., Chen, C.S., Reynolds, K., He, J., 2008. Global burden of obesity in 2005 and projections to 2030. *Int J Obes (Lond)* 32, 1431-1437.

Khanna, R., Soska, R., Lun, Y., Feng, J., Frascella, M., Young, B., Brignol, N., Pellegrino, L.,

Sitaraman, S.A., Desnick, R.J., Benjamin, E.R., Lockhart, D.J., Valenzano, K.J., 2010. The pharmacological chaperone 1-deoxygalactonojirimycin reduces tissue globotriaosylceramide levels in a mouse model of Fabry disease. *Mol Ther* 18, 23-33.

Kim, K.S., Larsen, N., Short, T., Plastow, G., Rothschild, M.F., 2000. A missense variant of the porcine melanocortin-4 receptor (MC4R) gene is associated with fatness, growth, and feed intake traits. *Mamm Genome* 11, 131-135.

Kobayashi, Y., Tsuchiya, K., Yamanome, T., Schioth, H.B., Kawauchi, H., Takahashi, A., 2008. Food deprivation increases the expression of melanocortin-4 receptor in the liver of barfin flounder, *Verasper moseri*. *Gen Comp Endocrinol* 155, 280-287.

Koegler, F.H., Grove, K.L., Schiffmacher, A., Smith, M.S., Cameron, J.L., 2001. Central melanocortin receptors mediate changes in food intake in the rhesus macaque. *Endocrinology* 142, 2586-2592.

Koshland, D.E., Jr., 1998. Conformational changes: how small is big enough? *Nat Med* 4, 1112-1114.

Krashes, M.J., Lowell, B.B., Garfield, A.S., 2016. Melanocortin-4 receptor-regulated energy homeostasis. *Nat Neurosci* 19, 206-219.

Lagerstrom, M.C., Klovins, J., Fredriksson, R., Fridmanis, D., Haitina, T., Ling, M.K., Berglund, M.M., Schioth, H.B., 2003. High affinity agonistic metal ion binding sites within the melanocortin 4 receptor illustrate conformational change of transmembrane region 3. *J Biol Chem* 278, 51521-51526.

Lane, J.R., Donthamsetti, P., Shonberg, J., Draper-Joyce, C.J., Dentry, S., Michino, M., Shi, L., Lopez, L., Scammells, P.J., Capuano, B., Sexton, P.M., Javitch, J.A., Christopoulos, A., 2014. A new mechanism of allostery in a G protein-coupled receptor dimer. *Nat Chem Biol*

10, 745-752.

Larsen, L.H., Echwald, S.M., Sorensen, T.I., Andersen, T., Wulff, B.S., Pedersen, O., 2005. Prevalence of mutations and functional analyses of melanocortin 4 receptor variants identified among 750 men with juvenile-onset obesity. *J Clin Endocr Metab* 90, 219-224.

Lee, Y.S., Poh, L.K., Kek, B.L., Loke, K.Y., 2008. Novel melanocortin 4 receptor gene mutations in severely obese children. *Clin Endocrinol (Oxf)* 68, 529-535.

Lefkowitz, R.J., 2013. A brief history of G-protein coupled receptors (Nobel Lecture). *Angew Chem Int Ed Engl* 52, 6366-6378.

Leidenheimer, N.J., Ryder, K.G., 2014. Pharmacological chaperoning: a primer on mechanism and pharmacology. *Pharmacol Res* 83, 10-19.

Li, R., Fan, W., Tian, G., Zhu, H., He, L., Cai, J., Huang, Q., Cai, Q., Li, B., Bai, Y., Zhang, Z., Zhang, Y., Wang, W., Li, J., Wei, F., Li, H., Jian, M., Li, J., Zhang, Z., Nielsen, R., Li, D., Gu, W., Yang, Z., Xuan, Z., Ryder, O.A., Leung, F.C., Zhou, Y., Cao, J., Sun, X., Fu, Y., Fang, X., Guo, X., Wang, B., Hou, R., Shen, F., Mu, B., Ni, P., Lin, R., Qian, W., Wang, G., Yu, C., Nie, W., Wang, J., Wu, Z., Liang, H., Min, J., Wu, Q., Cheng, S., Ruan, J., Wang, M., Shi, Z., Wen, M., Liu, B., Ren, X., Zheng, H., Dong, D., Cook, K., Shan, G., Zhang, H., Kosiol, C., Xie, X., Lu, Z., Zheng, H., Li, Y., Steiner, C.C., Lam, T.T., Lin, S., Zhang, Q., Li, G., Tian, J., Gong, T., Liu, H., Zhang, D., Fang, L., Ye, C., Zhang, J., Hu, W., Xu, A., Ren, Y., Zhang, G., Bruford, M.W., Li, Q., Ma, L., Guo, Y., An, N., Hu, Y., Zheng, Y., Shi, Y., Li, Z., Liu, Q., Chen, Y., Zhao, J., Qu, N., Zhao, S., Tian, F., Wang, X., Wang, H., Xu, L., Liu, X., Vinar, T., Wang, Y., Lam, T.W., Yiu, S.M., Liu, S., Zhang, H., Li, D., Huang, Y., Wang, X., Yang, G., Jiang, Z., Wang, J., Qin, N., Li, L., Li, J., Bolund, L., Kristiansen, K., Wong, G.K., Olson, M., Zhang, X., Li, S., Yang, H., Wang, J., Wang, J., 2010. The sequence and de

novo assembly of the giant panda genome. *Nature* 463, 311-317.

Lieberman, R.L., Wustman, B.A., Huertas, P., Powe, A.C., Jr., Pine, C.W., Khanna, R., Schlossmacher, M.G., Ringe, D., Petsko, G.A., 2007. Structure of acid β-glucosidase with pharmacological chaperone provides insight into Gaucher disease. *Nat Chem Biol* 3, 101-107.

Lindburg, D.G., Baragona, K., 2004. Giant Pandas: Biology and Conservation. University of California Press, Berkeley, CA.

Lobstein, T., Baur, L., Uauy, R., TaskForce, I.I.O., 2004. Obesity in children and young people: a crisis in public health. *Obes Rev* 5 Suppl 1, 4-104.

Longitudinal Assessment of Bariatric Surgery, C., Flum, D.R., Belle, S.H., King, W.C., Wahed, A.S., Berk, P., Chapman, W., Pories, W., Courcoulas, A., McCloskey, C., Mitchell, J., Patterson, E., Pomp, A., Staten, M.A., Yanovski, S.Z., Thirlby, R., Wolfe, B., 2009. Perioperative safety in the longitudinal assessment of bariatric surgery. *N Engl J Med* 361, 445-454.

Loo, T.W., Clarke, D.M., 1997. Correction of defective protein kinesis of human P-glycoprotein mutants by substrates and modulators. *J Biol Chem* 272, 709-712.

Loo, T.W., Clarke, D.M., 2007. Chemical and pharmacological chaperones as new therapeutic agents. *Expert Rev Mol Med* 9, 1-18.

Los, E.L., Deen, P.M., Robben, J.H., 2010. Potential of nonpeptide (ant)agonists to rescue vasopressin V2 receptor mutants for the treatment of X-linked nephrogenic diabetes insipidus. *J Neuroendocrinol* 22, 393-399.

Lubrano-Berthelier, C., Dubern, B., Lacorte, J.M., Picard, F., Shapiro, A., Zhang, S., Bertrais, S., Hercberg, S., Basdevant, A., Clement, K., Vaisse, C., 2006. Melanocortin 4 receptor

mutations in a large cohort of severely obese adults: prevalence, functional classification, genotype-phenotype relationship, and lack of association with binge eating. *J Clin Endocr Metab* 91, 1811-1818.

Lubrano-Berthelier, C., Durand, E., Dubern, B., Shapiro, A., Dazin, P., Weill, J., Ferron, C., Froguel, P., Vaisse, C., 2003. Intracellular retention is a common characteristic of childhood obesity-associated MC4R mutations. *Hum Mol Genet* 12, 145-153.

Manson, J.E., Nathan, D.M., Krolewski, A.S., Stampfer, M.J., Willett, W.C., Hennekens, C.H., 1992. A prospective study of exercise and incidence of diabetes among US male physicians. *JAMA* 268, 63-67.

Marks, D.L., Boucher, N., Lanouette, C.M., Perusse, L., Brookhart, G., Comuzzie, A.G., Chagnon, Y.C., Cone, R.D., 2004. Ala67Thr polymorphism in the Agouti-related peptide gene is associated with inherited leanness in humans. *Am J Med Genet A* 126A, 267-271.

Marks, J.L., Porte, D., Jr., Stahl, W.L., Baskin, D.G., 1990. Localization of insulin receptor mRNA in rat brain by in situ hybridization. *Endocrinology* 127, 3234-3236.

McDaniel, F.K., Molden, B.M., Mohammad, S., Baldini, G., McPike, L., Narducci, P., Granell, S., Baldini, G., 2012. Constitutive cholesterol-dependent endocytosis of melanocortin-4 receptor (MC4R) is essential to maintain receptor responsiveness to α-melanocyte-stimulating hormone (α-MSH). *J Biol Chem* 287, 21873-21890.

McNeely, W., Benfield, P., 1998. Orlistat. *Drugs* 56, 241-249.

Meimaridou, E., Gooljar, S.B., Ramnarace, N., Anthonypillai, L., Clark, A.J., Chapple, J.P., 2011. The cytosolic chaperone Hsc70 promotes traffic to the cell surface of intracellular retained melanocortin-4 receptor mutants. *Mol Endocrinol* 25, 1650-1660.

Mesaros, A., Koralov, S.B., Rother, E., Wunderlich, F.T., Ernst, M.B., Barsh, G.S., Rajewsky, K.,

Bruning, J.C., 2008. Activation of Stat3 signaling in AgRP neurons promotes locomotor activity. *Cell Metab* 7, 236-248.

Metherell, L.A., Chapple, J.P., Cooray, S., David, A., Becker, C., Ruschendorf, F., Naville, D., Begeot, M., Khoo, B., Nurnberg, P., Huebner, A., Cheetham, M.E., Clark, A.J., 2005. Mutations in MRAP, encoding a new interacting partner of the ACTH receptor, cause familial glucocorticoid deficiency type 2. *Nat Genet* 37, 166-170.

Miller, L.J., Holicky, E.L., Ulrich, C.D., Wieben, E.D., 1995. Abnormal processing of the human cholecystokinin receptor gene in association with gallstones and obesity. *Gastroenterology* 109, 1375-1380.

Miura, S., Zhang, J., Boros, J., Karnik, S.S., 2003. TM2-TM7 interaction in coupling movement of transmembrane helices to activation of the angiotensin II type-1 receptor. *J Biol Chem* 278, 3720-3725.

Mo, X.L., Tao, Y.X., 2013. Activation of MAPK by inverse agonists in six naturally occurring constitutively active mutant human melanocortin-4 receptors. *Biochim Biophys Acta* 1832, 1939-1948.

Mo, X.L., Yang, R., Tao, Y.X., 2012. Functions of transmembrane domain 3 of human melanocortin-4 receptor. *J Mol Endocrinol* 49, 221-235.

Mohammad, S., Baldini, G., Granell, S., Narducci, P., Martelli, A.M., Baldini, G., 2007. Constitutive traffic of melanocortin-4 receptor in neuro2A cells and immortalized hypothalamic neurons. *J Biol Chem* 282, 4963-4974.

Morello, J.P., Salahpour, A., Laperriere, A., Bernier, V., Arthus, M.F., Lonergan, M., Petaja-Repo, U., Angers, S., Morin, D., Bichet, D.G., Bouvier, M., 2000. Pharmacological chaperones rescue cell-surface expression and function of misfolded V2 vasopressin receptor mutants. *J*

Clin Invest 105, 887-895.

Morrison, J.A., Friedman, L.A., Gray-McGuire, C., 2007. Metabolic syndrome in childhood predicts adult cardiovascular disease 25 years later: the Princeton Lipid Research Clinics Follow-up Study. *Pediatrics* 120, 340-345.

Mountjoy, K.G., Jenny Wu, C.S., Dumont, L.M., Wild, J.M., 2003. Melanocortin-4 receptor messenger ribonucleic acid expression in rat cardiorespiratory, musculoskeletal, and integumentary systems. *Endocrinology* 144, 5488-5496.

Mountjoy, K.G., Kong, P.L., Taylor, J.A., Willard, D.H., Wilkison, W.O., 2001. Melanocortin receptor-mediated mobilization of intracellular free calcium in HEK293 cells. *Physiol Genomics* 5, 11-19.

Mountjoy, K.G., Mortrud, M.T., Low, M.J., Simerly, R.B., Cone, R.D., 1994. Localization of the melanocortin-4 receptor (MC4-R) in neuroendocrine and autonomic control circuits in the brain. *Mol Endocrinol* 8, 1298-1308.

Moyad, M.A., 2001. Review of potential risk factors for kidney (renal cell) cancer. S*emin Urol Oncol* 19, 280-293.

Newton, C.L., Whay, A.M., McArdle, C.A., Zhang, M., van Koppen, C.J., van de Lagemaat, R., Segaloff, D.L., Millar, R.P., 2011. Rescue of expression and signaling of human luteinizing hormone G protein-coupled receptor mutants with an allosterically binding small-molecule agonist. *Proc Natl Acad Sci U S A* 108, 7172-7176.

Nicholson, J.R., Kohler, G., Schaerer, F., Senn, C., Weyermann, P., Hofbauer, K.G., 2006. Peripheral administration of a melanocortin 4-receptor inverse agonist prevents loss of lean body mass in tumor-bearing mice. *J Pharmacol Exp Ther* 317, 771-777.

Nijenhuis, W.A., Garner, K.M., VanRozen, R.J., Adan, R.A., 2003. Poor cell surface expression

of human melanocortin-4 receptor mutations associated with obesity. *J Biol Chem* 278, 22939-22945.

Nijenhuis, W.A., Oosterom, J., Adan, R.A., 2001. AgRP(83-132) acts as an inverse agonist on the human-melanocortin-4 receptor. *Mol Endocrinol* 15, 164-171.

Noon, L.A., Franklin, J.M., King, P.J., Goulding, N.J., Hunyady, L., Clark, A.J., 2002. Failed export of the adrenocorticotrophin receptor from the endoplasmic reticulum in non-adrenal cells: evidence in support of a requirement for a specific adrenal accessory factor. *J Endocrinol* 174, 17-25.

Noorwez, S.M., Kuksa, V., Imanishi, Y., Zhu, L., Filipek, S., Palczewski, K., Kaushal, S., 2003. Pharmacological chaperone-mediated in vivo folding and stabilization of the P23H-opsin mutant associated with autosomal dominant retinitis pigmentosa. *J Biol Chem* 278, 14442-14450.

Noorwez, S.M., Malhotra, R., McDowell, J.H., Smith, K.A., Krebs, M.P., Kaushal, S., 2004. Retinoids assist the cellular folding of the autosomal dominant retinitis pigmentosa opsin mutant P23H. *J Biol Chem* 279, 16278-16284.

Noorwez, S.M., Ostrov, D.A., McDowell, J.H., Krebs, M.P., Kaushal, S., 2008. A high-throughput screening method for small-molecule pharmacologic chaperones of misfolded rhodopsin. *Invest Ophthalmol Vis Sci* 49, 3224-3230.

Nowacka-Woszuk, J., Cieslak, J., Skowronska, B., Majewska, K.A., Stankiewicz, W., Fichna, P., Switonski, M., 2011. Missense mutations and polymorphisms of the MC4R gene in Polish obese children and adolescents in relation to the relative body mass index. *J Appl Genet* 52, 319-323.

Ogden, C.L., Carroll, M.D., Fryar, C.D., Flegal, K.M., 2015. Prevalence of Obesity Among

Adults and Youth: United States, 2011-2014. *NCHS Data Brief*, 1-8.

Ollmann, M.M., Wilson, B.D., Yang, Y.K., Kerns, J.A., Chen, Y., Gantz, I., Barsh, G.S., 1997. Antagonism of central melanocortin receptors in vitro and in vivo by agouti-related protein. *Science* 278, 135-138.

Papp, E., Csermely, P., 2006. Chemical chaperones: mechanisms of action and potential use. *Handb Exp Pharmacol*, 405-416.

Patten, C.S., Daniels, D., Suzuki, A., Fluharty, S.J., Yee, D.K., 2007. Structural and signaling requirements of the human melanocortin 4 receptor for MAP kinase activation. *Regul Pept* 142, 111-122.

Petaja-Repo, U.E., Hogue, M., Bhalla, S., Laperriere, A., Morello, J.P., Bouvier, M., 2002. Ligands act as pharmacological chaperones and increase the efficiency of δ opioid receptor maturation. *EMBO J* 21, 1628-1637.

Pierroz, D.D., Ziotopoulou, M., Ungsunan, L., Moschos, S., Flier, J.S., Mantzoros, C.S., 2002. Effects of acute and chronic administration of the melanocortin agonist MTII in mice with diet-induced obesity. *Diabetes* 51, 1337-1345.

Plum, L., Ma, X., Hampel, B., Balthasar, N., Coppari, R., Munzberg, H., Shanabrough, M., Burdakov, D., Rother, E., Janoschek, R., Alber, J., Belgardt, B.F., Koch, L., Seibler, J., Schwenk, F., Fekete, C., Suzuki, A., Mak, T.W., Krone, W., Horvath, T.L., Ashcroft, F.M., Bruning, J.C., 2006. Enhanced PIP3 signaling in POMC neurons causes KATP channel activation and leads to diet-sensitive obesity. *J Clin Invest* 116, 1886-1901.

Poggioli, R., Vergoni, A.V., Bertolini, A., 1986. ACTH-(1-24) and alpha-MSH antagonize feeding behavior stimulated by kappa opiate agonists. *Peptides* 7, 843-848.

Pogozheva, I.D., Chai, B.X., Lomize, A.L., Fong, T.M., Weinberg, D.H., Nargund, R.P.,

Mulholland, M.W., Gantz, I., Mosberg, H.I., 2005. Interactions of human melanocortin 4 receptor with nonpeptide and peptide agonists. *Biochemistry* 44, 11329-11341.

Poitout, L., Brault, V., Sackur, C., Bernetiere, S., Camara, J., Plas, P., Roubert, P., 2007. Identification of a novel series of benzimidazoles as potent and selective antagonists of the human melanocortin-4 receptor. *Bioorg Med Chem Lett* 17, 4464-4470.

Pritchard, L.E., Turnbull, A.V., White, A., 2002. Pro-opiomelanocortin processing in the hypothalamus: impact on melanocortin signalling and obesity. *J Endocrinol* 172, 411-421.

Qiu, J., Zhang, C., Borgquist, A., Nestor, C.C., Smith, A.W., Bosch, M.A., Ku, S., Wagner, E.J., Ronnekleiv, O.K., Kelly, M.J., 2014. Insulin excites anorexigenic proopiomelanocortin neurons via activation of canonical transient receptor potential channels. *Cell Metab* 19, 682-693.

Rabkin, S.W., Chen, Y., Leiter, L., Liu, L., Reeder, B.A., 1997. Risk factor correlates of body mass index. Canadian Heart Health Surveys Research Group. *CMAJ* 157 Suppl 1, S26-31.

Rahmeh, R., Damian, M., Cottet, M., Orcel, H., Mendre, C., Durroux, T., Sharma, K.S., Durand, G., Pucci, B., Trinquet, E., Zwier, J.M., Deupi, X., Bron, P., Baneres, J.L., Mouillac, B., Granier, S., 2012. Structural insights into biased G protein-coupled receptor signaling revealed by fluorescence spectroscopy. *Proc Natl Acad Sci U S A* 109, 6733-6738.

Reiter, E., Ahn, S., Shukla, A.K., Lefkowitz, R.J., 2012. Molecular mechanism of beta-arrestin-biased agonism at seven-transmembrane receptors. *Annu Rev Pharmacol Toxicol* 52, 179-197.

Rene, P., Le Gouill, C., Pogozheva, I.D., Lee, G., Mosberg, H.I., Farooqi, I.S., Valenzano, K.J., Bouvier, M., 2010. Pharmacological chaperones restore function to MC4R mutants responsible for severe early-onset obesity. *J Pharmacol Exp Ther* 335, 520-532.

Rexrode, K.M., Hennekens, C.H., Willett, W.C., Colditz, G.A., Stampfer, M.J., Rich-Edwards, J.W., Speizer, F.E., Manson, J.E., 1997. A prospective study of body mass index, weight change, and risk of stroke in women. *JAMA* 277, 1539-1545.

Riediger, T., Traebert, M., Schmid, H.A., Scheel, C., Lutz, T.A., Scharrer, E., 2003. Site-specific effects of ghrelin on the neuronal activity in the hypothalamic arcuate nucleus. *Neurosci Lett* 341, 151-155.

Rimm, E.B., Stampfer, M.J., Giovannucci, E., Ascherio, A., Spiegelman, D., Colditz, G.A., Willett, W.C., 1995. Body size and fat distribution as predictors of coronary heart disease among middle-aged and older US men. *Am J Epidemiol* 141, 1117-1127.

Ringe, D., Petsko, G.A., 2009. What are pharmacological chaperones and why are they interesting? *J Biol* 8, 80.

Ringholm, A., Fredriksson, R., Poliakova, N., Yan, Y.L., Postlethwait, J.H., Larhammar, D., Schioth, H.B., 2002. One melanocortin 4 and two melanocortin 5 receptors from zebrafish show remarkable conservation in structure and pharmacology. *J Neurochem* 82, 6-18.

Ringholm, A., Klovins, J., Fredriksson, R., Poliakova, N., Larson, E.T., Kukkonen, J.P., Larhammar, D., Schioth, H.B., 2003. Presence of melanocortin (MC4) receptor in spiny dogfish suggests an ancient vertebrate origin of central melanocortin system. *Eur J Biochem* 270, 213-221.

Robben, J.H., Sze, M., Knoers, N.V., Deen, P.M., 2006. Rescue of vasopressin V2 receptor mutants by chemical chaperones: specificity and mechanism. *Mol Biol Cell* 17, 379-386.

Robert, J., Clauser, E., Petit, P.X., Ventura, M.A., 2005. A novel C-terminal motif is necessary for the export of the vasopressin V1b/V3 receptor to the plasma membrane. *J Biol Chem* 280, 2300-2308.

Romiti, A., Buzzetti, R., Salandri, A., Festuccia, F., Giovannini, C.A., Santella, S., Montesani, C., Giovannini, C., 1998. Thyroid tumors in obesity. *Minerva Endocrinol* 23, 27-29.

Rossi, M., Kim, M.S., Morgan, D.G., Small, C.J., Edwards, C.M., Sunter, D., Abusnana, S., Goldstone, A.P., Russell, S.H., Stanley, S.A., Smith, D.M., Yagaloff, K., Ghatei, M.A., Bloom, S.R., 1998. A C-terminal fragment of Agouti-related protein increases feeding and antagonizes the effect of alpha-melanocyte stimulating hormone in vivo. *Endocrinology* 139, 4428-4431.

Roth, C.L., Ludwig, M., Woelfle, J., Fan, Z.C., Brumm, H., Biebermann, H., Tao, Y.X., 2009. A novel melanocortin-4 receptor gene mutation in a female patient with severe childhood obesity. *Endocrine* 36, 52-59.

Roubert, P., Dubern, B., Plas, P., Lubrano-Berthelier, C., Alihi, R., Auger, F., Deoliveira, D.B., Dong, J.Z., Basdevant, A., Thurieau, C., Clement, K., 2010. Novel pharmacological MC4R agonists can efficiently activate mutated MC4R from obese patient with impaired endogenous agonist response. *J Endocrinol* 207, 177-183.

Rouskas, K., Meyre, D., Stutzmann, F., Paletas, K., Papazoglou, D., Vatin, V., Marchand, M., Kouvatsi, A., Froguel, P., 2012. Loss-of-function mutations in MC4R are very rare in the Greek severely obese adult population. *Obesity (Silver Spring)* 20, 2278-2282.

Rubenstein, R.C., Egan, M.E., Zeitlin, P.L., 1997. In vitro pharmacologic restoration of CFTR-mediated chloride transport with sodium 4-phenylbutyrate in cystic fibrosis epithelial cells containing ΔF508-CFTR. *J Clin Invest* 100, 2457-2465.

Sabin, M.A., Ford, A.L., Holly, J.M., Hunt, L.P., Crowne, E.C., Shield, J.P., 2006. Characterisation of morbidity in a UK, hospital based, obesity clinic. *Arch Dis Child* 91, 126-130.

Sainsbury, A., Schwarzer, C., Couzens, M., Fetissov, S., Furtinger, S., Jenkins, A., Cox, H.M., Sperk, G., Hokfelt, T., Herzog, H., 2002. Important role of hypothalamic Y2 receptors in body weight regulation revealed in conditional knockout mice. *Proc Natl Acad Sci U S A* 99, 8938-8943.

Sampson, H.M., Robert, R., Liao, J., Matthes, E., Carlile, G.W., Hanrahan, J.W., Thomas, D.Y., 2011. Identification of a NBD1-binding pharmacological chaperone that corrects the trafficking defect of F508del-CFTR. *Chem Biol* 18, 231-242.

Santoro, N., Cirillo, G., Xiang, Z., Tanas, R., Greggio, N., Morino, G., Iughetti, L., Vottero, A., Salvatoni, A., Di Pietro, M., Balsamo, A., Crino, A., Grandone, A., Haskell-Luevano, C., Perrone, L., del Giudice, E.M., 2009. Prevalence of pathogenetic MC4R mutations in Italian children with early onset obesity, tall stature and familial history of obesity. *BMC Med Genet* 10, 25.

Sawyer, T.K., Sanfilippo, P.J., Hruby, V.J., Engel, M.H., Heward, C.B., Burnett, J.B., Hadley, M.E., 1980. 4-Norleucine, 7-D-phenylalanine-alpha-melanocyte-stimulating hormone: a highly potent alpha-melanotropin with ultralong biological activity. *Proc Natl Acad Sci U S A* 77, 5754-5758.

Schioth, H.B., Lagerstrom, M.C., Watanobe, H., Jonsson, L., Vergoni, A.V., Ringholm, A., Skarphedinsson, J.O., Skuladottir, G.V., Klovins, J., Fredriksson, R., 2003. Functional role, structure, and evolution of the melanocortin-4 receptor. *Ann N Y Acad Sci* 994, 74-83.

Schioth, H.B., Muceniece, R., Wikberg, J.E., 1996. Characterisation of the melanocortin 4 receptor by radioligand binding. *Pharmacol Toxicol* 79, 161-165.

Schrier, R.W., Gross, P., Gheorghiade, M., Berl, T., Verbalis, J.G., Czerwiec, F.S., Orlandi, C., Investigators, S., 2006. Tolvaptan, a selective oral vasopressin V2-receptor antagonist, for

hyponatremia. *N Engl J Med* 355, 2099-2112.

Sebag, J.A., Hinkle, P.M., 2007. Melanocortin-2 receptor accessory protein MRAP forms antiparallel homodimers. *Proc Natl Acad Sci U S A* 104, 20244-20249.

Sebag, J.A., Zhang, C., Hinkle, P.M., Bradshaw, A.M., Cone, R.D., 2013. Developmental control of the melanocortin-4 receptor by MRAP2 proteins in zebrafish. *Science* 341, 278-281.

Sebhat, I.K., Martin, W.J., Ye, Z., Barakat, K., Mosley, R.T., Johnston, D.B., Bakshi, R., Palucki, B., Weinberg, D.H., MacNeil, T., Kalyani, R.N., Tang, R., Stearns, R.A., Miller, R.R., Tamvakopoulos, C., Strack, A.M., McGowan, E., Cashen, D.E., Drisko, J.E., Hom, G.J., Howard, A.D., MacIntyre, D.E., van der Ploeg, L.H., Patchett, A.A., Nargund, R.P., 2002. Design and pharmacology of N-[(3R)-1,2,3,4-tetrahydroisoquinolinium- 3-ylcarbonyl]-(1R)-1-(4-chlorobenzyl)- 2-[4-cyclohexyl-4-(1H-1,2,4-triazol- 1-ylmethyl)piperidin-1-yl]-2-oxoethylamine (1), a potent, selective, melanocortin subtype-4 receptor agonist. *J Med Chem* 45, 4589-4593.

Sellers, T.A., Kushi, L.H., Potter, J.D., Kaye, S.A., Nelson, C.L., McGovern, P.G., Folsom, A.R., 1992. Effect of family history, body-fat distribution, and reproductive factors on the risk of postmenopausal breast cancer. *N Engl J Med* 326, 1323-1329.

Shimizu, H., Inoue, K., Mori, M., 2007. The leptin-dependent and -independent melanocortin signaling system: regulation of feeding and energy expenditure. *J Endocrinol* 193, 1-9.

Siebenhofer, A., Horvath, K., Jeitler, K., Berghold, A., Stich, A.K., Matyas, E., Pignitter, N., Siering, U., 2009. Long-term effects of weight-reducing drugs in hypertensive patients. *Cochrane Database Syst Rev*, CD007654.

Siljee-Wong, J.E., 2011. Melanocortin MC(4) receptor expression sites and local function. *Eur J Pharmacol* 660, 234-240.

Skorczyk, A., Stachowiak, M., Szczerbal, I., Klukowska-Roetzler, J., Schelling, C., Dolf, G., Switonski, M., 2007. Polymorphism and chromosomal location of the MC4R (melanocortin-4 receptor) gene in the dog and red fox. *Gene* 392, 247-252.

Smith, A.I., Funder, J.W., 1988. Proopiomelanocortin processing in the pituitary, central nervous system, and peripheral tissues. *Endocr Rev* 9, 159-179.

Srinivasan, S., Lubrano-Berthelier, C., Govaerts, C., Picard, F., Santiago, P., Conklin, B.R., Vaisse, C., 2004. Constitutive activity of the melanocortin-4 receptor is maintained by its N-terminal domain and plays a role in energy homeostasis in humans. *J Clin Invest* 114, 1158-1164.

Stampfer, M.J., Maclure, K.M., Colditz, G.A., Manson, J.E., Willett, W.C., 1992. Risk of symptomatic gallstones in women with severe obesity. *Am J Clin Nutr* 55, 652-658.

Staubert, C., Tarnow, P., Brumm, H., Pitra, C., Gudermann, T., Gruters, A., Schoneberg, T., Biebermann, H., Rompler, H., 2007. Evolutionary aspects in evaluating mutations in the melanocortin 4 receptor. *Endocrinology* 148, 4642-4648.

Ste Marie, L., Miura, G.I., Marsh, D.J., Yagaloff, K., Palmiter, R.D., 2000. A metabolic defect promotes obesity in mice lacking melanocortin-4 receptors. *Proc Natl Acad Sci U S A* 97, 12339-12344.

Steiner, A.L., Kipnis, D.M., Utiger, R., Parker, C., 1969. Radioimmunoassay for the measurement of adenosine 3',5'-cyclic phosphate. *Proc Natl Acad Sci U S A* 64, 367-373.

Stutzmann, F., Tan, K., Vatin, V., Dina, C., Jouret, B., Tichet, J., Balkau, B., Potoczna, N., Horber, F., O'Rahilly, S., Farooqi, I.S., Froguel, P., Meyre, D., 2008. Prevalence of melanocortin-4 receptor deficiency in Europeans and their age-dependent penetrance in multigenerational pedigrees. *Diabetes* 57, 2511-2518.

Sutton, G.M., Duos, B., Patterson, L.M., Berthoud, H.R., 2005. Melanocortinergic modulation of cholecystokinin-induced suppression of feeding through extracellular signal-regulated kinase signaling in rat solitary nucleus. *Endocrinology* 146, 3739-3747.

Tan, K., Pogozheva, I.D., Yeo, G.S., Hadaschik, D., Keogh, J.M., Haskell-Leuvano, C., O'Rahilly, S., Mosberg, H.I., Farooqi, I.S., 2009. Functional characterization and structural modeling of obesity associated mutations in the melanocortin 4 receptor. *Endocrinology* 150, 114-125.

Tao, Y.X., 2005. Molecular mechanisms of the neural melanocortin receptor dysfunction in severe early onset obesity. *Mol Cell Endocrinol* 239, 1-14.

Tao, Y.X., 2006. Inactivating mutations of G protein-coupled receptors and diseases: Structure-function insights and therapeutic implications. *Pharmacol Ther* 111, 949-973.

Tao, Y.X., 2009. Mutations in melanocortin-4 receptor and human obesity. *Prog Mol Biol Transl Sci* 88, 173-204.

Tao, Y.X., 2010. The melanocortin-4 receptor: Physiology, pharmacology, and pathophysiology. *Endocr Rev* 31, 506-543.

Tao, Y.X., 2014. Constitutive activity in melanocortin-4 receptor: biased signaling of inverse agonists. *Adv Pharmacol* 70, 135-154.

Tao, Y.X., Conn, P.M., 2014. Chaperoning G protein-coupled receptors: From cell biology to therapeutics. *Endocr Rev* 35, 602-647.

Tao, Y.X., Huang, H., 2014. Ipsen 5i is a novel potent pharmacoperone for intracellularly retained melanocortin-4 receptor mutants. *Front Endocrinol (Lausanne)* 5, 131.

Tao, Y.X., Segaloff, D.L., 2003. Functional characterization of melanocortin-4 receptor mutations associated with childhood obesity. *Endocrinology* 144, 4544-4551.

Tao, Y.X., Segaloff, D.L., 2005. Functional analyses of melanocortin-4 receptor mutations

identified from patients with binge eating disorder and nonobese or obese subjects. *J Clin Endocr Metab* 90, 5632-5638.

Tao, Y.X., Yuan, Z.H., Xie, J., 2013. G protein-coupled receptors as regulators of energy homeostasis. *Prog Mol Biol Transl Sci* 114, 1-43.

Tarnow, P., Schoneberg, T., Krude, H., Gruters, A., Biebermann, H., 2003. Mutationally induced disulfide bond formation within the third extracellular loop causes melanocortin 4 receptor inactivation in patients with obesity. *J Biol Chem* 278, 48666-48673.

Tena-Sempere, M., 2013. Interaction between energy homeostasis and reproduction: central effects of leptin and ghrelin on the reproductive axis. *Horm Metab Res* 45, 919-927.

Terranova, L., Busetto, L., Vestri, A., Zappa, M.A., 2012. Bariatric surgery: cost-effectiveness and budget impact. *Obes Surg* 22, 646-653.

Thearle, M.S., Muller, Y.L., Hanson, R.L., Mullins, M., Abdussamad, M., Tran, J., Knowler, W.C., Bogardus, C., Krakoff, J., Baier, L.J., 2012. Greater impact of melanocortin-4 receptor deficiency on rates of growth and risk of type 2 diabetes during childhood compared with adulthood in Pima Indians. *Diabetes* 61, 250-257.

Tirosh, A., Shai, I., Afek, A., Dubnov-Raz, G., Ayalon, N., Gordon, B., Derazne, E., Tzur, D., Shamis, A., Vinker, S., Rudich, A., 2011. Adolescent BMI trajectory and risk of diabetes versus coronary disease. *N Engl J Med* 364, 1315-1325.

Torgerson, J.S., Hauptman, J., Boldrin, M.N., Sjostrom, L., 2004. XENical in the prevention of diabetes in obese subjects (XENDOS) study: a randomized study of orlistat as an adjunct to lifestyle changes for the prevention of type 2 diabetes in obese patients. *Diabetes Care* 27, 155-161.

Trogdon, J.G., Finkelstein, E.A., Feagan, C.W., Cohen, J.W., 2012. State- and payer-specific

estimates of annual medical expenditures attributable to obesity. *Obesity (Silver Spring)* 20, 214-220.

Uversky, V.N., Li, J., Fink, A.L., 2001. Trimethylamine-*N*-oxide-induced folding of α-synuclein. *FEBS Lett* 509, 31-35.

Vagenende, V., Yap, M.G., Trout, B.L., 2009. Mechanisms of protein stabilization and prevention of protein aggregation by glycerol. *Biochemistry* 48, 11084-11096.

Vaisse, C., Clement, K., Durand, E., Hercberg, S., Guy-Grand, B., Froguel, P., 2000. Melanocortin-4 receptor mutations are a frequent and heterogeneous cause of morbid obesity. *J Clin Invest* 106, 253-262.

Vaisse, C., Clement, K., Guy-Grand, B., Froguel, P., 1998. A frameshift mutation in human MC4R is associated with a dominant form of obesity. *Nat Genet* 20, 113-114.

Valli-Jaakola, K., Lipsanen-Nyman, M., Oksanen, L., Hollenberg, A.N., Kontula, K., Bjorbaek, C., Schalin-Jantti, C., 2004. Identification and characterization of melanocortin-4 receptor gene mutations in morbidly obese Finnish children and adults. *J Clin Endocr Metab* 89, 940-945.

Vergoni, A.V., Bertolini, A., Guidetti, G., Karefilakis, V., Filaferro, M., Wikberg, J.E., Schioth, H.B., 2000. Chronic melanocortin 4 receptor blockage causes obesity without influencing sexual behavior in male rats. *J Endocrinol* 166, 419-426.

Vergoni, A.V., Poggioli, R., Bertolini, A., 1986. Corticotropin inhibits food intake in rats. *Neuropeptides* 7, 153-158.

Vink, T., Hinney, A., van Elburg, A.A., van Goozen, S.H., Sandkuijl, L.A., Sinke, R.J., Herpertz-Dahlmann, B.M., Hebebrand, J., Remschmidt, H., van Engeland, H., Adan, R.A., 2001. Association between an agouti-related protein gene polymorphism and anorexia nervosa.

Mol Psychiatr 6, 325-328.

Vongs, A., Lynn, N.M., Rosenblum, C.I., 2004. Activation of MAP kinase by MC4-R through PI3 kinase. *Regul Pept* 120, 113-118.

Vos, T.J., Caracoti, A., Che, J.L., Dai, M., Farrer, C.A., Forsyth, N.E., Drabic, S.V., Horlick, R.A., Lamppu, D., Yowe, D.L., Balani, S., Li, P., Zeng, H., Joseph, I.B., Rodriguez, L.E., Maguire, M.P., Patane, M.A., Claiborne, C.F., 2004. Identification of 2-[2-[2-(5-bromo-2-methoxyphenyl)-ethyl]-3-fluorophenyl]-4,5-dihydro-1H-imidazole (ML00253764), a small molecule melanocortin 4 receptor antagonist that effectively reduces tumor-induced weight loss in a mouse model. *J Med Chem* 47, 1602-1604.

Wagner, C.G., McMahon, C.D., Marks, D.L., Daniel, J.A., Steele, B., Sartin, J.L., 2004. A role for agouti-related protein in appetite regulation in a species with continuous nutrient delivery. *Neuroendocrinology* 80, 210-218.

Wainwright, C.E., Elborn, J.S., Ramsey, B.W., Marigowda, G., Huang, X., Cipolli, M., Colombo, C., Davies, J.C., De Boeck, K., Flume, P.A., Konstan, M.W., McColley, S.A., McCoy, K., McKone, E.F., Munck, A., Ratjen, F., Rowe, S.M., Waltz, D., Boyle, M.P., 2015. Lumacaftor-Ivacaftor in patients with cystic fibrosis homozygous for Phe508del *CFTR*. *N Engl J Med* 373, 220-231.

Wang, C.L., Liang, L., Wang, H.J., Fu, J.F., Hebebrand, J., Hinney, A., 2006. Several mutations in the melanocortin 4 receptor gene are associated with obesity in Chinese children and adolescents. *J Endocrinol Invest* 29, 894-898.

Wang, X.H., Wang, H.M., Zhao, B.L., Yu, P., Fan, Z.C., 2014. Rescue of defective MC4R cell-surface expression and signaling by a novel pharmacoperone Ipsen 17. *J Mol Endocrinol* 53, 17-29.

Wang, Z.Q., Huang, J.S., Zhou, J.H., Shi, L., Jiang, X.F., Tao, Y.X., 2016. Pharmacologic analyses of four chicken melanocortin-4 receptor mutations. *Domest Anim Endocrinol* 54, 68-75.

Wang, Z.Q., Tao, Y.X., 2011. Functional studies on twenty novel naturally occurring melanocortin-4 receptor mutations. *Biochim Biophys Acta* 1812, 1190-1199.

Ward, N.A., Hirst, S., Williams, J., Findlay, J.B., 2012. Pharmacological chaperones increase the cell-surface expression of intracellularly retained mutants of the melanocortin 4 receptor with unique rescuing efficacy profiles. *Biochem Soc Trans* 40, 717-720.

Warnock, D.G., Bichet, D.G., Holida, M., Goker-Alpan, O., Nicholls, K., Thomas, M., Eyskens, F., Shankar, S., Adera, M., Sitaraman, S., Khanna, R., Flanagan, J.J., Wustman, B.A., Barth, J., Barlow, C., Valenzano, K.J., Lockhart, D.J., Boudes, P., Johnson, F.K., 2015. Oral migalastat HCl leads to greater systemic exposure and tissue levels of active α-galactosidase A in Fabry patients when co-administered with infused agalsidase. *PloS ONE* 10, e0134341.

Wiley, J.C., Pettan-Brewer, C., Ladiges, W.C., 2011. Phenylbutyric acid reduces amyloid plaques and rescues cognitive behavior in AD transgenic mice. *Aging Cell* 10, 418-428.

Willesen, M.G., Kristensen, P., Romer, J., 1999. Co-localization of growth hormone secretagogue receptor and NPY mRNA in the arcuate nucleus of the rat. *Neuroendocrinology* 70, 306-316.

Wirth, M.M., Giraudo, S.Q., 2000. Agouti-related protein in the hypothalamic paraventricular nucleus: effect on feeding. *Peptides* 21, 1369-1375.

Witteman, J.C., Willett, W.C., Stampfer, M.J., Colditz, G.A., Sacks, F.M., Speizer, F.E., Rosner, B., Hennekens, C.H., 1989. A prospective study of nutritional factors and hypertension among US women. *Circulation* 80, 1320-1327.

Xiang, Z., Litherland, S.A., Sorensen, N.B., Proneth, B., Wood, M.S., Shaw, A.M., Millard, W.J.,

Haskell-Luevano, C., 2006. Pharmacological characterization of 40 human melanocortin-4 receptor polymorphisms with the endogenous proopiomelanocortin-derived agonists and the agouti-related protein (AGRP) antagonist. *Biochemistry* 45, 7277-7288.

Xiang, Z., Pogozheva, I.D., Sorenson, N.B., Wilczynski, A.M., Holder, J.R., Litherland, S.A., Millard, W.J., Mosberg, H.I., Haskell-Luevano, C., 2007. Peptide and small molecules rescue the functional activity and agonist potency of dysfunctional human melanocortin-4 receptor polymorphisms. *Biochemistry* 46, 8273-8287.

Xiang, Z., Proneth, B., Dirain, M.L., Litherland, S.A., Haskell-Luevano, C., 2010. Pharmacological characterization of 30 human melanocortin-4 receptor polymorphisms with the endogenous proopiomelanocortin-derived agonists, synthetic agonists, and the endogenous agouti-related protein antagonist. *Biochemistry* 49, 4583-4600.

Yam, G.H., Bosshard, N., Zuber, C., Steinmann, B., Roth, J., 2006. Pharmacological chaperone corrects lysosomal storage in Fabry disease caused by trafficking-incompetent variants. Am *J Physiol Cell Physiol* 290, C1076-C1082.

Yan, J., Tao, Y.X., 2011. Pharmacological characterization of canine melancortin-4 receptor and its natural variant V213F. *Domest Anim Endocrinol* 41, 91-97.

Yang, F., Huang, H., Tao, Y.X., 2015a. Biased signaling in naturally occurring mutations in human melanocortin-3 receptor gene. *Int J Biol Sci* 11, 423-433.

Yang, Y., Cai, M., Chen, M., Qu, H., McPherson, D., Hruby, V., Harmon, C.M., 2009. Key amino acid residues in the melanocortin-4 receptor for nonpeptide THIQ specific binding and signaling. *Regul Pept* 155, 46-54.

Yang, Y., Chen, M., Dimmitt, R., Harmon, C.M., 2014. Structural insight into the MC4R conformational changes via different agonist-mediated receptor signaling. *Biochemistry* 53,

7086-7092.

Yang, Z., Huang, Z.L., Tao, Y.X., 2015b. Functions of DPLIY motif and helix 8 of human melanocortin-3 receptor. *J Mol Endocrinol* 55, 107-117.

Yeo, G.S., Farooqi, I.S., Aminian, S., Halsall, D.J., Stanhope, R.G., O'Rahilly, S., 1998. A frameshift mutation in MC4R associated with dominantly inherited human obesity. *Nat Genet* 20, 111-112.

Yeo, G.S., Lank, E.J., Farooqi, I.S., Keogh, J., Challis, B.G., O'Rahilly, S., 2003. Mutations in the human melanocortin-4 receptor gene associated with severe familial obesity disrupts receptor function through multiple molecular mechanisms. *Hum Mol Genet* 12, 561-574.

Yuste-Checa, P., Brasil, S., Gamez, A., Underhaug, J., Desviat, L.R., Ugarte, M., Perez-Cerda, C., Martinez, A., Perez, B., 2017. Pharmacological chaperoning: A potential treatment for PMM2-CDG. *Hum Mutat* 38, 160-168.

Zhou, Z., Gong, Q., January, C.T., 1999. Correction of defective protein trafficking of a mutant HERG potassium channel in human long QT syndrome. Pharmacological and temperature effects. *J Biol Chem* 274, 31123-31126.

Zimran, A., Altarescu, G., Elstein, D., 2013. Pilot study using ambroxol as a pharmacological chaperone in type 1 Gaucher disease. *Blood Cells Mol Dis* 50, 134-137.